NASA TECHNICAL MEMORANDUM

NASA TM-78208

TRANSFER FUNCTION TESTS OF THE JOY LONGWALL SHEARER

By Paul H. Fisher, Jr.
Electronics and Control Laboratory

December 1978

NASA

George C. Marshall Space Flight Center
Marshall Space Flight Center, Alabama

TECHNICAL REPORT STANDARD TITLE PAGE

1. REPORT NO.	2. GOVERNMENT ACCESSION NO.	3. RECIPIENT'S CATALOG NO.
NASA TM-78208		

4 TITLE AND SUBTITLE	5. REPORT DATE
Transfer Function Tests of the Joy Longwall Shearer	December 1978
	6. PERFORMING ORGANIZATION CODE
7. AUTHOR(S)	8. PERFORMING ORGANIZATION REPORT #
Paul H. Fisher, Jr.	
9. PERFORMING ORGANIZATION NAME AND ADDRESS	10. WORK UNIT NO.
George C. Marshall Space Flight Center Marshall Space Flight Center, Alabama 35812	11. CONTRACT OR GRANT NO.
	13. TYPE OF REPORT & PERIOD COVERED
12 SPONSORING AGENCY NAME AND ADDRESS	Technical Memorandum
National Aeronautics and Space Administration Washington, D.C. 20546	14. SPONSORING AGENCY CODE

15. SUPPLEMENTARY NOTES

Prepared by Electronics and Control Laboratory, Science and Engineering

16. ABSTRACT

A series of operational tests was performed in March 1977, on the Joy longwall shearer located at the Bureau of Mines in Bructon, Pennsylvania. The purpose of these tests was to determine the transfer function and operational characteristics of the system. These characteristics will be used to generate a simulation model of the longwall shearer used in the development of the closed-loop vertical control system.

17. KEY WORDS	18. DISTRIBUTION STATEMENT
	Unclassified — Unlimited

19. SECURITY CLASSIF. (of this report)	20. SECURITY CLASSIF. (of this page)	21. NO. OF PAGES	22. PRICE
Unclassified	Unclassified	87	NTIS

TABLE OF CONTENTS

LIST OF ILLUSTRATIONS

LIST OF ILLUSTRATIONS (Continued)

LIST OF ILLUSTRATIONS (Continued)

LIST OF ILLUSTRATIONS (Concluded)

LIST OF TABLES

TECHNICAL MEMORANDUM 78208

TRANSFER FUNCTION TESTS OF THE JOY LONGWALL SHEARER

INTRODUCTION

A series of operational tests was performed in March 1977 on the Joy longwall shearer located at the Bureau of Mines in Bructon, Pennsylvania. The purpose of these tests was to determine the transfer function and operational characteristics of the system. These characteristics will be used to generate a simulation model of the longwall shearer used in the development of the closed-loop vertical control system.

DESCRIPTION OF TEST SETUP

The longwall shearer after instrumentation is shown in Figure 1. The figure shows the left and right boom, cutting drum, left and right control panels, the conveyor pans, and rack. All tests were performed in this work area and no external loads were applied to the cutting drums or booms. Before the tests, the tilt cylinders (ROLL) were positioned so the chassis was horizontal and the cowl was rotated to a vertical position to permit the boom to be lowered to a horizontal position.

The dual boom system showing the sensor locations and input commands are shown in Figure 2. Table 1 identifies the symbols in Figure 2. The location of the sensors on the longwall shearer are shown in Figures 3 through 6. Input commands to the system (8 V) were selected from a pulse generator (which provided for a selection of various pulse durations and frequencies) or from a sine wave generator (for a range of frequencies and amplitudes). These inputs were used to drive the right and left booms individually or simultaneously. The input command to the left boom (C_L) and right boom (C_R) were interfaced through an Oceanic connector to the control valves and recorded on magnetic tape with the other system parameters.

TABLE 1. SYMBOL IDENTIFICATION

Channel	Recorder A	Symbol	Recorder B	Symbol
1	Reference Pulse		Reference Pulse	
2	Piezoaccelerometer	A_{PL}	Piezoaccelerometer	A_{PR}
3	Servoaccelerometer	A_{SL}	Servoaccelerometer	A_{SR}
4	Radial Accelerometer	A_{RL}	Radial Accelerometer	A_{RR}
5	Rate Gyro of Left Boom	$\dot{\beta}_L$	Rate Gyro of Right Boom	$\dot{\beta}_R$
6	Boom Cylinder Position	X_L	Boom Cylinder Position	X_R
7	Pressure between Needle Check Valve and Pilot Check Valve	P_1	Pressure between Needle Check Valve and Pilot Check Valve	P_4
8	Between Needle and Check Valve and Boom Cylinder	P_2	Between Needle and Check Valve and Boom Cylinder	P_5
9	Lower Boom Pressure Line	P_3	Lower Boom Pressure Line	P_6
10	Supply Pressure	P_S	Left Boom Position Pot	Y_L
11	Command to Left Control Valve	C_L	Command to Right Control Valve	C_R

The system pressures were monitored with pressure transducers calibrated from 0 to 2500 psi for a 0 to 5 V output from signal conditioners. The supply pressure regulator was set at 2200 psi, but the pressure sensor (P_S) was located between the pump and the regulator. Other pressure sensors (P_i) i + 1 . . . 6 were located as shown in Figure 2. During several tests, pressures exceeding 2500 psi within the system saturated the pressure sensors. Hydraulic temperature (T) was monitored in the return line. The hydraulic temperatures were found to be excessive and a heat exchanger was installed.

The position of the boom cylinders was obtained by mounting linear potentiometers to the cylinder body and the slider to the boom cylinder rod. The boom cylinder stroke is 9.5 in. and, when extended, the potentiometer output was set at 4.5 V. The resultant boom angle (β) is 36.3 deg. A boom angle of zero occurs when the boom is collinear with the chassis. The potentiometer output is then 0.8 V and the boom cylinder stroke is 3.25 in. The boom cylinder position for the left (X_L) and right (X_R) boom is shown in Figure 2. The boom cylinder stroke (S) is related to the cylinder positions ($X_{L,R}$) provided in this report by:

$$S = 0.6579\,X + 3.25.$$

The left boom pressures are shown in Figure 3. The vertical actuator in Figure 4 is one of two tilt cylinders (ROLL). The left and right boom cylinder position potentiometers are shown in Figures 4 and 5. The locations of the temperature probe and the supply pressure transducer are shown in Figure 6. Several protective side panels were removed from the longwall shearer to provide access for mounting the sensors.

The boom height potentiometer (Y_L) in Figure 7 was monitored on the left boom to detect boom position relative to the ground reference. A potentiometer stand for low boom angles and a stand extension were used for larger boom angles to support the potentiometer (Y_L). A scale factor of 1.724 in./V was used for this output.

Angular boom rates were detected at the rate gyro package shown in Figure 7 ($\dot{\beta}_L$). The operational range of this sensor is ±20 deg/sec with a natural frequency of 23 Hz. Calibration curves for the rate gyros are shown in Figure 8 for $\dot{\beta}_R$ and Figure 9 for $\dot{\beta}_L$.

The sensor disc, which contains the rate gyro and the tangential and normal accelerometers, was aligned such that the tangential accelerometers were perpendicular to the centerline of the boom. The output voltage from the accelerometers was scaled from 0 to 5 V by the signal conditioners such that zero acceleration was 2.5 V. The recorded outputs in this report of A_{SR} and A_{SL} has had the Earth's gravity input biased out. The accelerometers are shown in Figure 7 for the left boom. Two ±5 g sensors were used for A_S and A_P and a ±1 g sensor for A_R. Higher frequencies (above 20 Hz) were sensed with the piezosensor A_P while the lower frequencies (0 to 100 Hz) were sensed with the servoaccelerometer A_S.

The outputs from the sensors were routed to the signal conditioner and distribution box and then to the two Ampex 1300 tape recorders. Selected parameters were monitored and recorded on an eight channel Brush recorder. The Ampex recorder speed provided a 20 000 Hz frequency response, but data acquired on the Brush is flat out to only 55 Hz.

Eleven channels of data were recorded on each tape recorder. Channels 1 and 11 were calibrated for ±8 V and the remaining channels were calibrated ±5 V. Recorder playback scale factors are 3.53 for the ±5 V channels and 5.66 for the ±8 V channels. The data channel identification is given in Table 1. The data recorders and support equipment are shown in Figure 10.

DESCRIPTION OF TESTS PERFORMED

The closed-loop vertical control system will be used to detect the difference between a desired cutting depth of coal and the actual cutting depth that occurs and maintain that difference within prescribed limits. Commands from the controller to the longwall shearer control valve will be constant in magnitude but of variable duration. Since the present longwall shearer control valve is a proportional valve, a series of system tests was performed to investigate the linear and nonlinear system characteristics. (A list of these tests is given in Table 2.) These tests resulted in the identification of characteristics needed to develop an improved simulation model of the longwall shearer. A systems analysis to identify or explain the reason for the characteristics observed or recorded is not intended in this report. This would require a more indepth study than has been directed for this task.

TABLE 2. TESTS PERFORMED TO INVESTIGATE LINEAR AND NONLINEAR SYSTEM CHARACTERISTICS

1. Raised and Lowered Right and Left Booms
   - A. Individually and Simultaneously
   - B. Continuous Command
   - C. Pulsed Command
2. Oscillate About a Reference Position
   - A. Boom Horizontal
   - B. Boom Raised
   - C. Sinusoidal Input
   - D. Pulsed Input
   - E. Simultaneous Commands
3. Command Threshold
   - A. Pulsed Input
   - B. Sinusoidal Input
4. Frequency Response
5. Translation of Longwall Shearer on Track
   - A. Minimum Speed
   - B. Mid-Speed
   - C. Maximum Speed

The frequency response of the left boom is shown in Figure 11. This was obtained from a constant amplitude input C_L for selected frequencies over the range indicated. The predominate effects are the attenuation that occurs above 0.6 Hz and the coupling of the signal and response of the right boom. This is listed in Table 2 as Item 4.

A series of runs identified in Figure 12 were plotted on the Brush recorder during the tests. These selected parameters provide a ready insight to the system's response. An expanded time scale and additional parameters of these runs are included in Figures 13 through 53. The needle and check

valve and the double pilot check valve are shown in Figures 54 and 55. The resultant response of the system parameters listed in Table 2 follows Figure 17. Before these runs were made, a set of tapes (1A and 1B) were made to obtain an understanding of the system. As a result of these preliminary runs, a double pilot check valve was replaced on the right boom. An internal leakage prevented the boom from maintaining a constant position. An unbalanced rate between raising and lowering the boom was balanced by adjusting the needle check valve (Figs. 2 and 54). An activation threshold was identified for both on-off and proportional control valve operation. Small amplitude inputs to the proportional valve (chatter) resulted in a boom oscillation whenever the boom was lowered. Although several needle valve positions were selected, there was always an input amplitude that excited this limit cycle condition when the boom was lowered. This characteristic is not excited when the system is operated in the on-off mode. The needle valve was set for balanced rates before data tapes 2A, 2B, 3A, and 3B were made. An increase in hydraulic temperature occurred during initial system tests prior to tapes 2 and 3 and the temperature was allowed to reach 200°F before tests were terminated. The Shell Tellus No. 33 oil used in the system has an operational temperature range from 0 to 220°F. (The Tellus oil No. 33 has been designated as No. 68 since January 1977.) As shown in Figure 2, a heat exchanger was added to the system which maintained the monitored temperature point below 150°F during successive runs. An observed hot spot in the area of the hydraulic pump occurred during the acquisitions of data and, although the temperature probe recorded less than 150°F, data gathering was discontinued. The following day, an equipment shut-down occurred prior to making transverse runs on the track. This shut-down was attributed to a thermal overload.

The following runs were obtained from No. 2 data tapes:

Run 1 — Left boom up then down, stopping before full stroke of the actuator.

Run 2 — Right boom up then down, stopping before full actuator stroke.

Run 3 — Simultaneous command to lower left boom and raise right boom. The left boom lower rate is the same as Run 1; however, a reduced rate occurs in the right boom during simultaneous operation.

Run 4 — Simultaneous command to raise the boom to end of stroke. The left boom extended to the hard stop before the right boom is extended to the end of stroke.

Run 5 — Pulsed input to the right boom, increasing pulse duration until response occurs. The threshold was determined to be 300 msec. A response is also noted in the left boom rate but not the boom cylinder position.

Run 6 — A 300 msec pulse command to raise the right boom then a simultaneous continuous raise then lower left boom command. Cross coupling is evident between both booms.

Run 7 — Pulsed input increased to 500 msec to raise right boom, then adjusted down pulse time for a sustained oscillation of a low boom position. The down pulse duration was 760 msec.

Run 8 — The right boom was raised and maintained the same duration pulses as in Run 7.

Run 9 — A continuous command to raise and lower left boom while the right boom is pulsed about a fixed position. The pulses of right boom are the same as in Run 7.

Run 10 — The left boom threshold was determined to be a 260 msec pulse.

Run 11 — A continuous command to the right boom to raise, then lower the left boom pulsed to raise the boom.

Run 12 — A 500 msec up pulse and a 600 msec down pulse permitted the left boom to oscillate about a constant position.

Run 13 — Raised boom to new position to check oscillation about a new position.

Run 14 — Continuous command to raise, then lower right boom while left boom oscillates at pulsed times given in Run 12.

Run 15 — Left and right boom oscillate about a point for a pulse time given in Runs 7 and 12. Both booms are dropping but at a different rate.

Run 16 — Left and right boom oscillate about a point for a 1 sec duration up pulse. The down pulse was adjusted to maintain a constant position on the right boom.

Run 17 — Left and right boom oscillate about a point for a 1 sec duration up pulse for the left boom.

Run 18 — The 1 sec duration pulses when applied simultaneously to both booms resulted in an in-phase pulsing and resultant decrease in the position of each boom. The individual oscillations about a point in Runs 16 and 17 could not be maintained when commanded together.

Run 19 — Not recorded.

Run 20 — Same as Run 18 but with both booms in a lower position.

Additional runs and data are available and are recorded on tape; however, it cannot be included in this report because of the bulk of the material. Any additional information or data that are on the tapes can be obtained upon request to EC24.

A simulation model of the longwall shearer was developed from these test results and is provided in Appendix A.

CONCLUSION

The data obtained during this investigation were for an unloaded condition, since the drum was not cutting coal or driven into the coal seam by the linear drive along the track. The magnitude of the observed coupling between the booms is expected to change in the operational mode when the cutting drums and boom are under load. The loads on the system will result in higher system temperature and hydraulic pressures than have been indicated in this report.

It has been determined that the needle check valve is a significant component in the dynamic response characteristics of the system. The needle valve can be opened such that the rates to lower the boom exceed those to raise it. A decrease in boom rates occurred when the booms were raised simultaneously, but this did not occur when they were simultaneously lowered. The complete

closing of the needle valve restricts the flow so that the boom can only be raised. The needle valve position determines the down pulse duration for sustained oscillation, the rate the boom can be lowered, the frequency response curve, and the chatter level for a proportional input command.

An increase in the activation threshold for pulsed inputs was observed and should be reflected in the simulation model along with the other significant characteristics determined by this study.

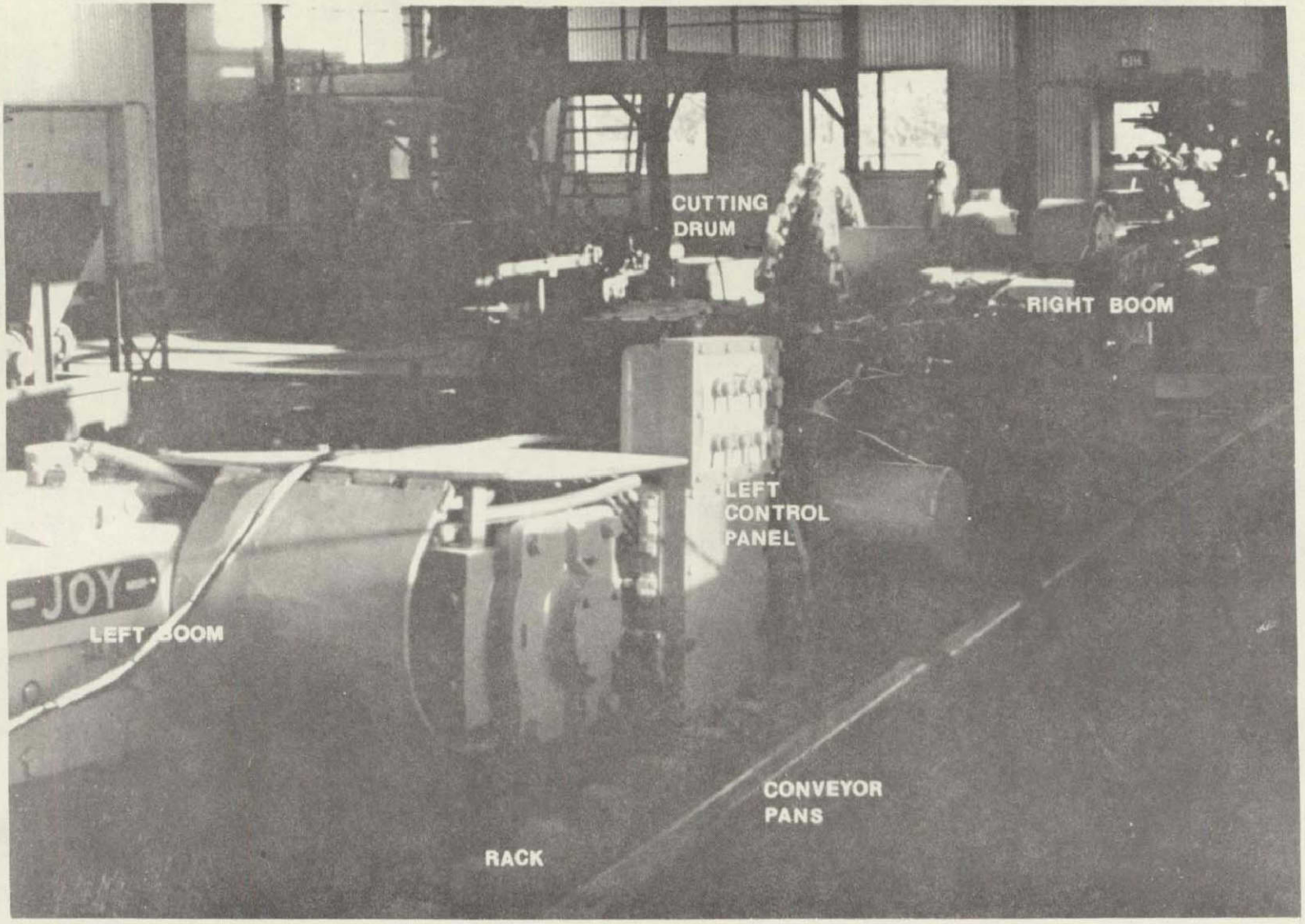

Figure 1. Longwall shearer at Bruceton, Pennsylvania.

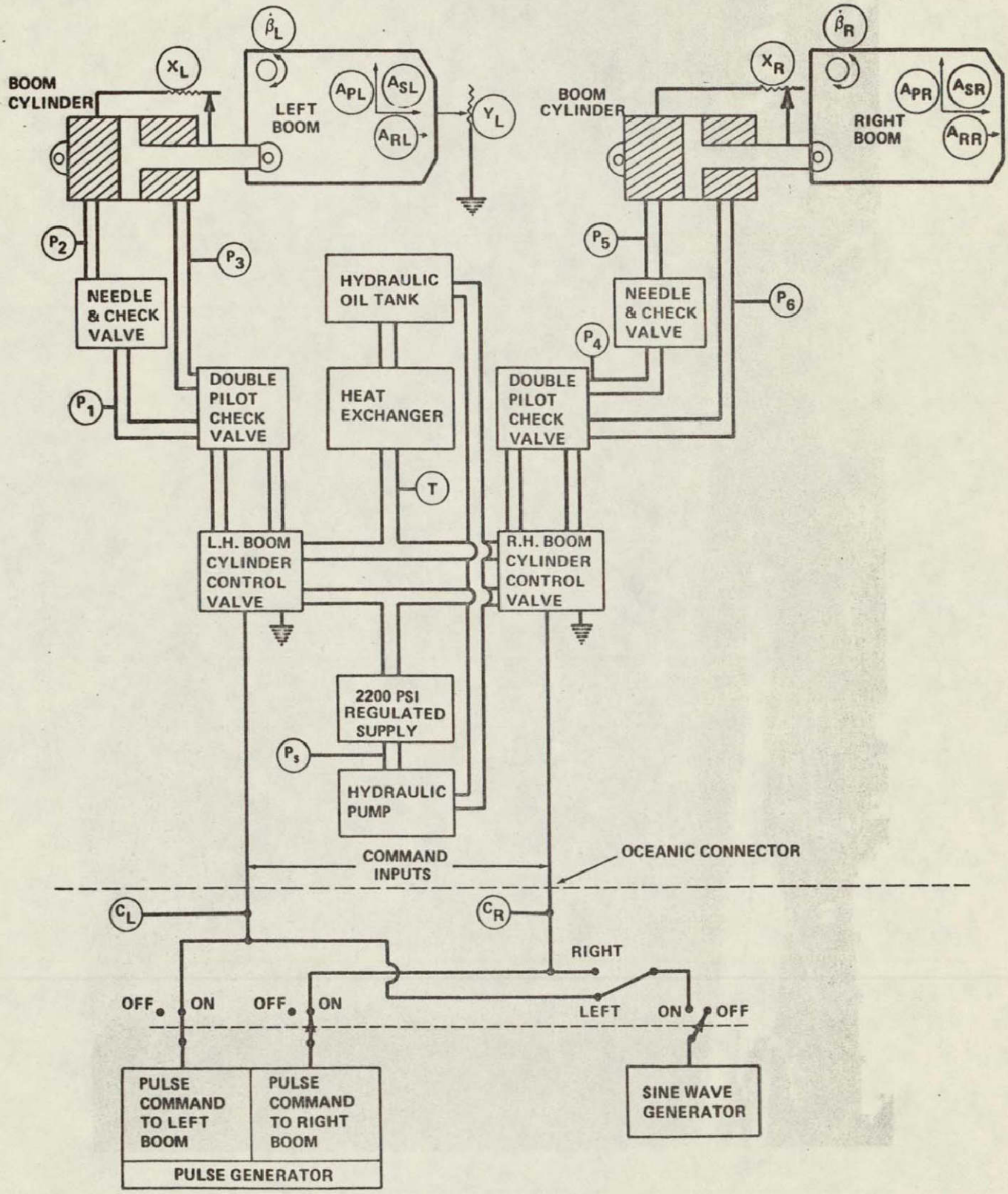

Figure 2. Longwall shearer measurement schematic.

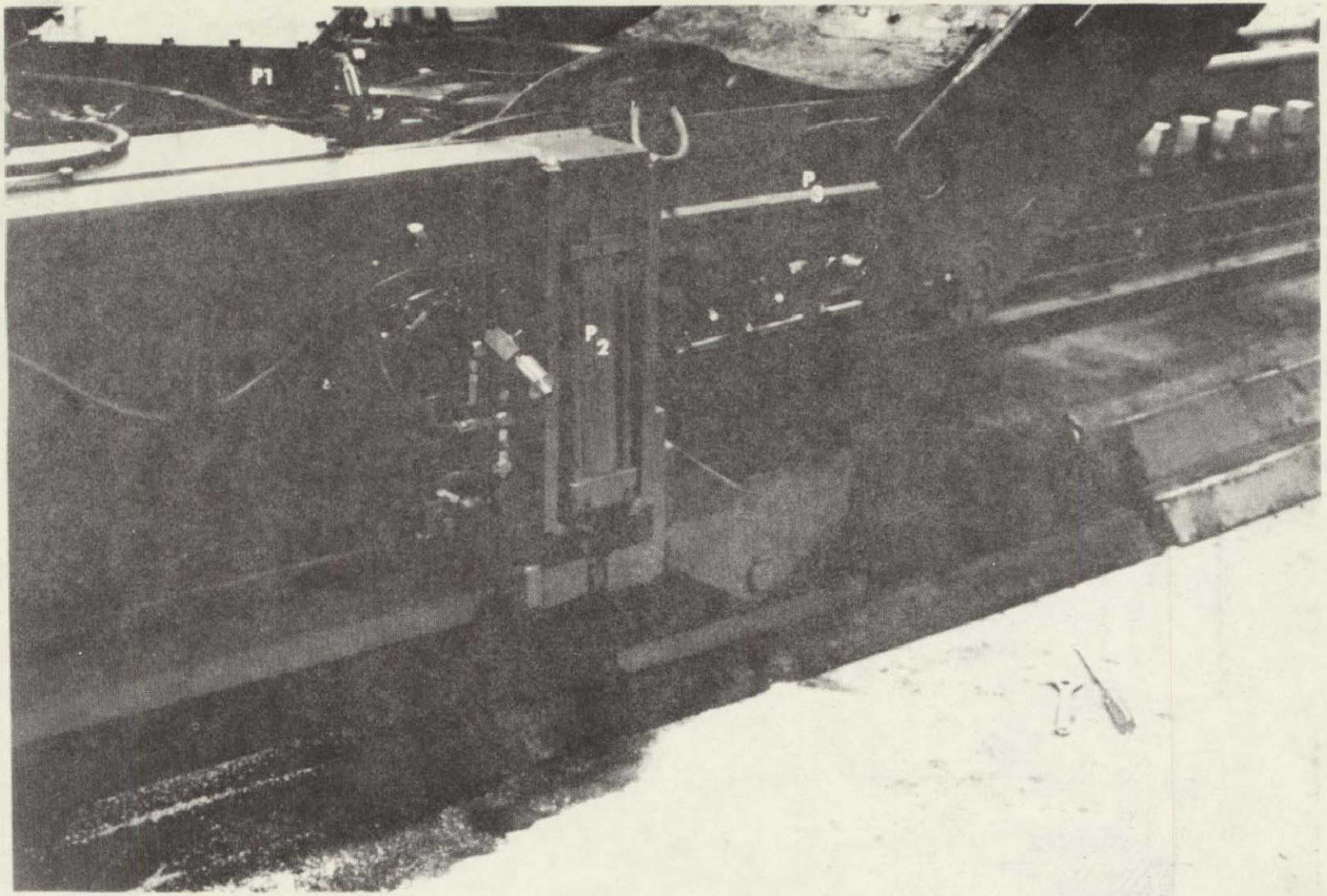

Figure 3. Left boom pressure sensors.

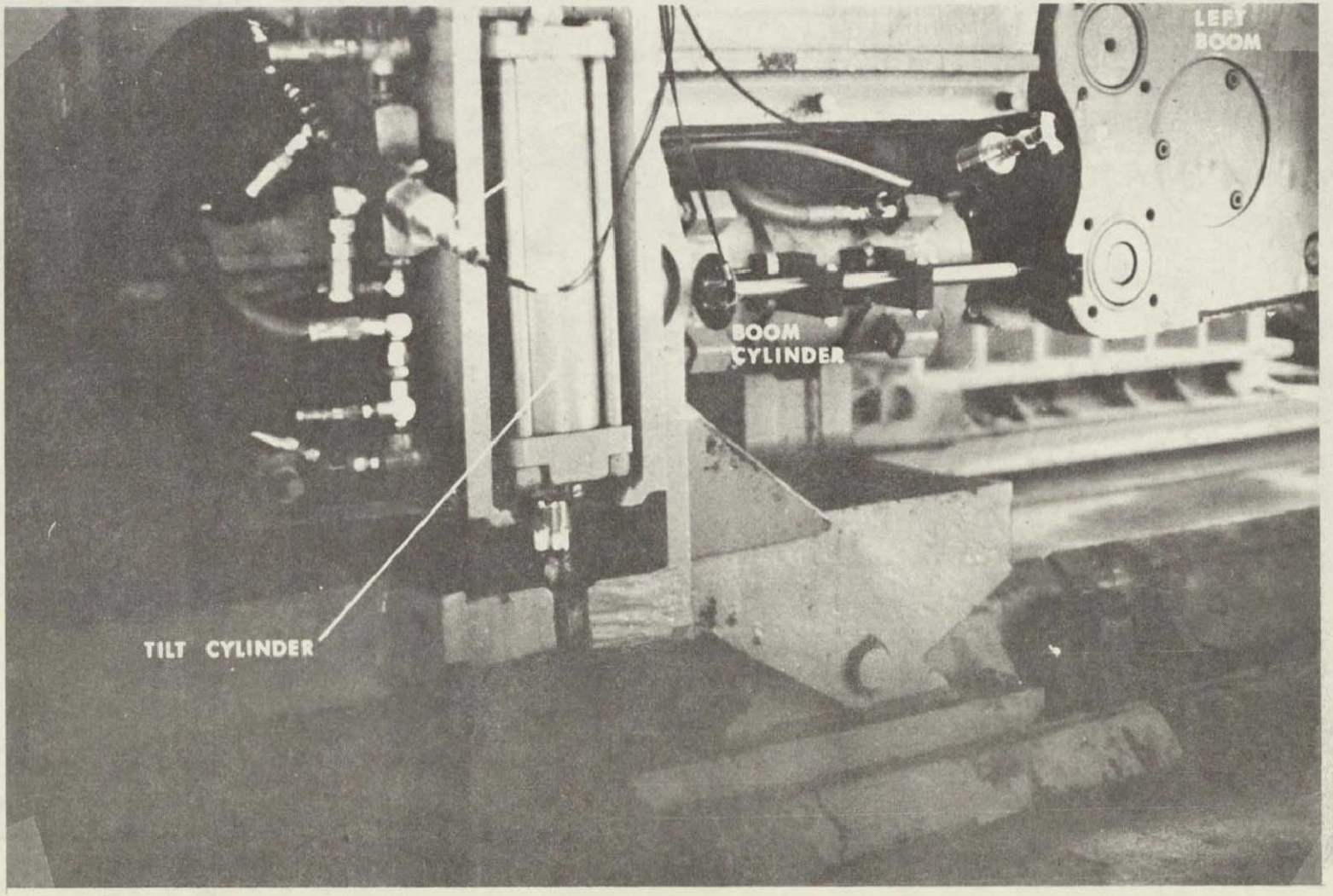

Figure 4. Left boom cylinder and sensors.

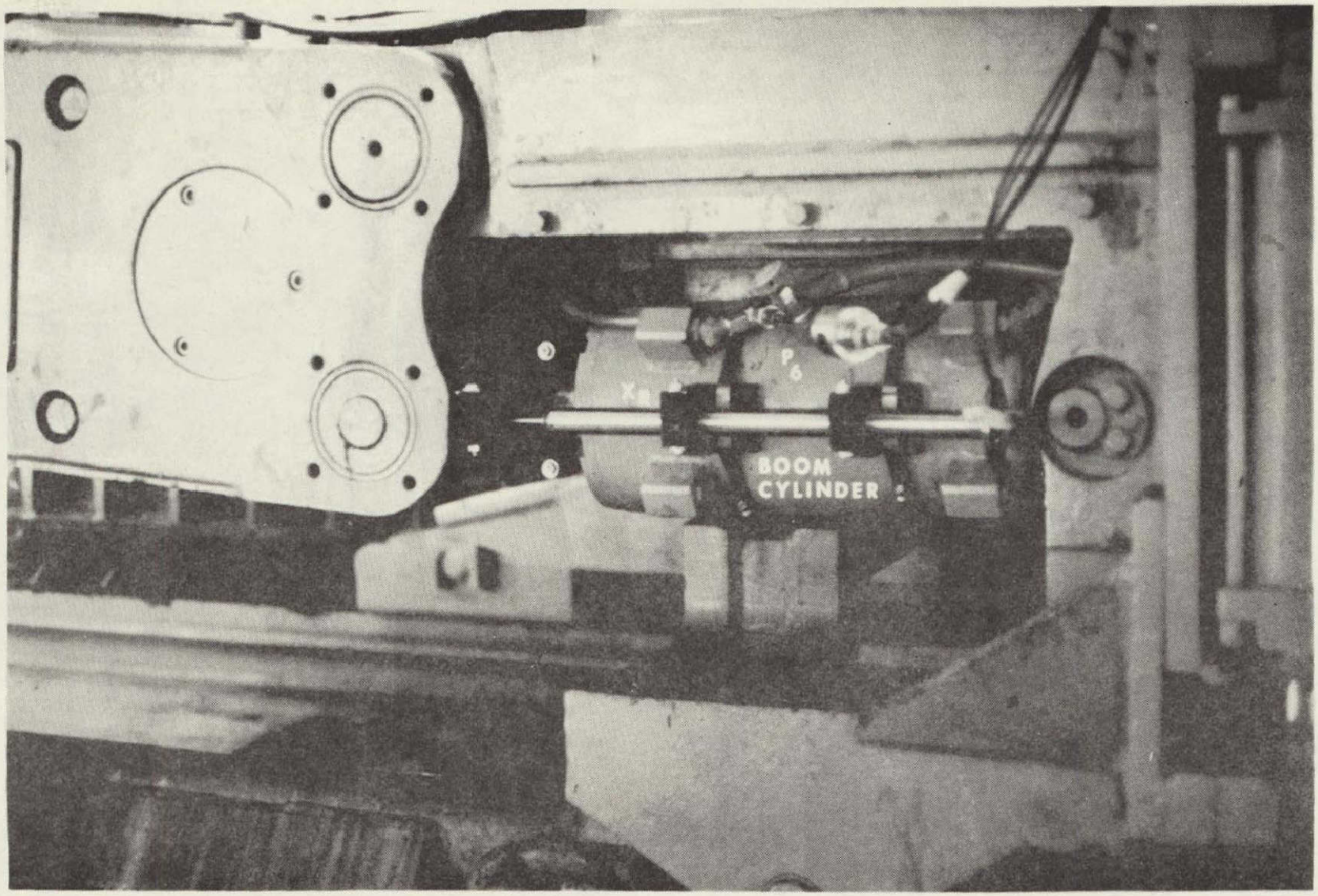

Figure 5. Right boom cylinder and sensors.

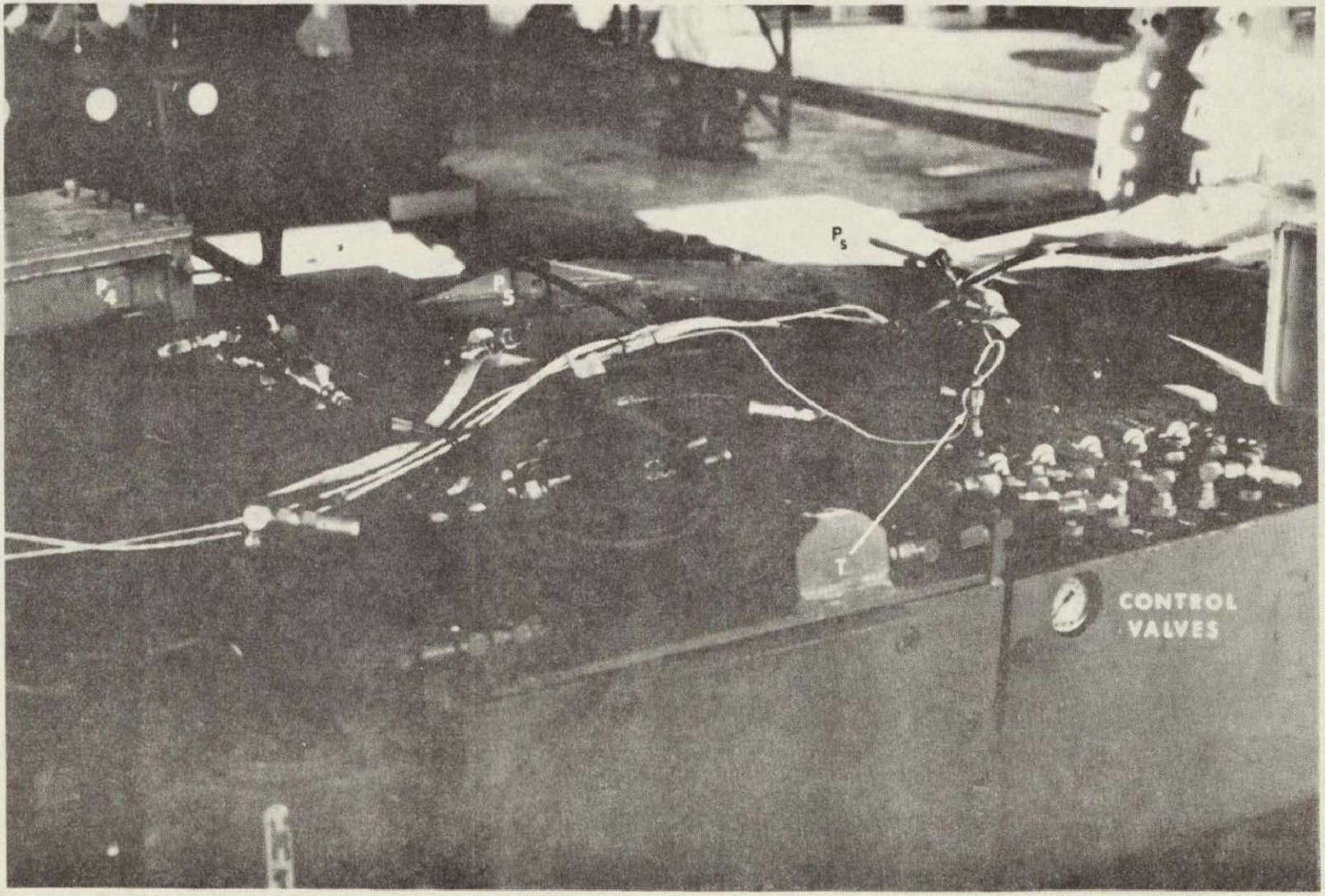

Figure 6. Temperature probe and pressure sensors.

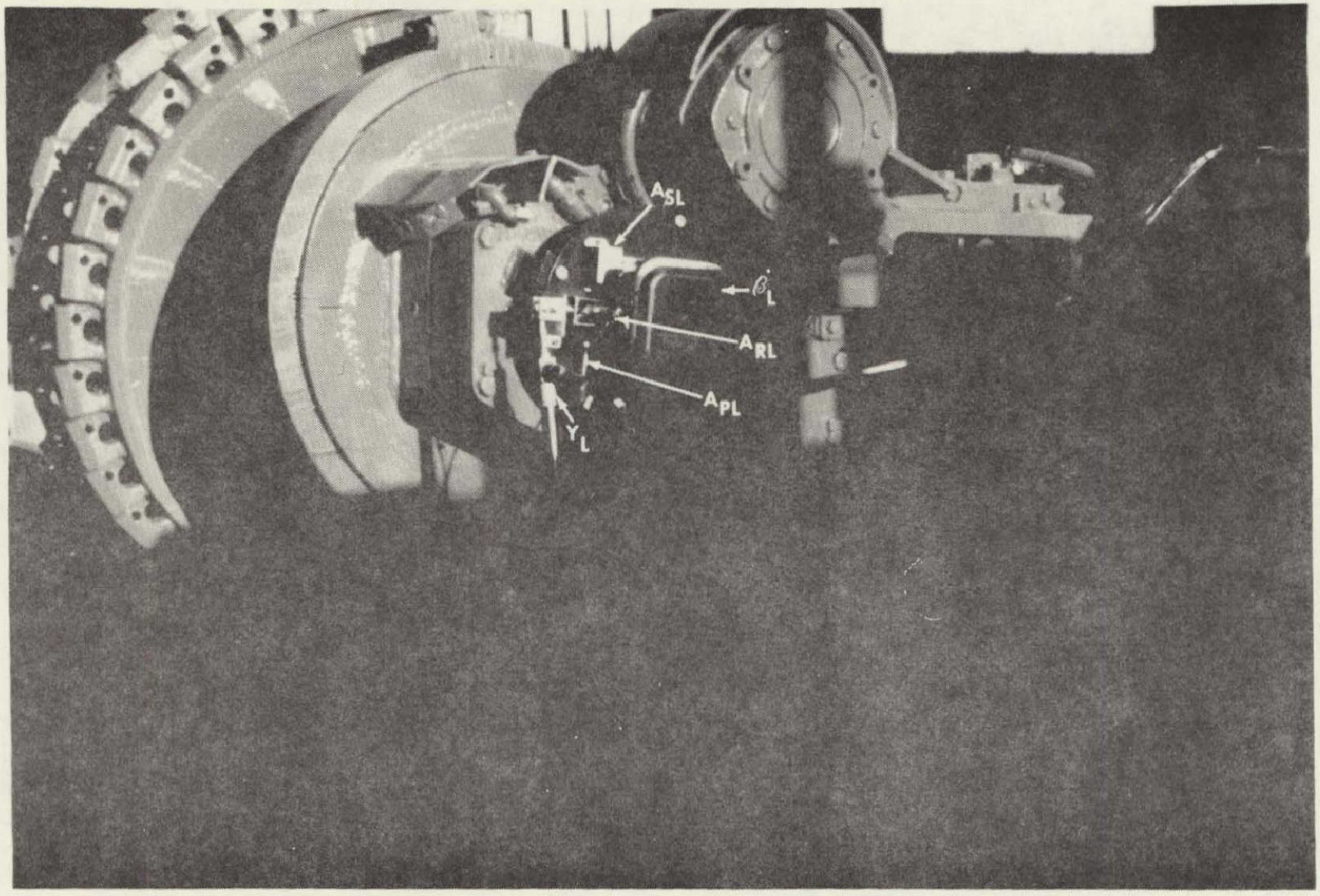

Figure 7. Left boom acceleration, velocity, and position sensors.

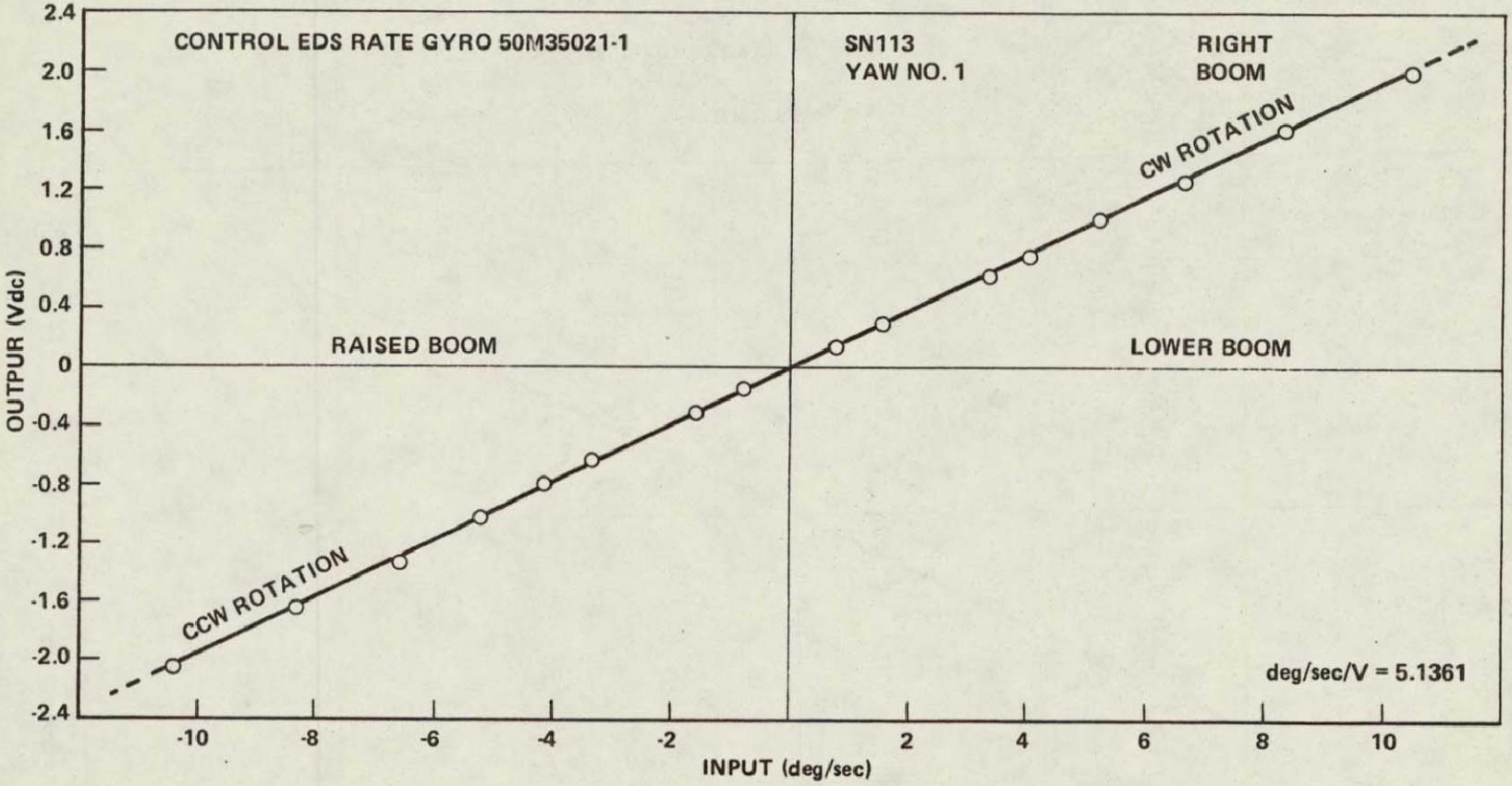

Figure 8. Calibration curve for the rate gyro for $\dot{\beta}_R$.

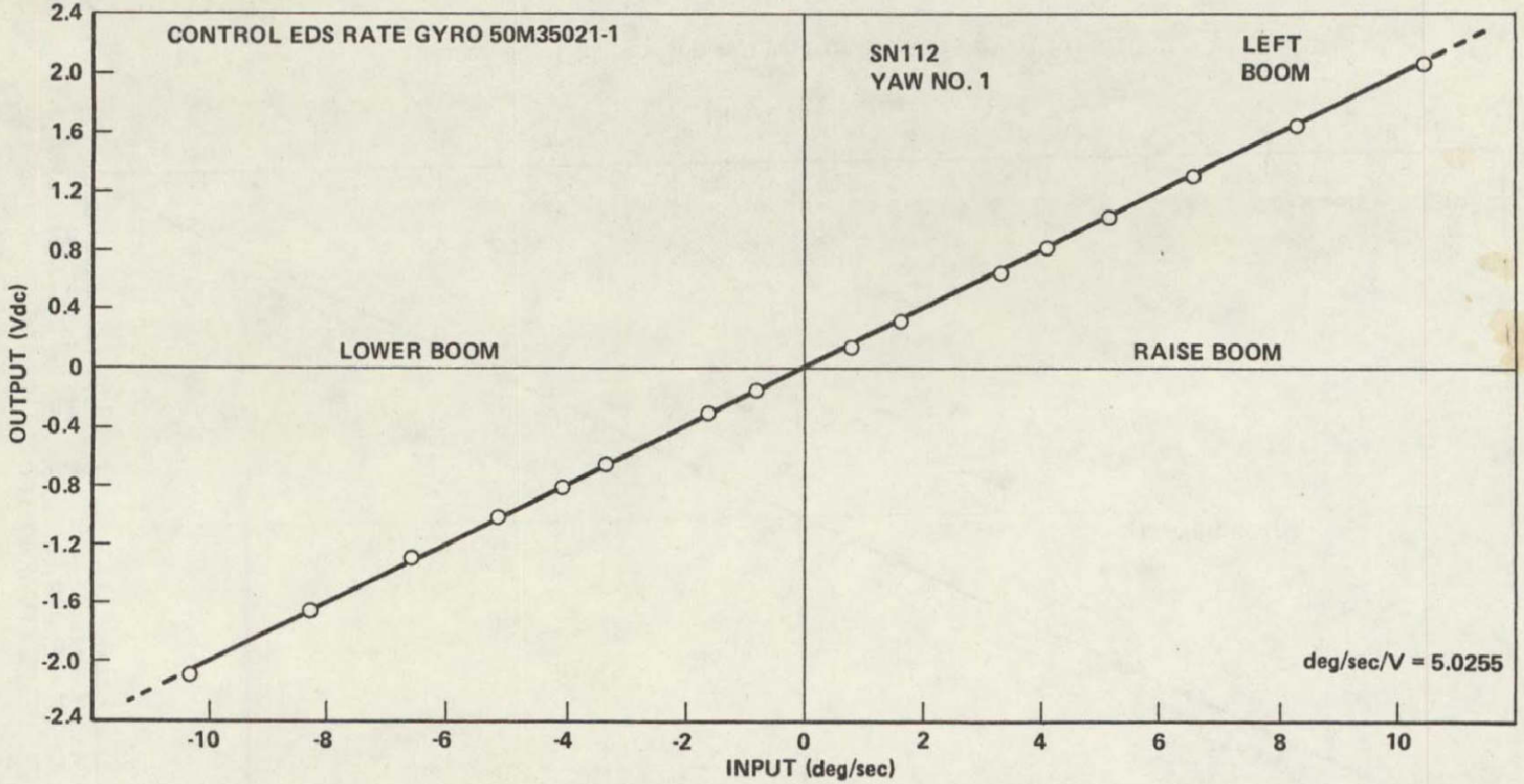

Figure 9. Calibration curve for the rate gyro for $\dot{\beta}_L$.

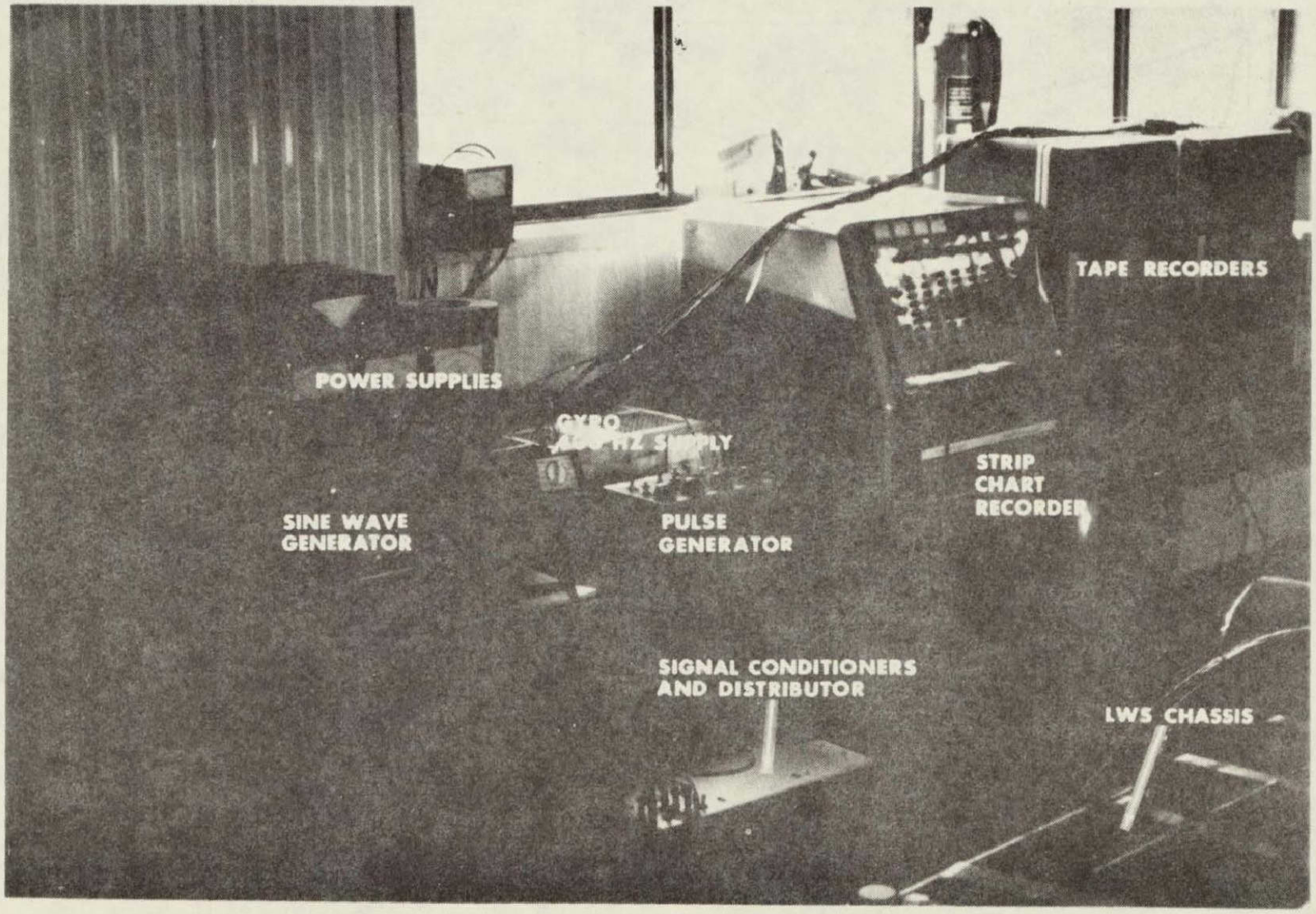

Figure 10. Test and recording equipment.

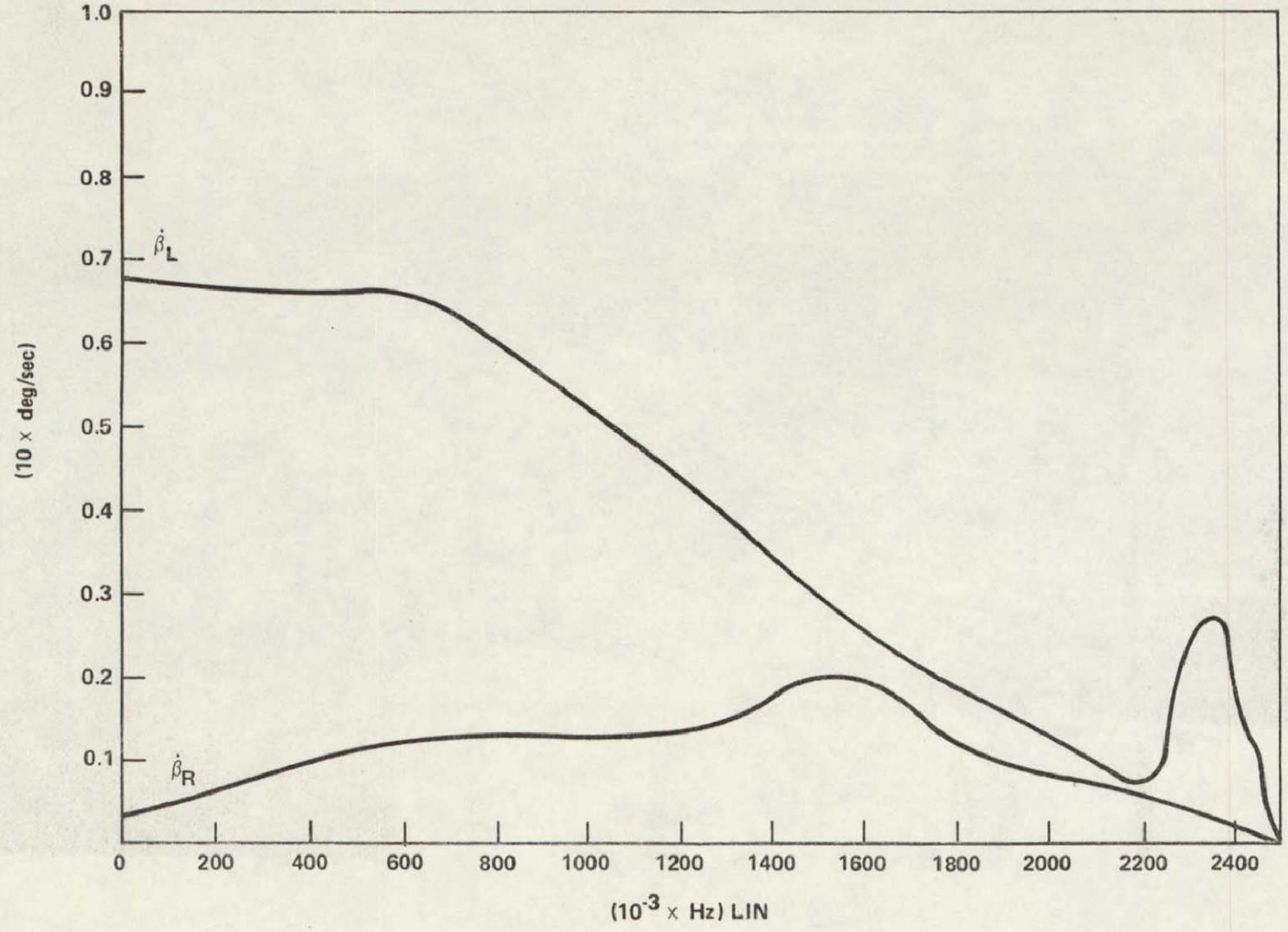

Figure 11. Longwall shearer frequency response for a C_L input.

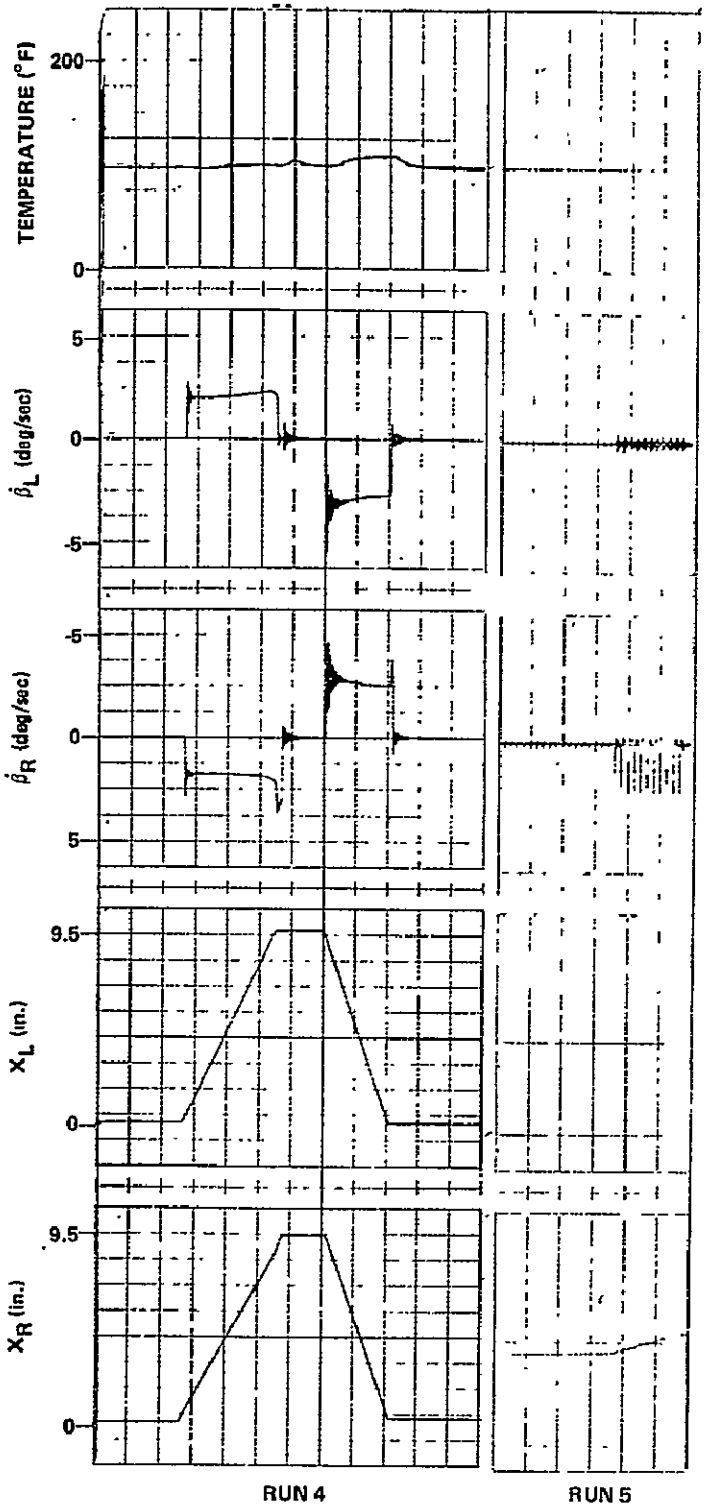

Figure 12. (Continued).

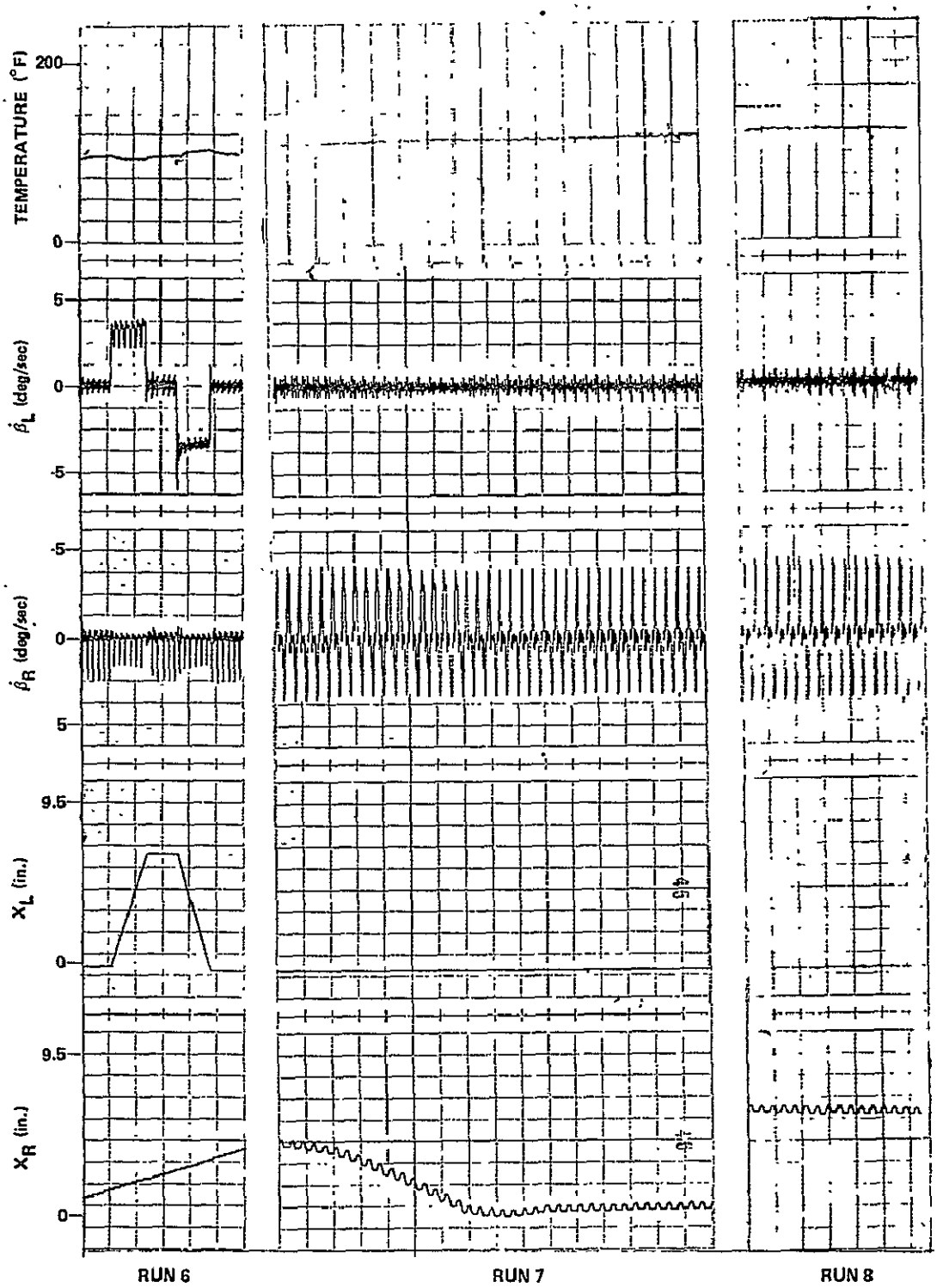

Figure 12. (Continued).

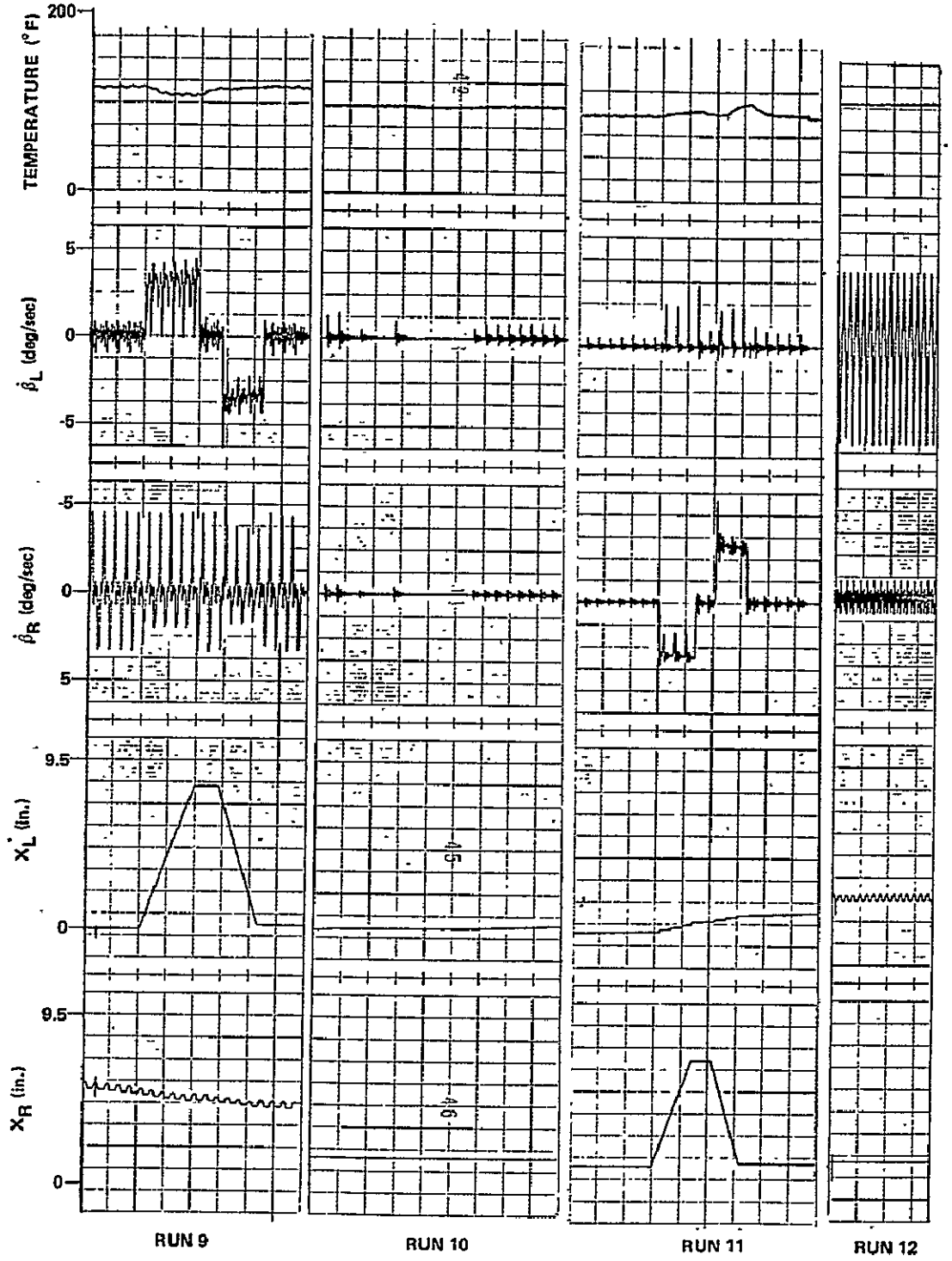

Figure 12. (Continued).

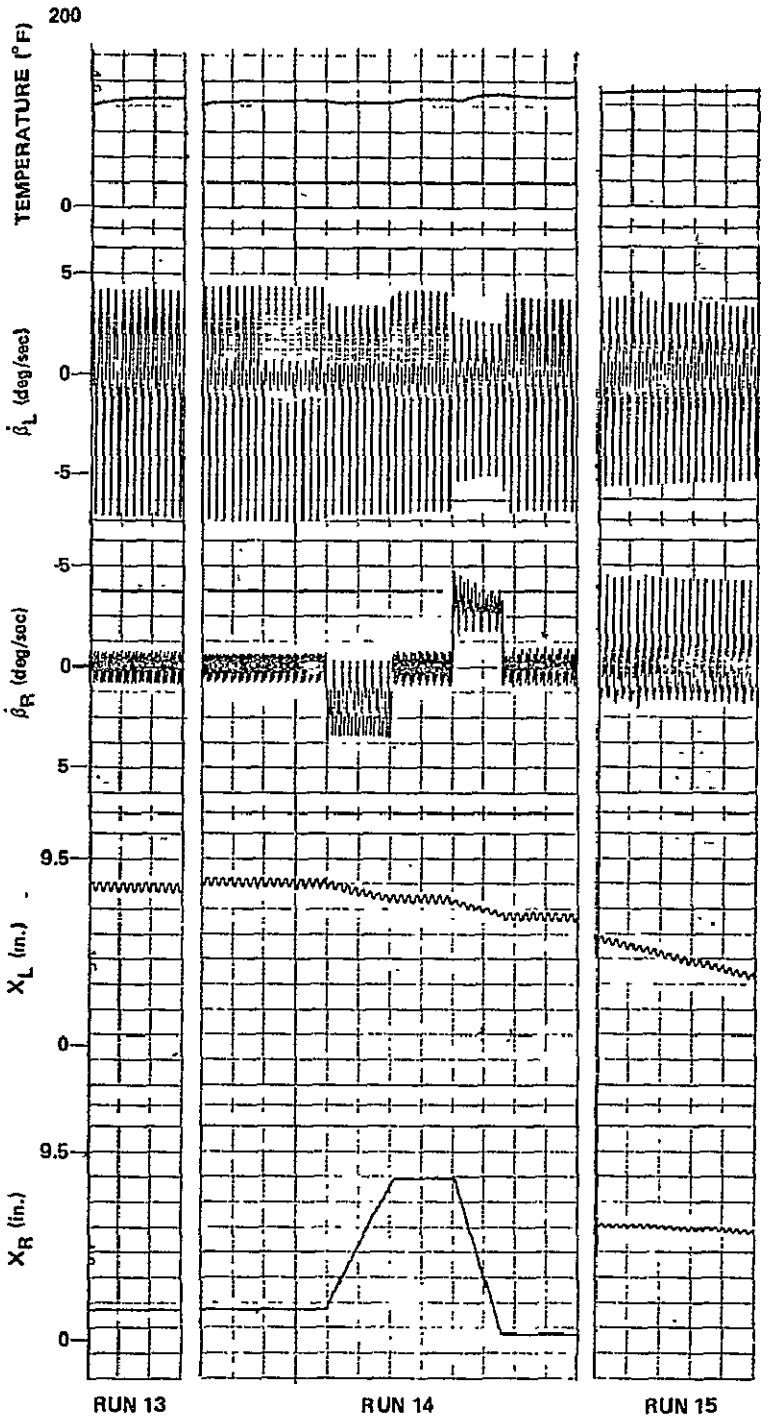

Figure 12. (Continued).

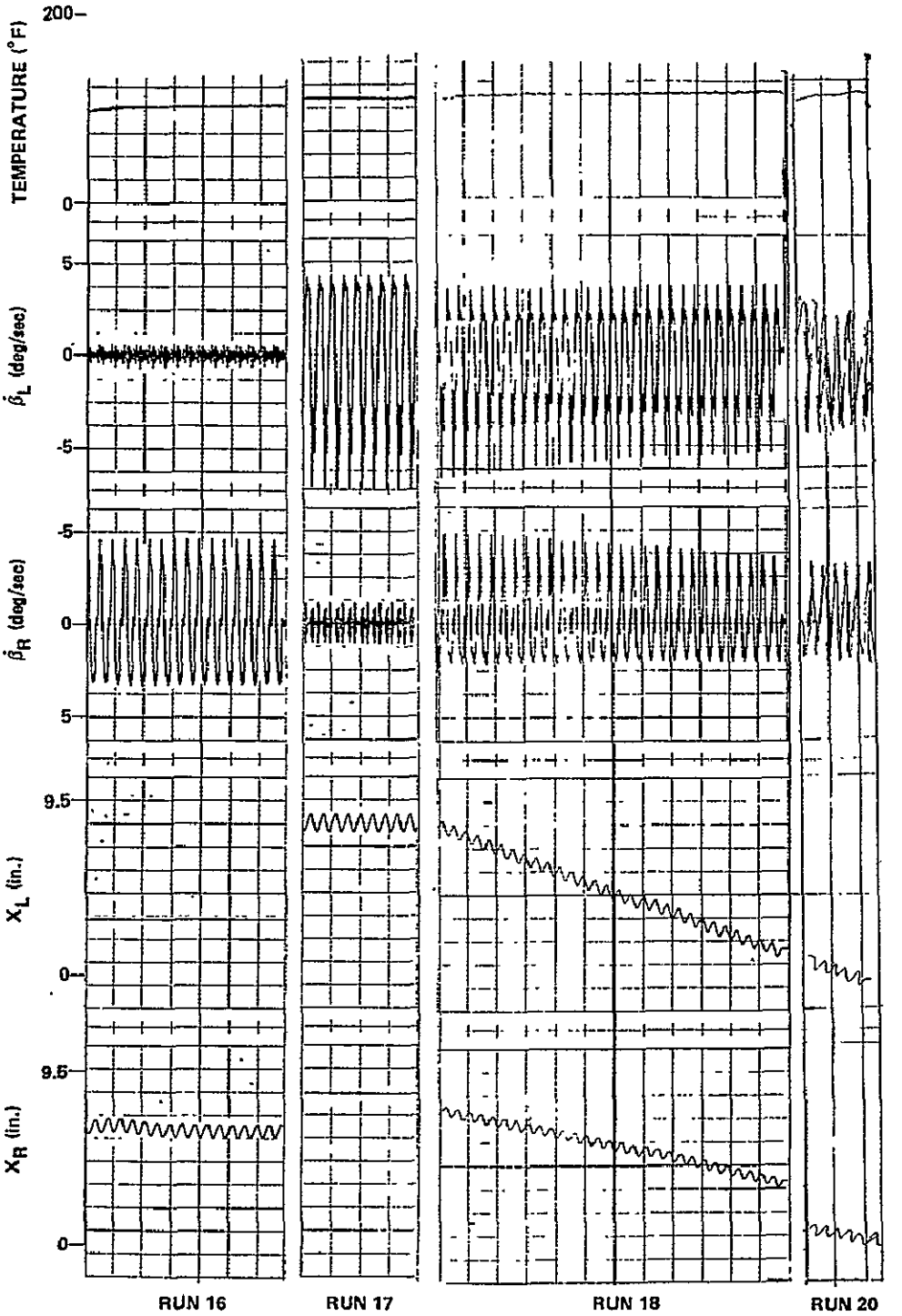

Figure 12. (Concluded).

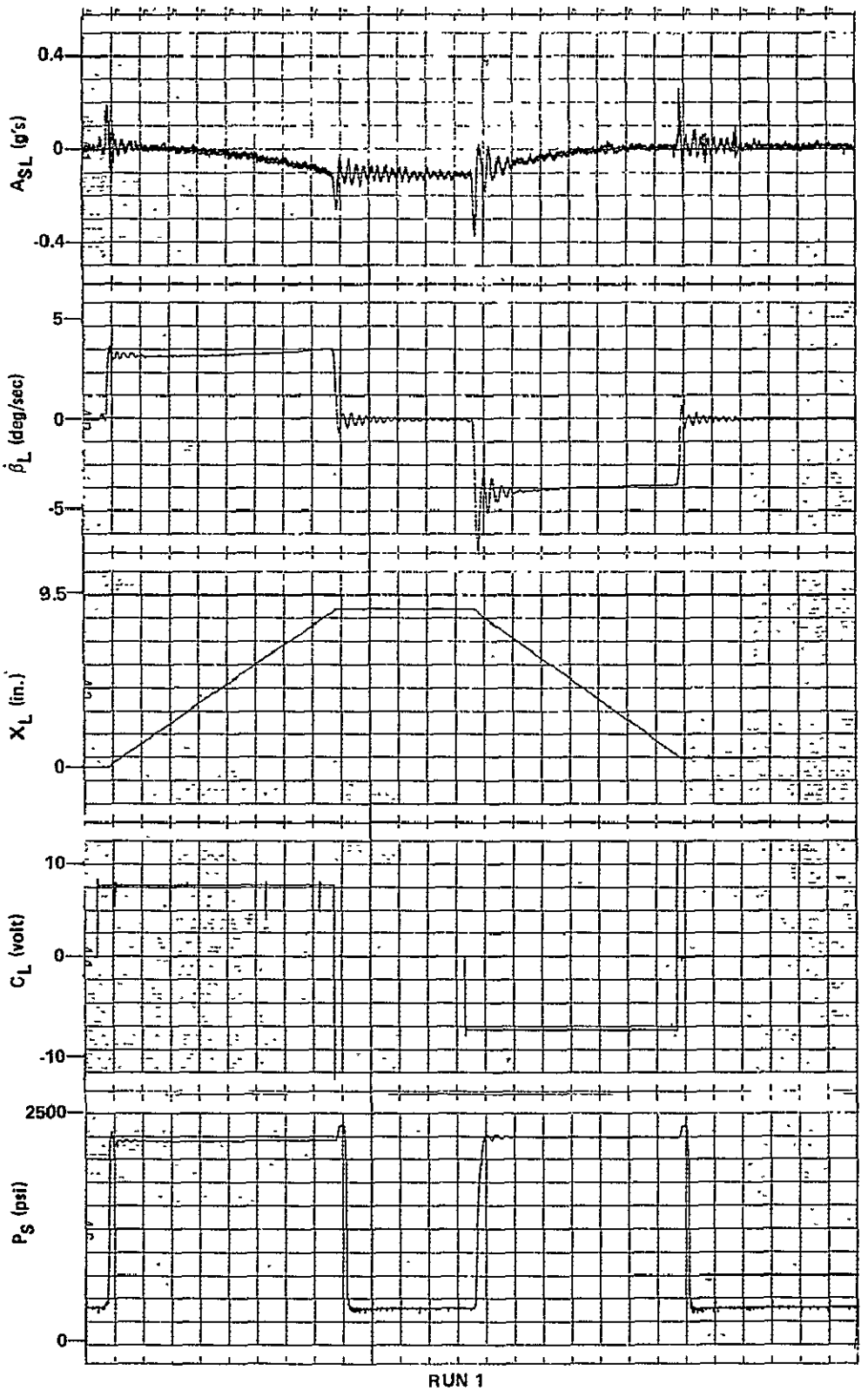

Figure 13. Dynamic response of the left boom for Run 1.

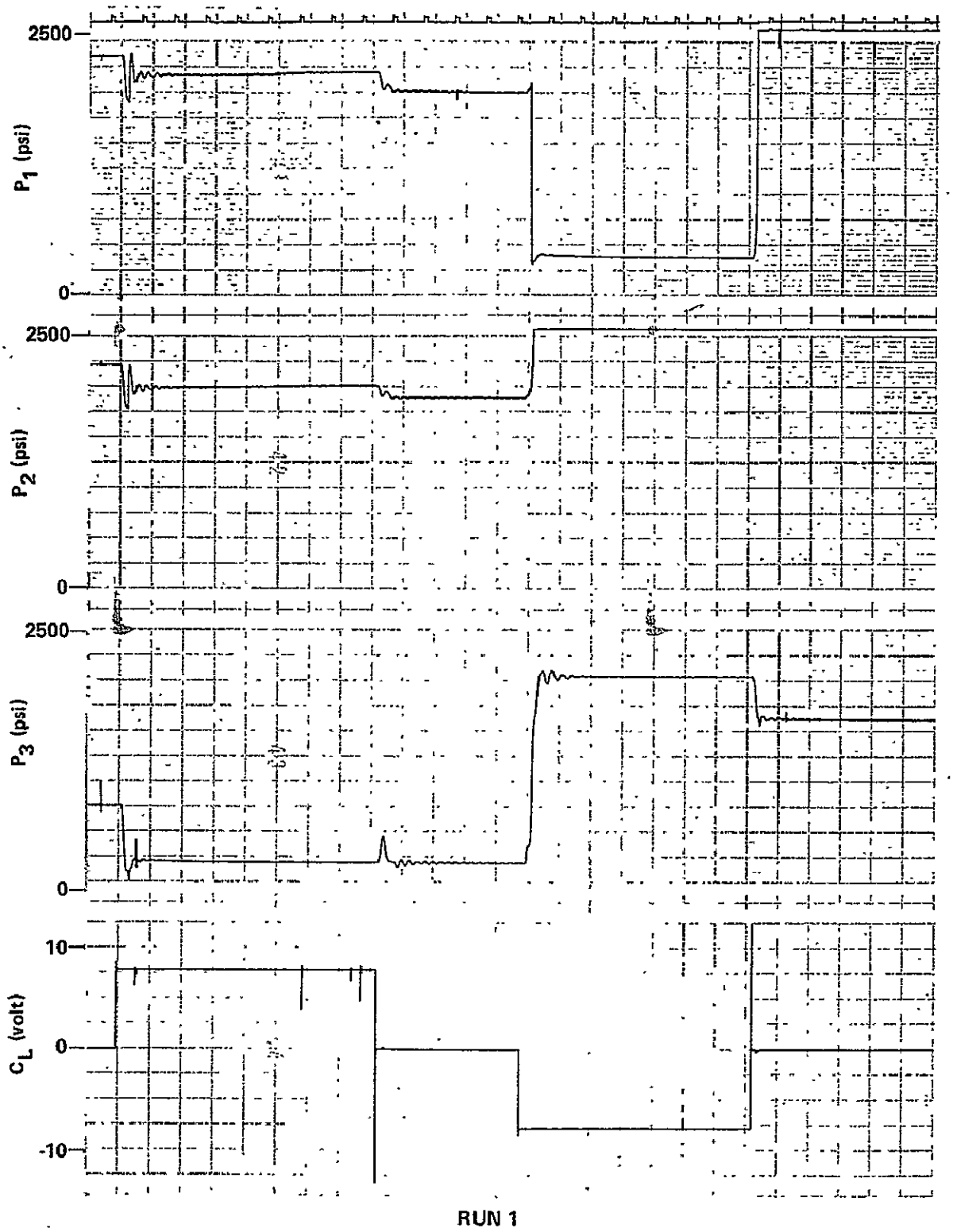

Figure 14. Pressure response of the left boom for Run 1.

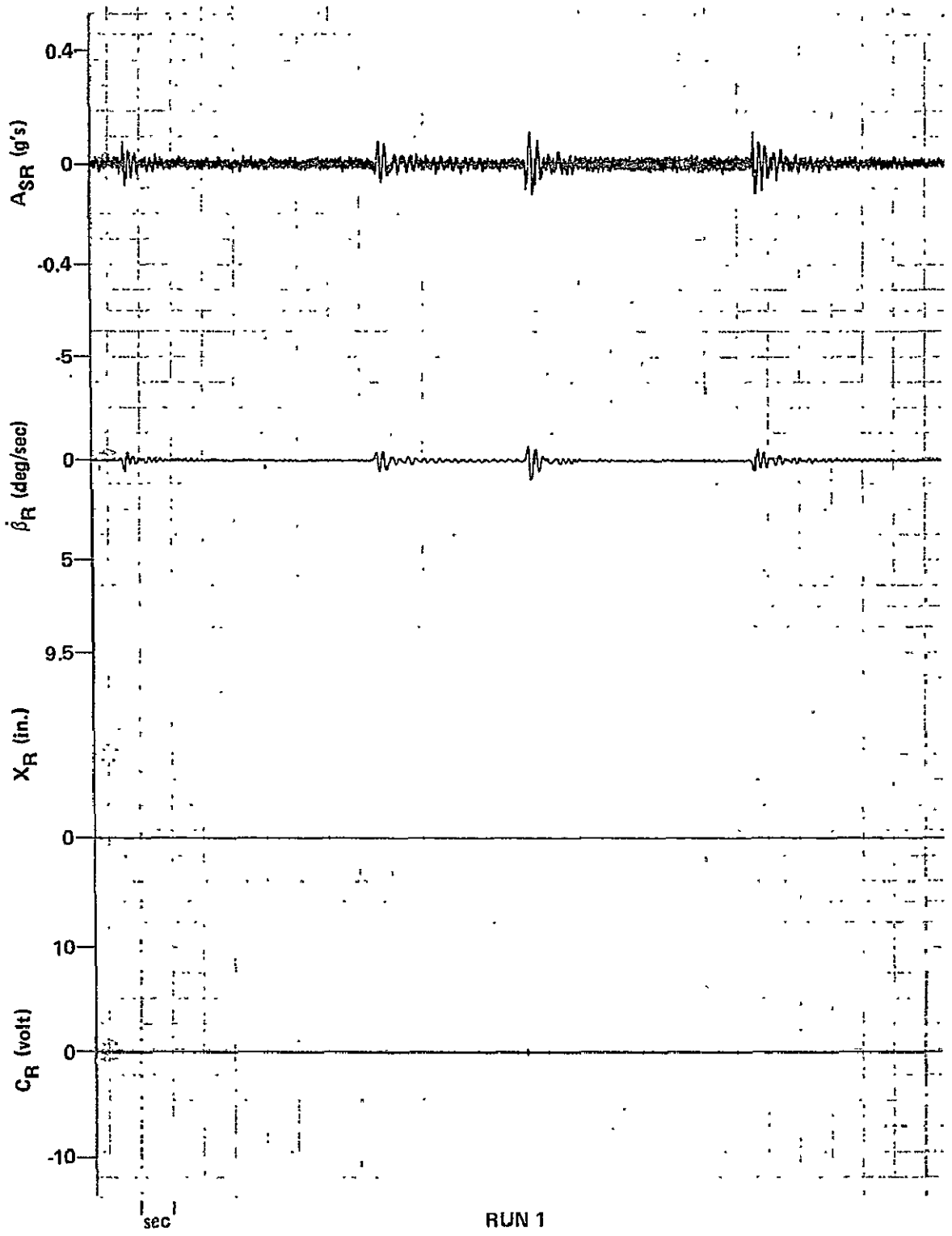

Figure 15. Dynamic response of the right boom for Run 1.

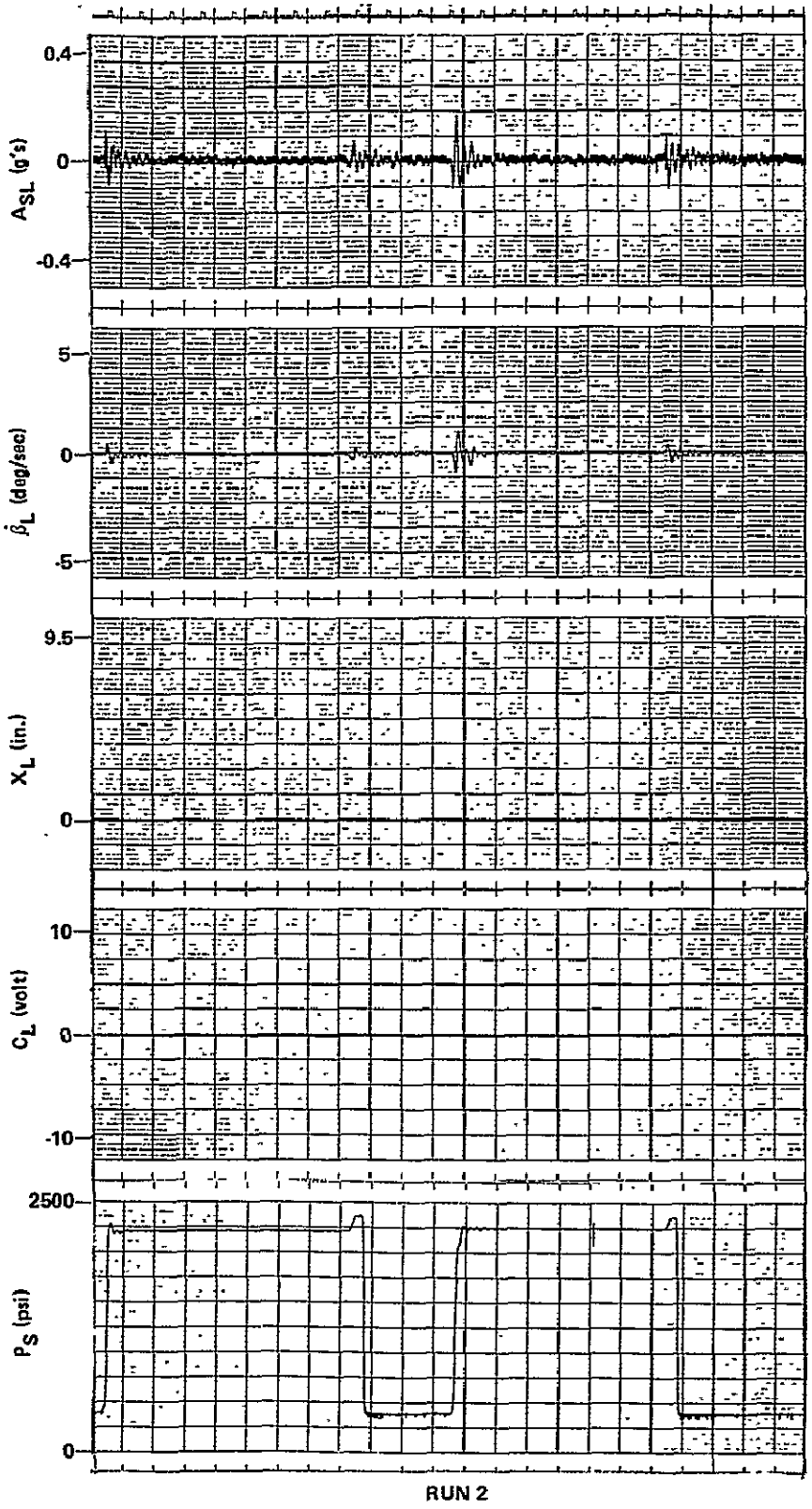

Figure 16. Dynamic response of the left boom for Run 2.

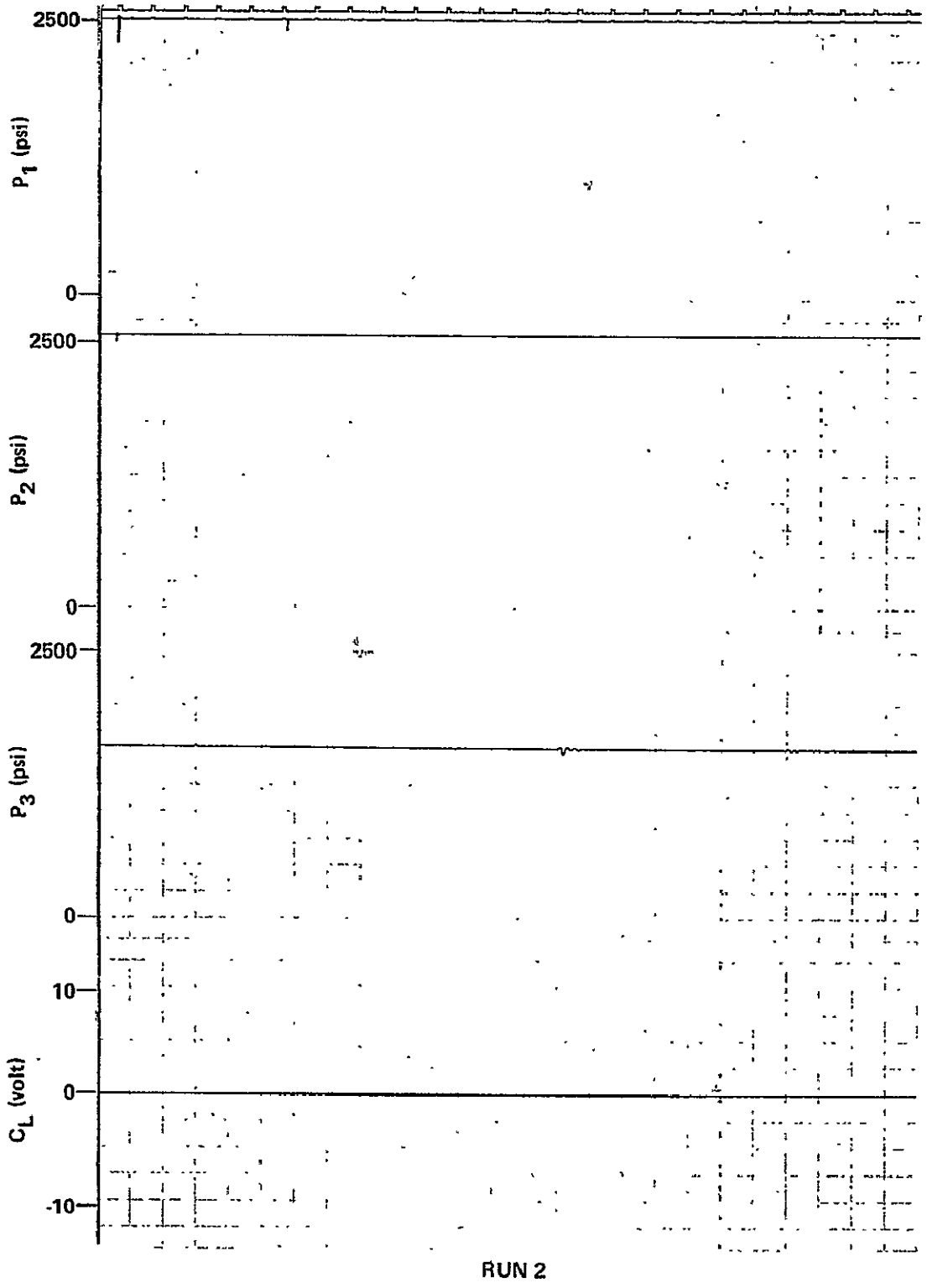

Figure 17. Pressure response of the left boom for Run 2.

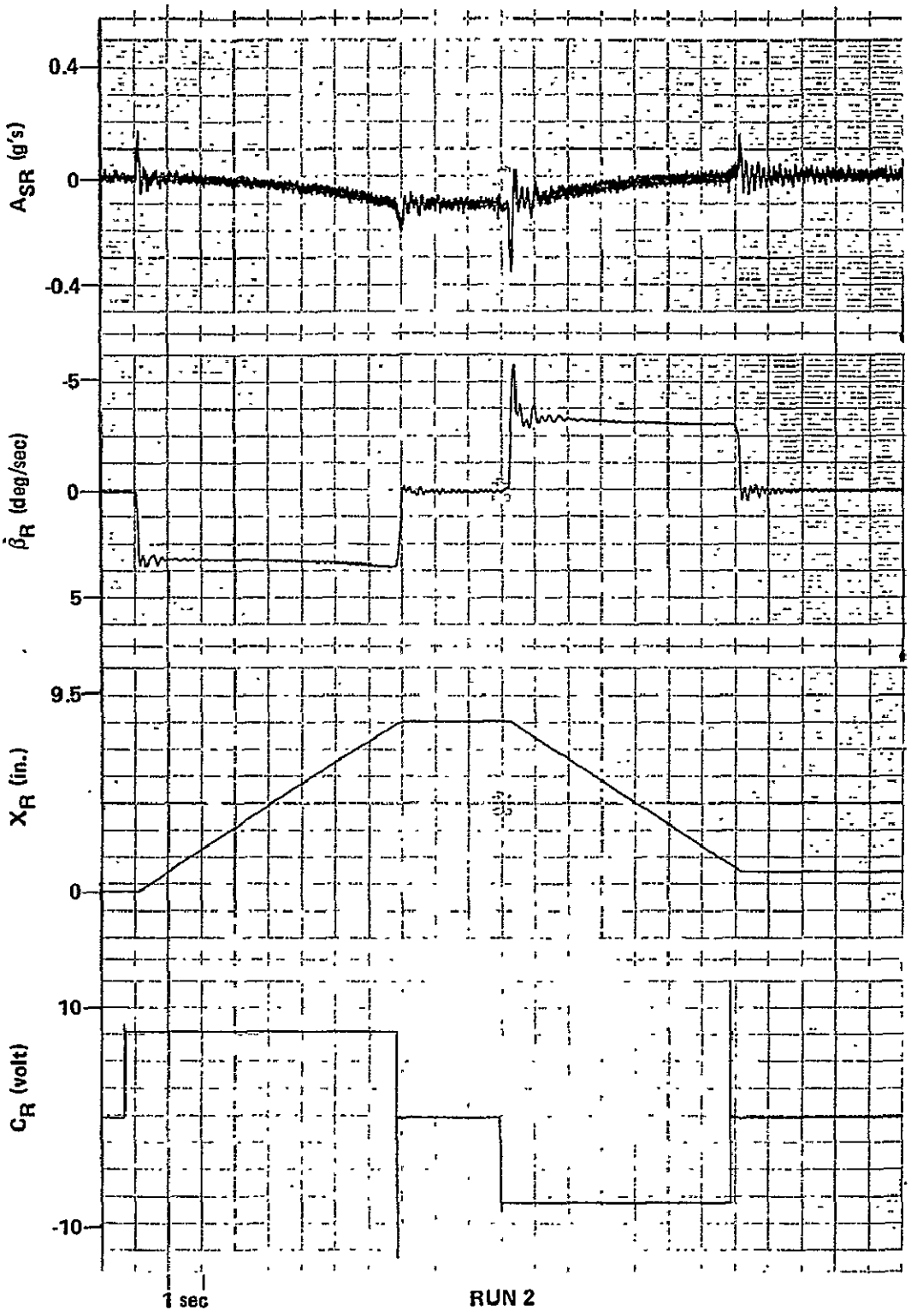

Figure 18. Dynamic response of the right boom for Run 2.

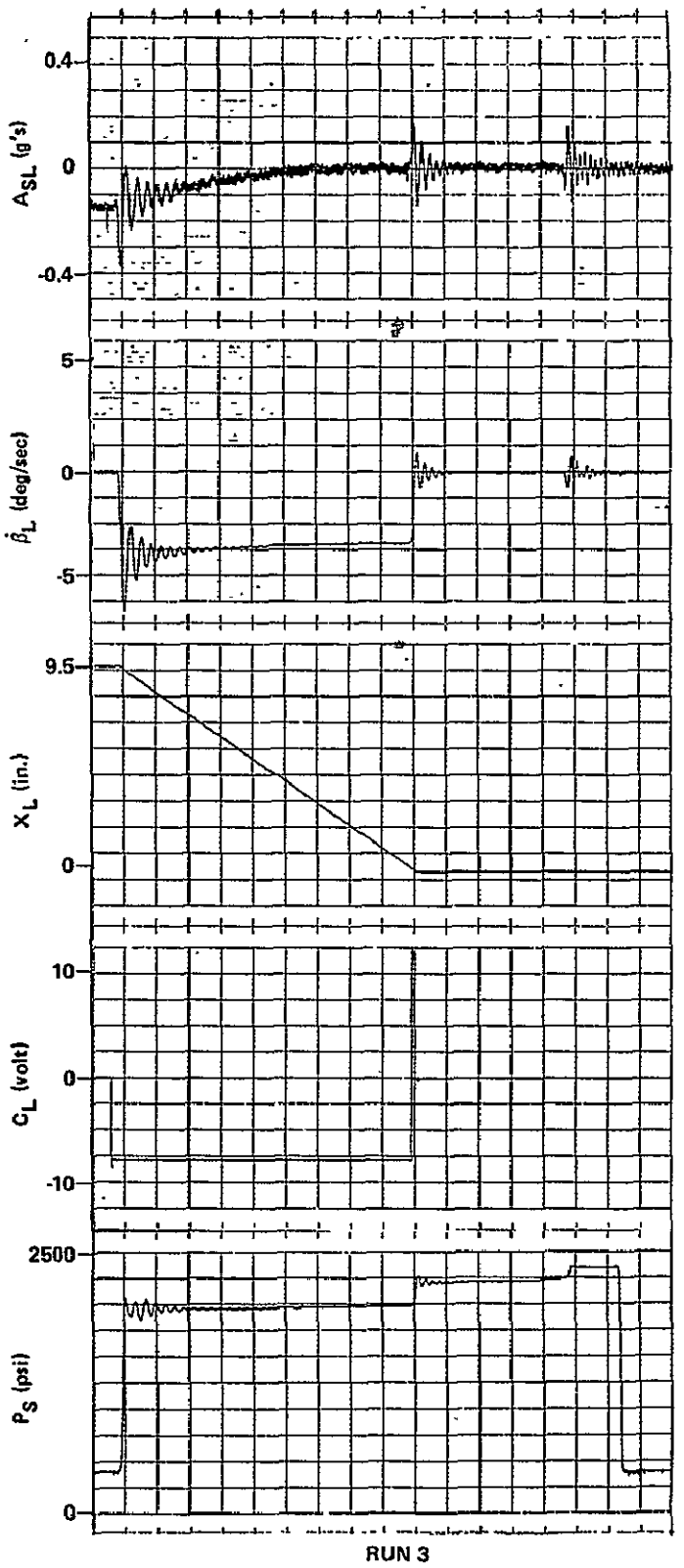

Figure 19. Dynamic response of the left boom for Run 3.

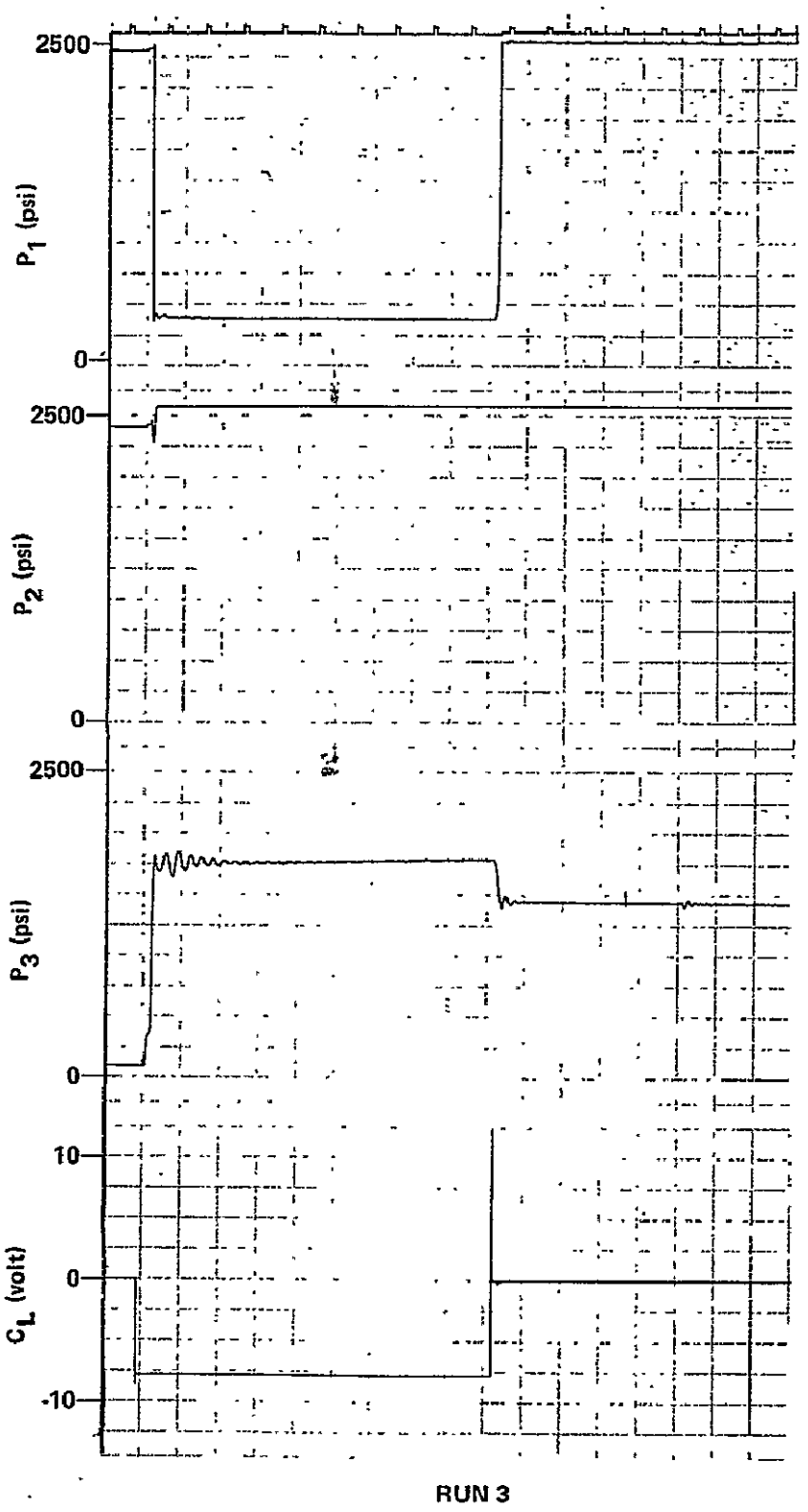

Figure 20. Pressure response of the left boom for Run 3.

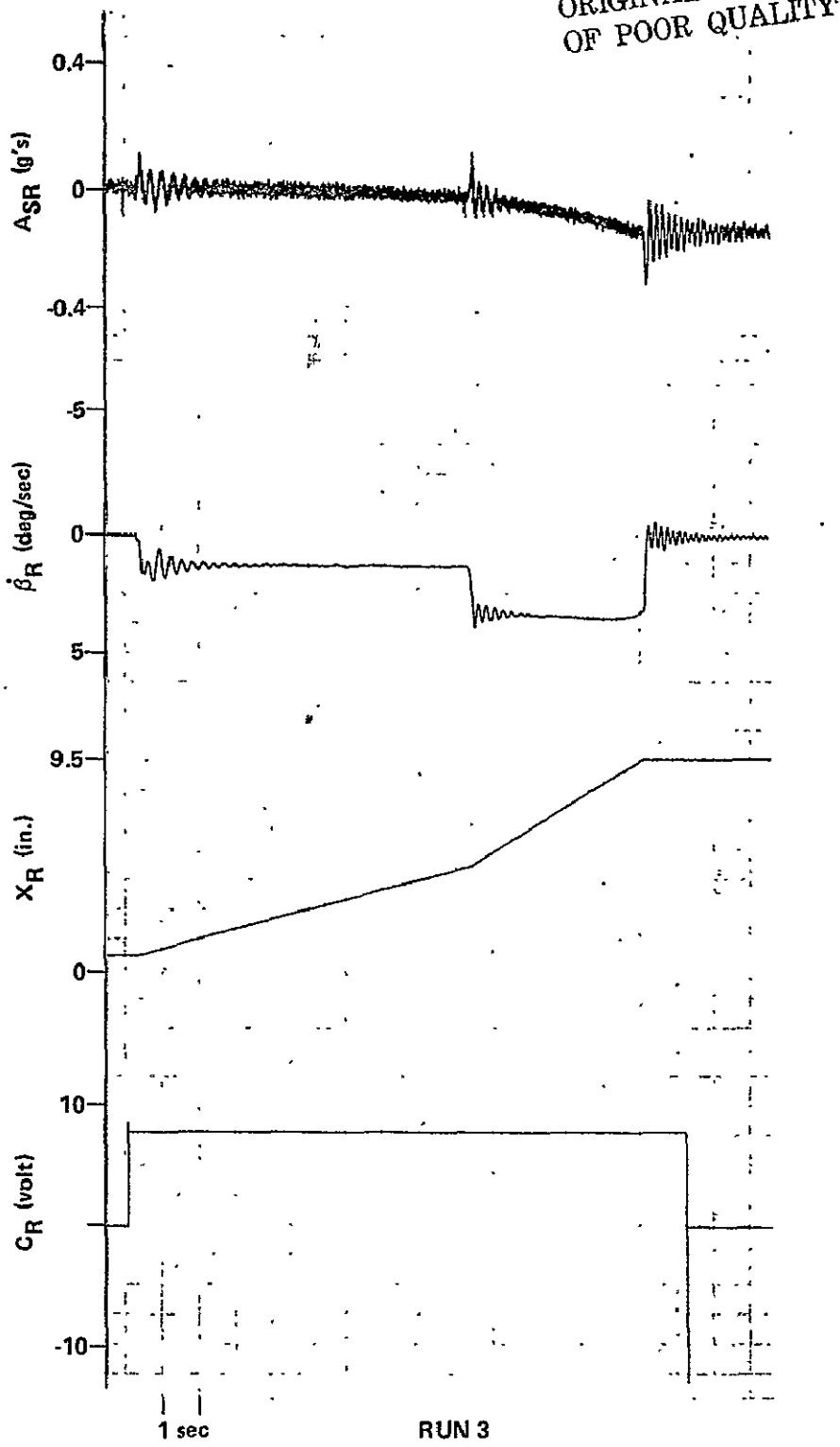

Figure 21. Dynamic response of the right boom for Run 3.

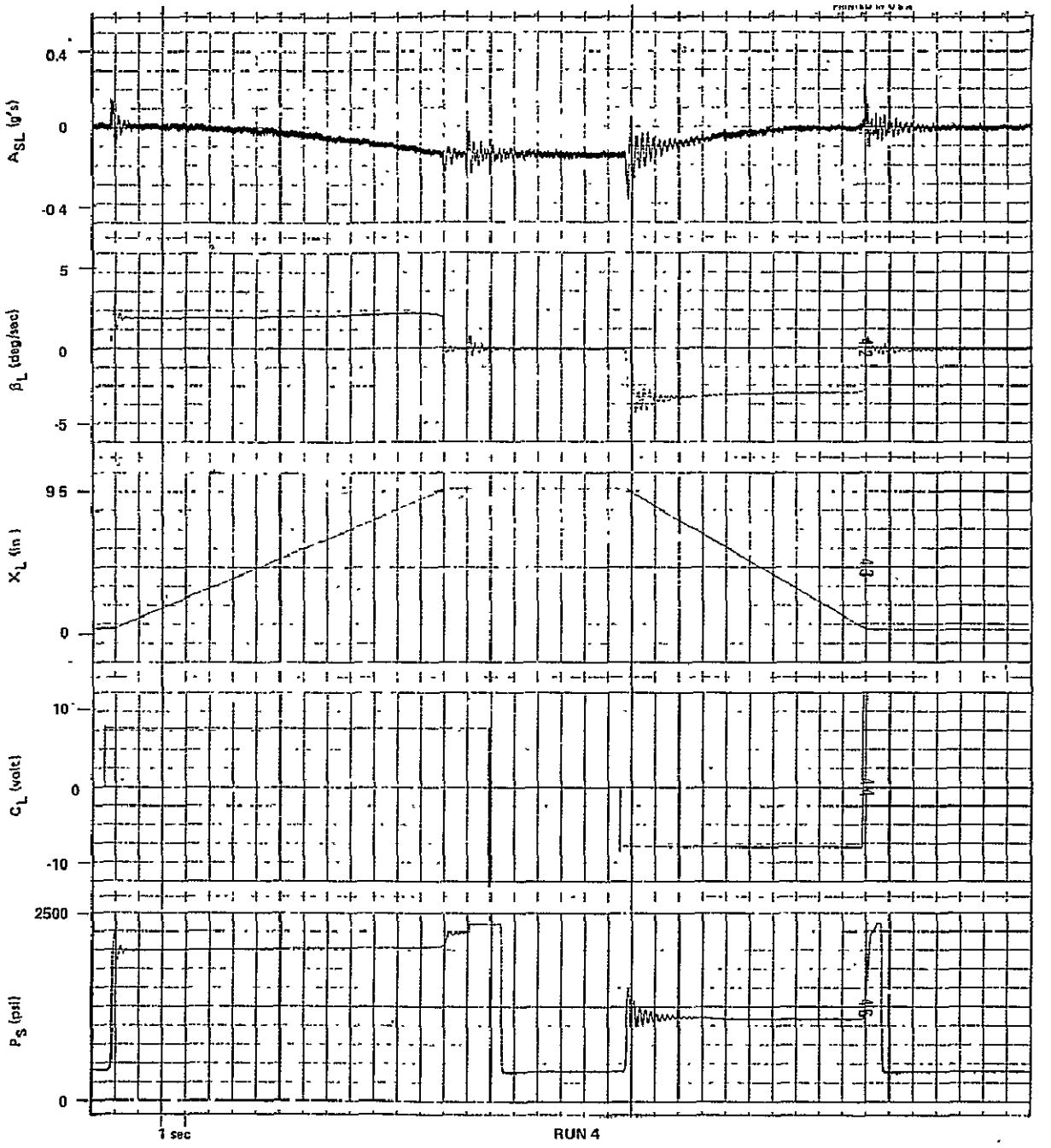

Figure 22. Dynamic response of the left boom for Run 4.

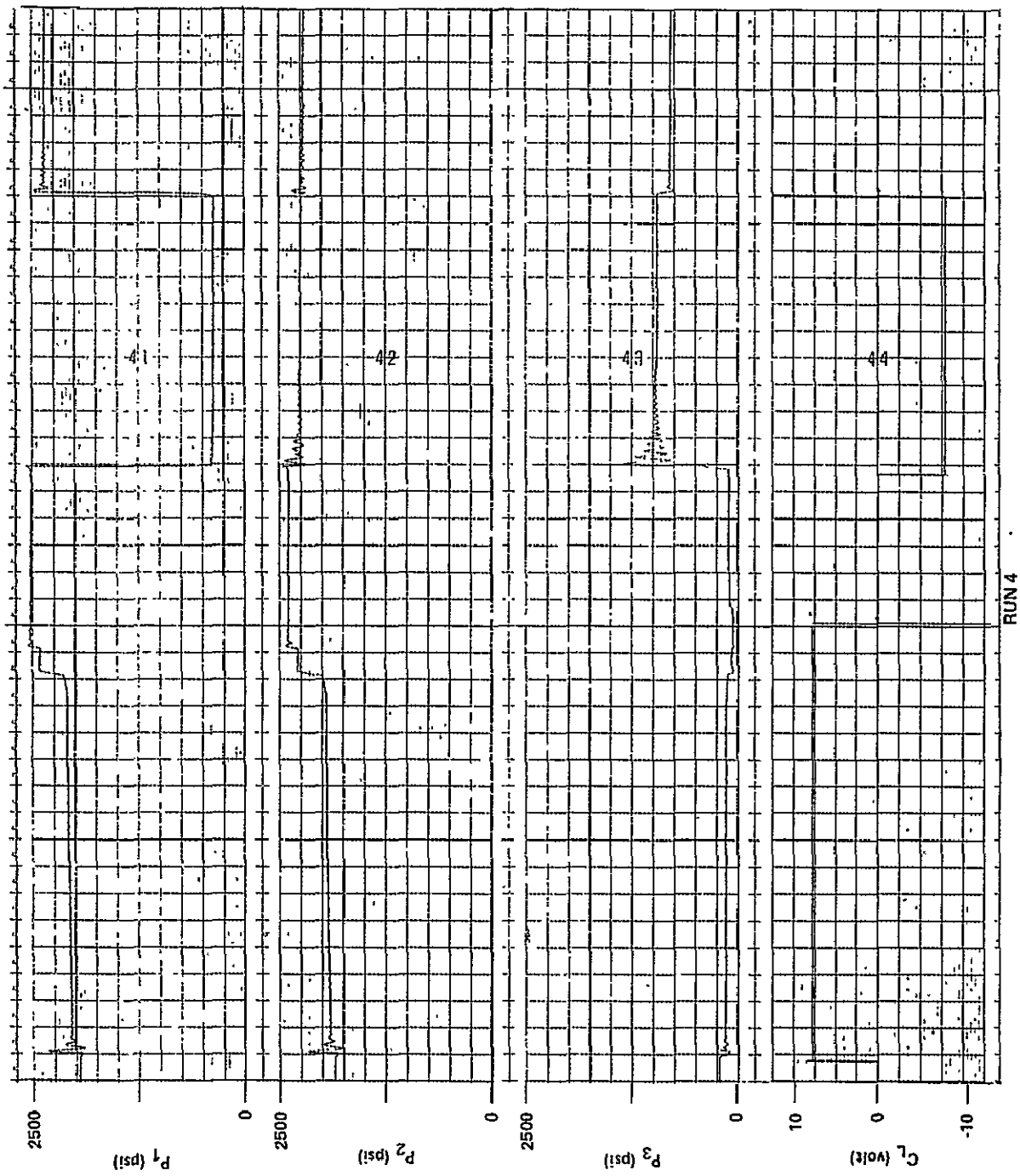

Figure 23. Pressure response of left boom for Run 4.

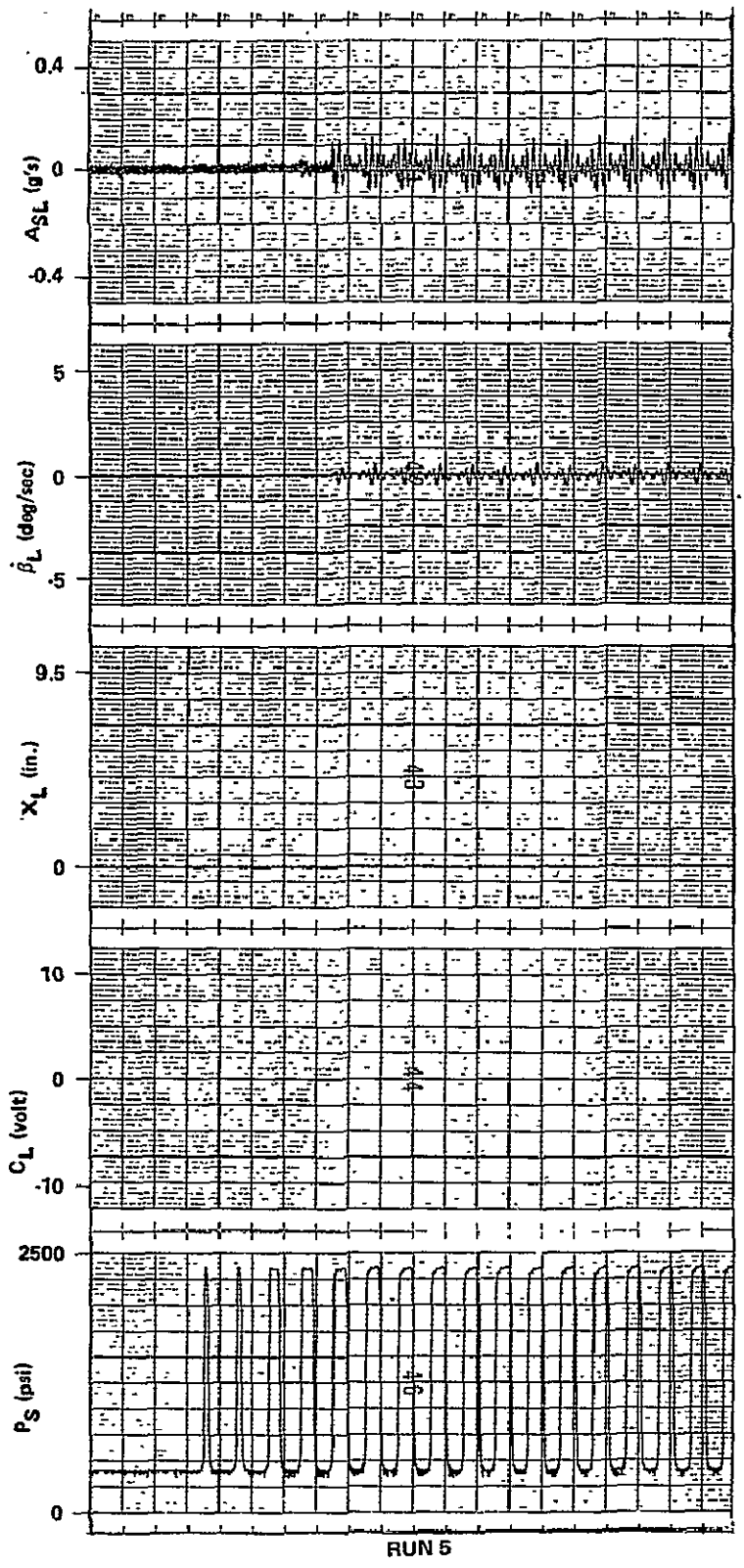

Figure 24. Dynamic response of the left boom for Run 5.

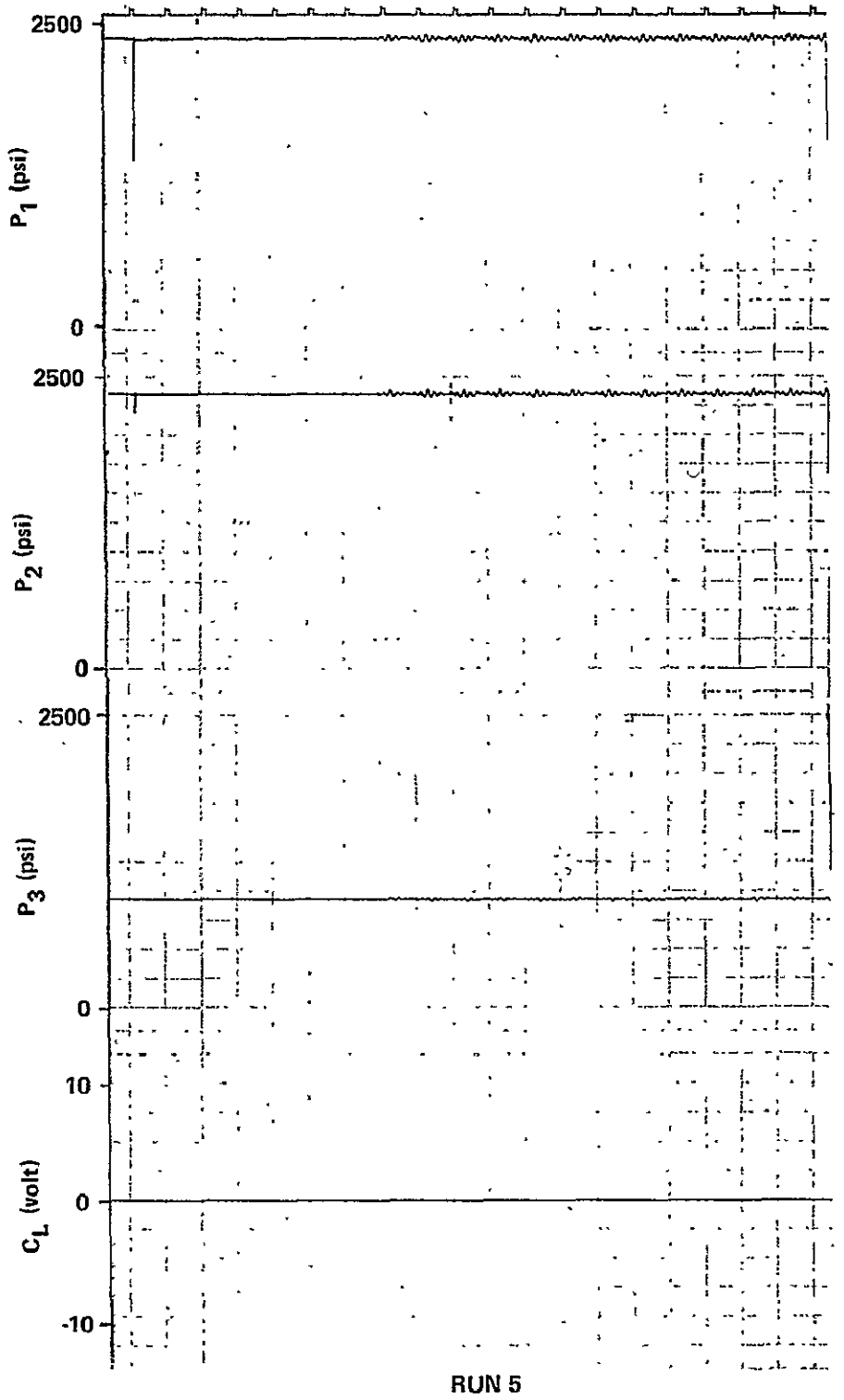

Figure 25. Pressure response of the left boom for Run 5.

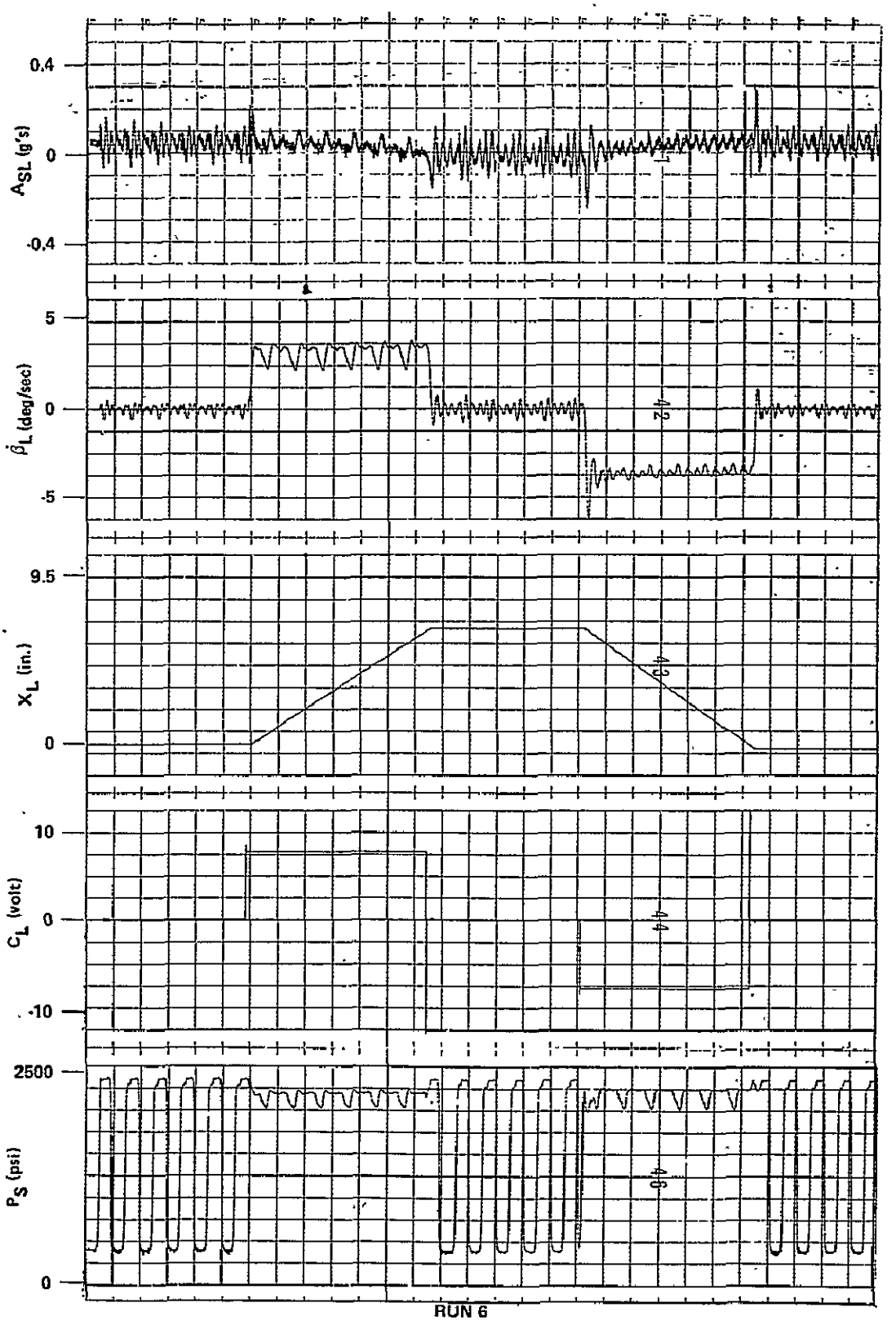

Figure 26. Dynamic response of the left boom for Run 6.

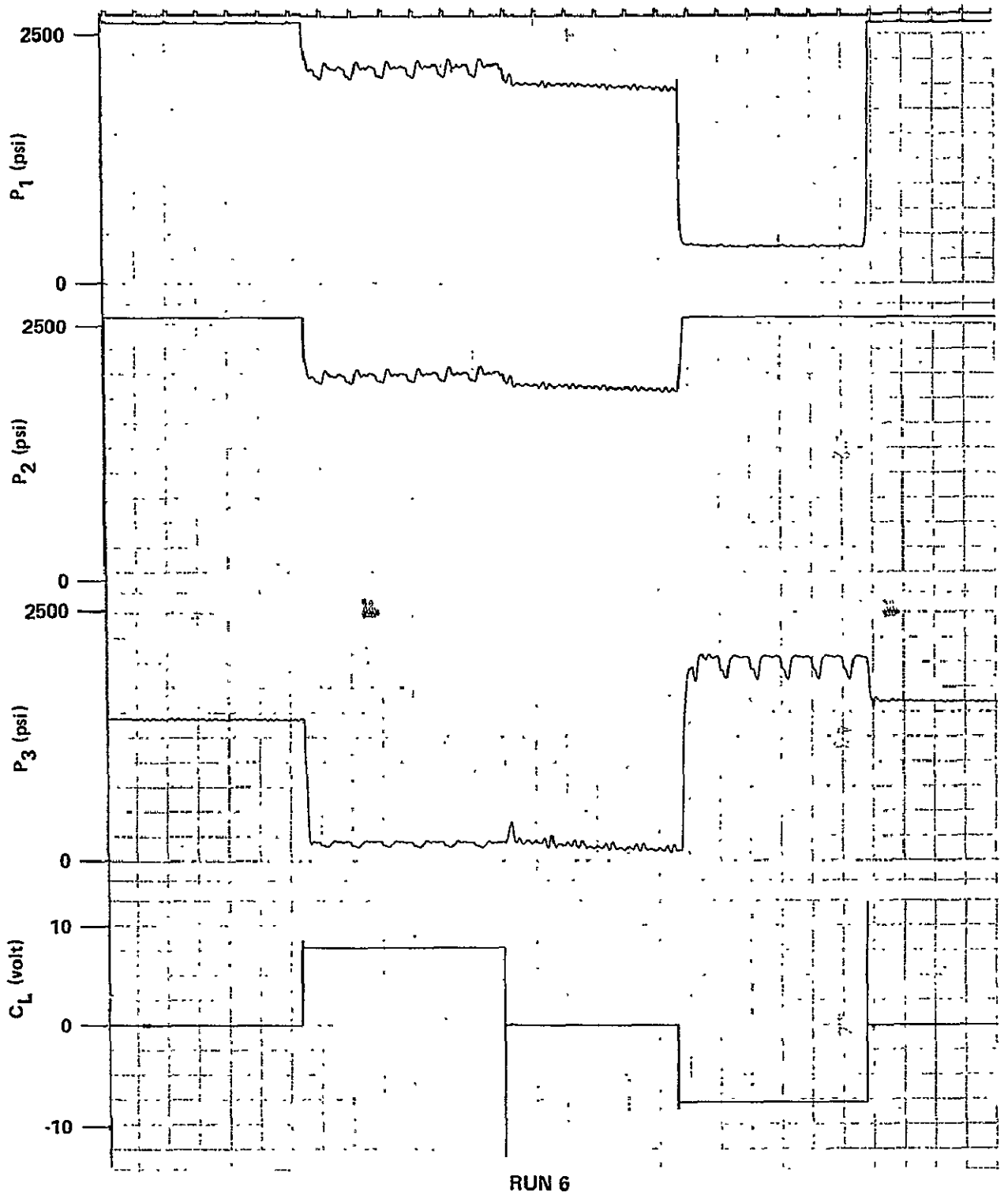

Figure 27. Pressure response of the left boom for Run 6.

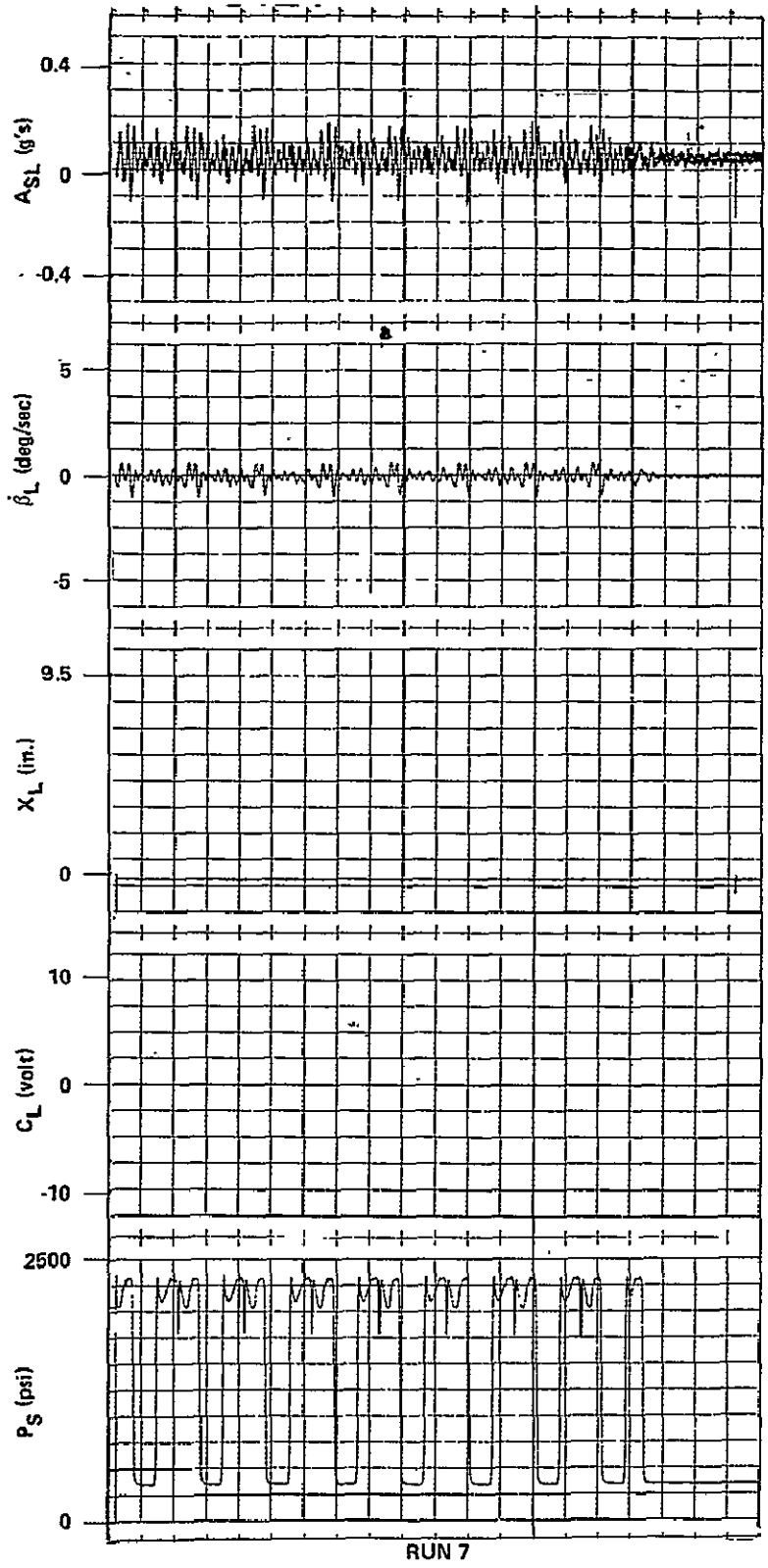

Figure 28. Dynamic response of the left boom for Run 7.

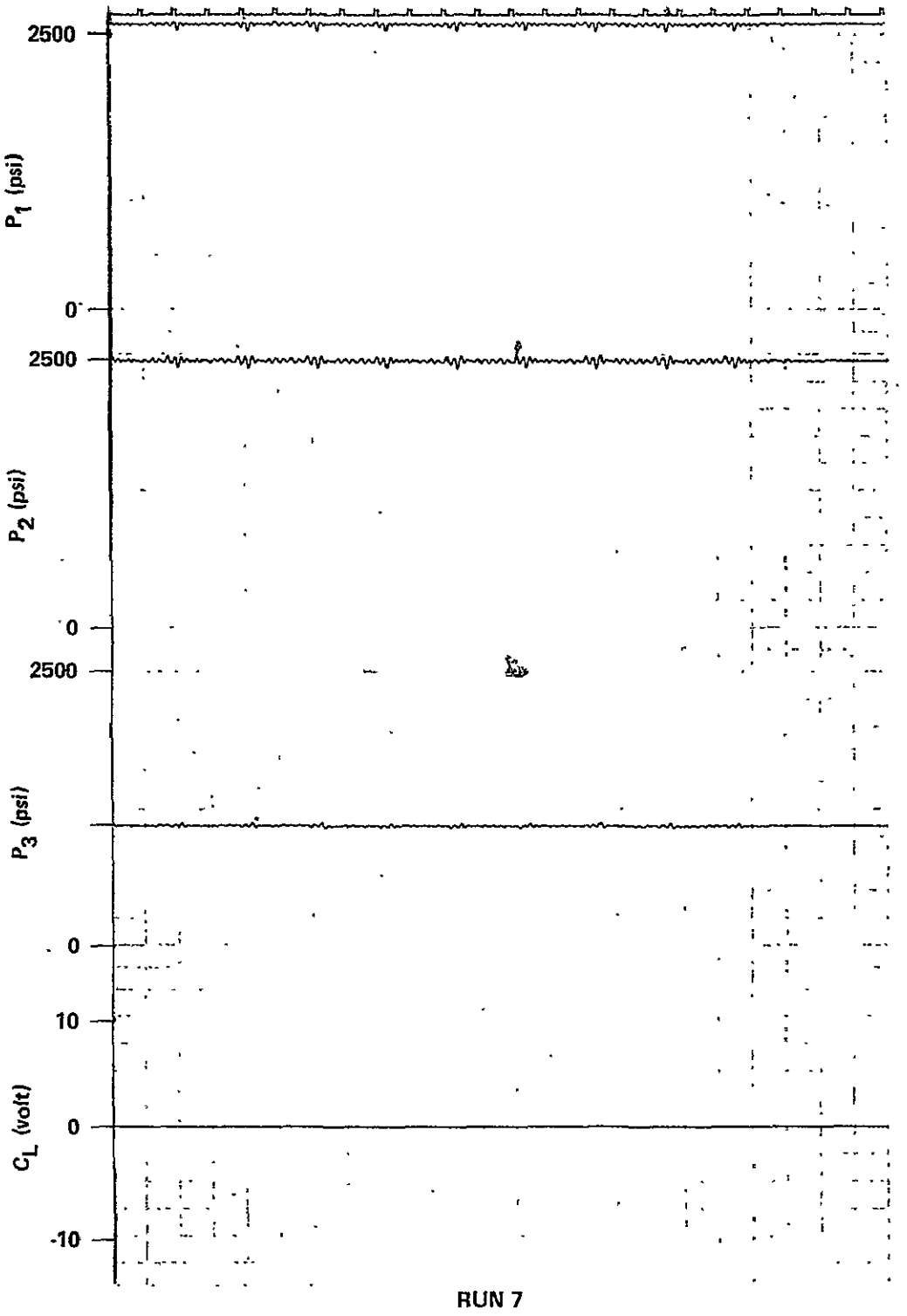

Figure 29. Pressure response of the left boom for Run 7.

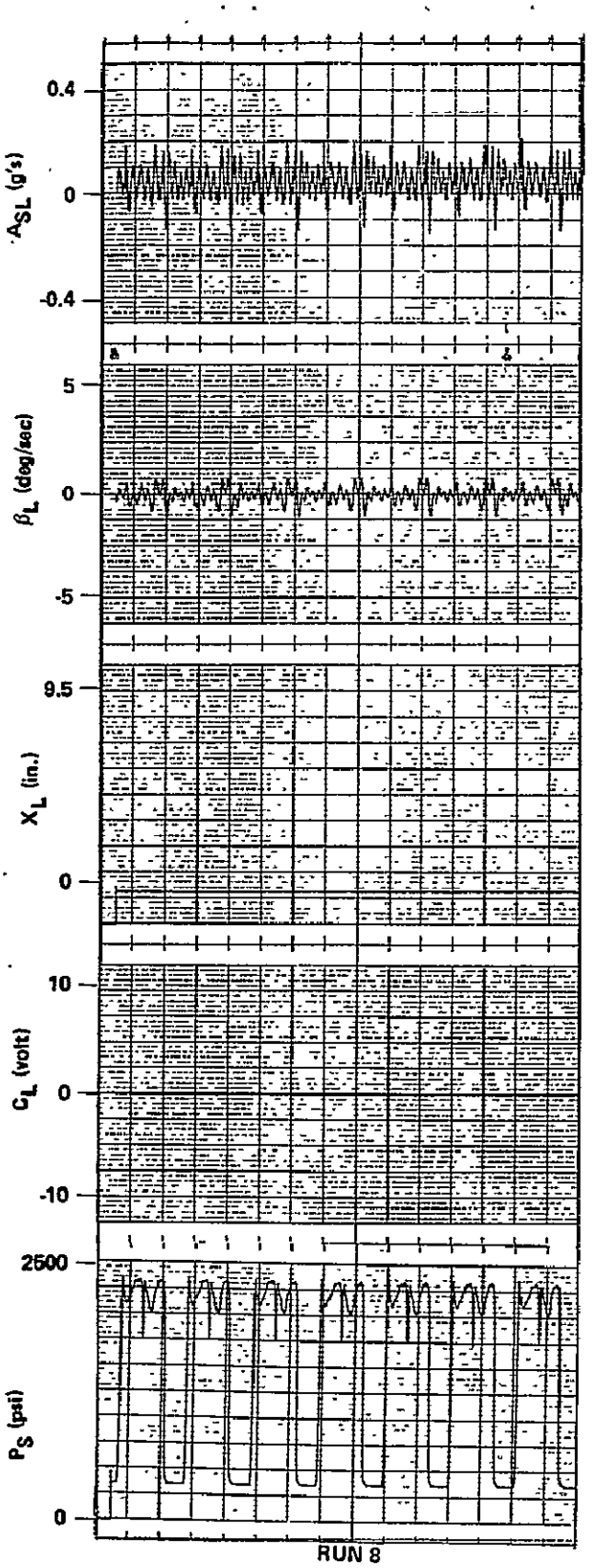

Figure 30. Dynamic response of the left boom for Run 8.

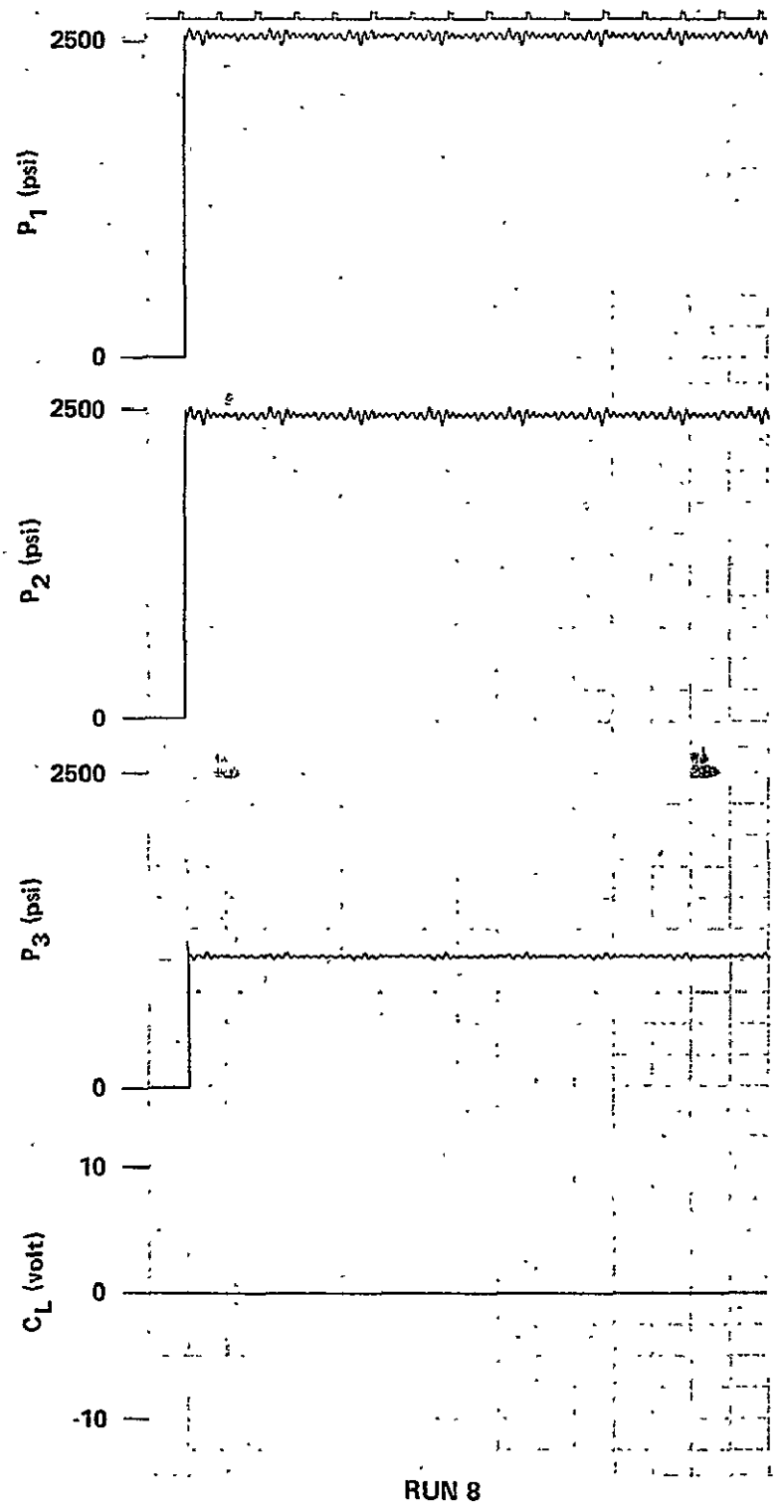

Figure 31. Pressure response of the left boom for Run 8.

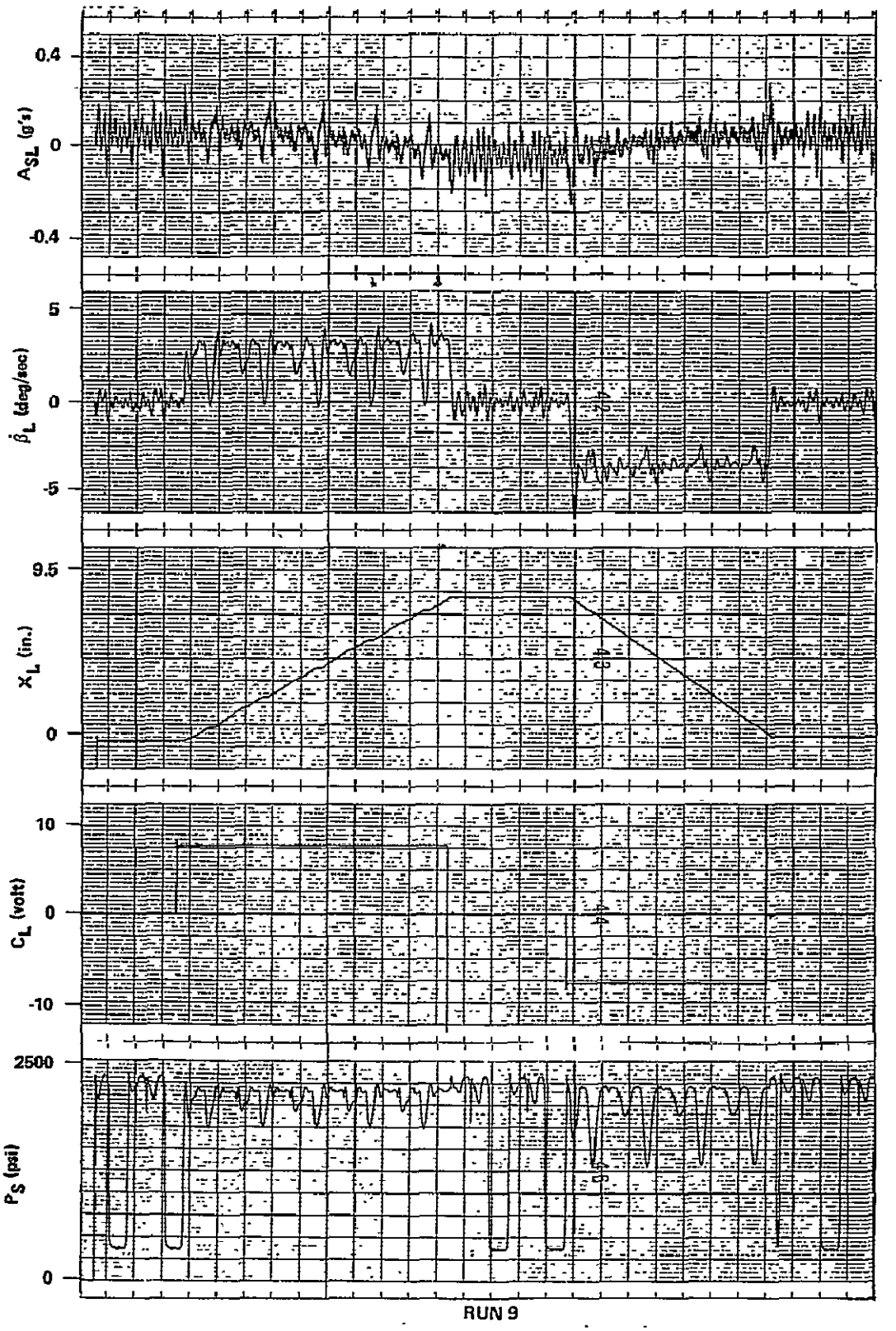

Figure 32. Dynamic response of the left boom for Run 9.

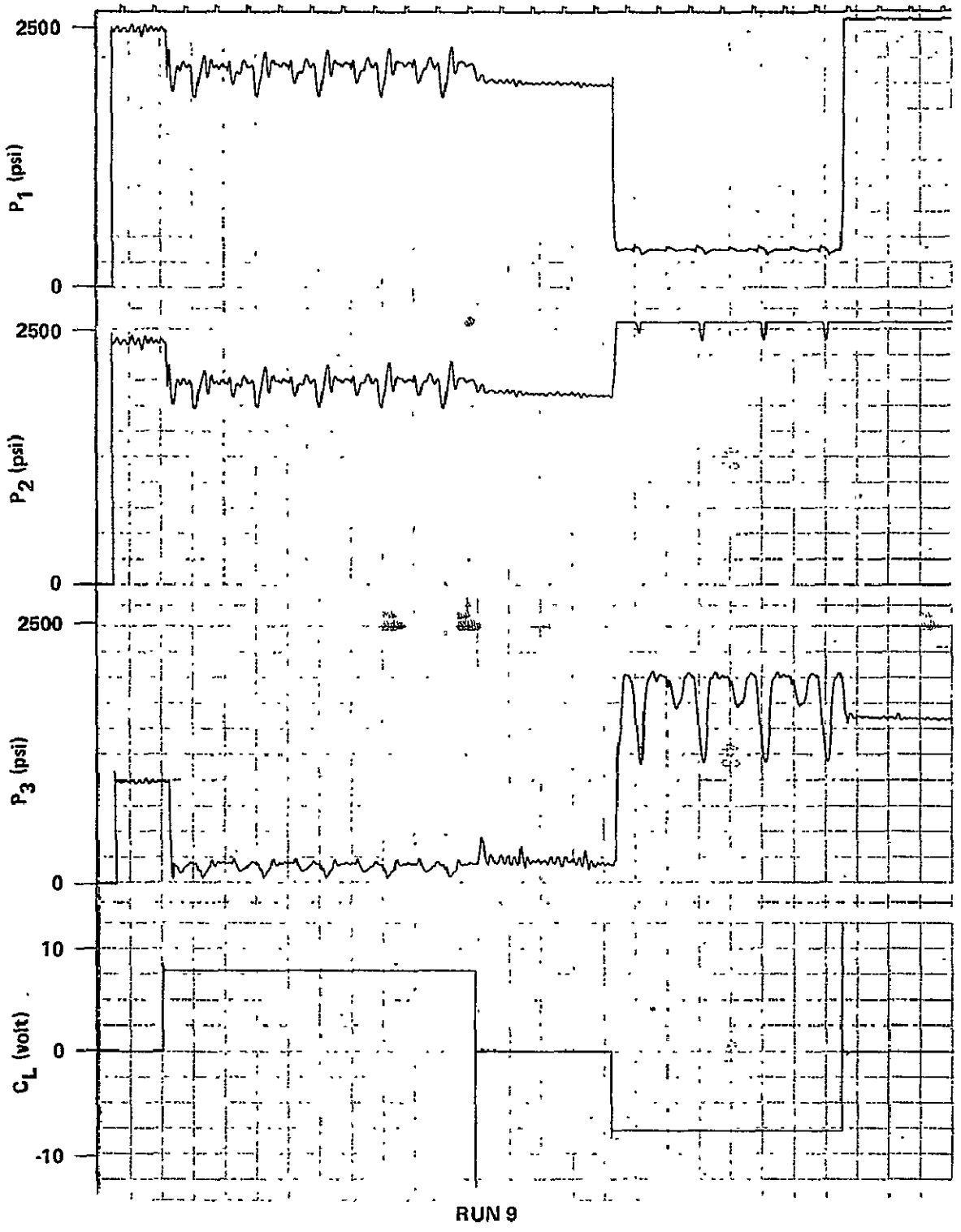

Figure 33. Pressure response of the left boom for Run 9.

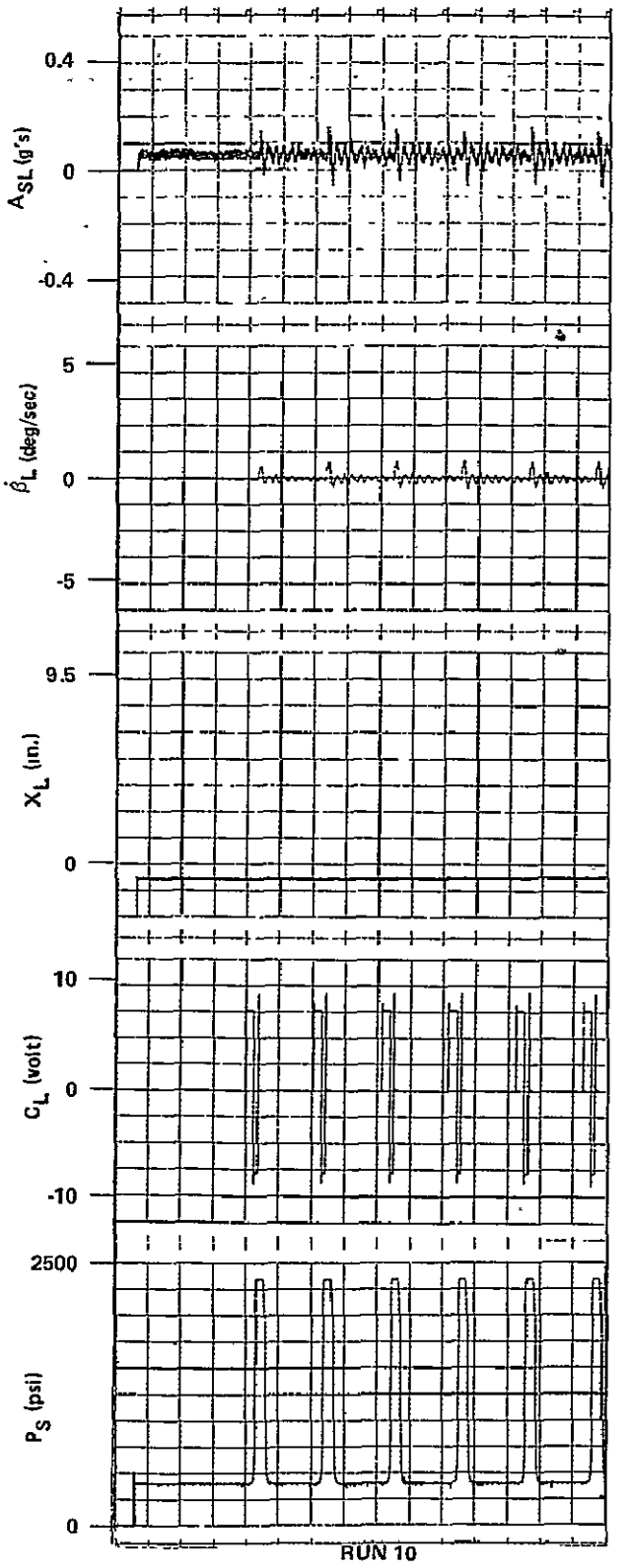

Figure 34. Dynamic response of the left boom for Run 10.

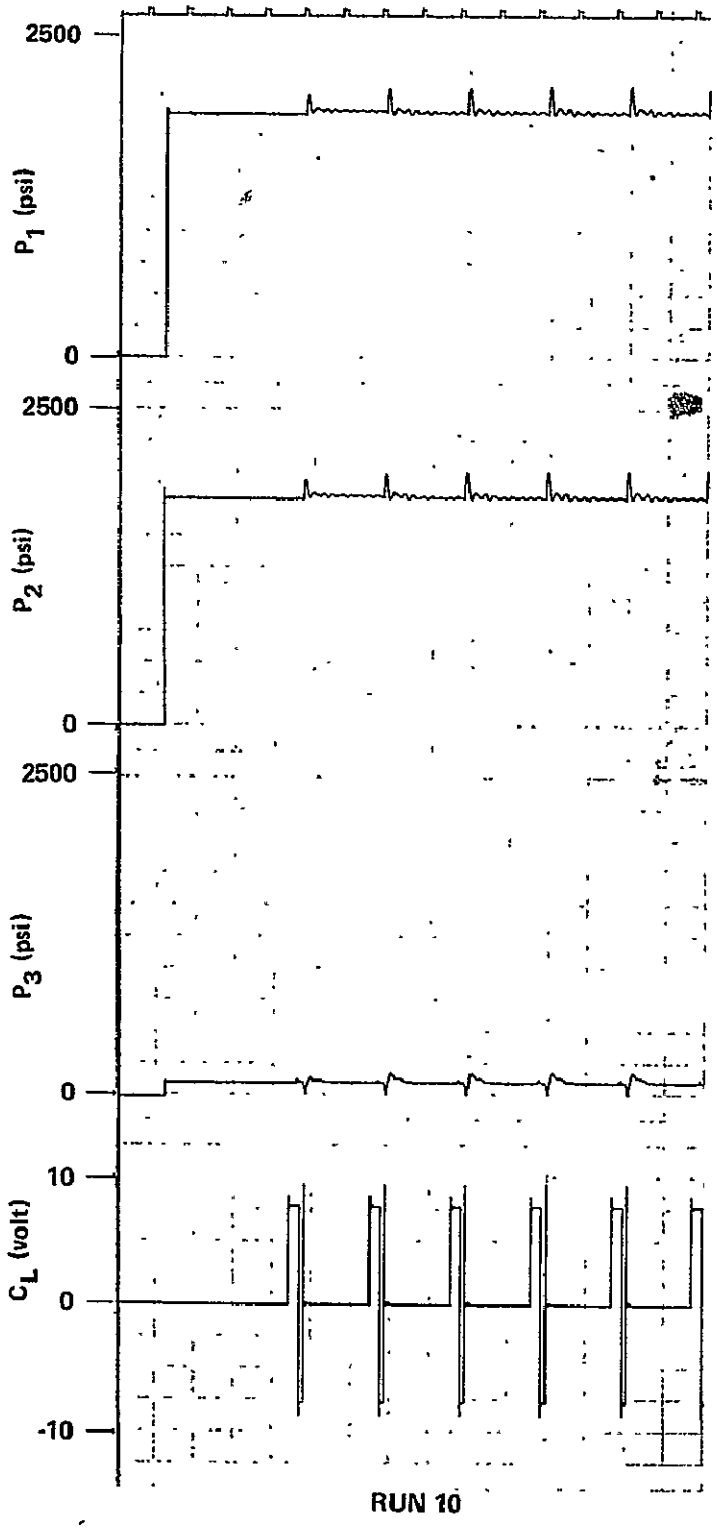

Figure 35. Pressure response of the left boom for Run 10.

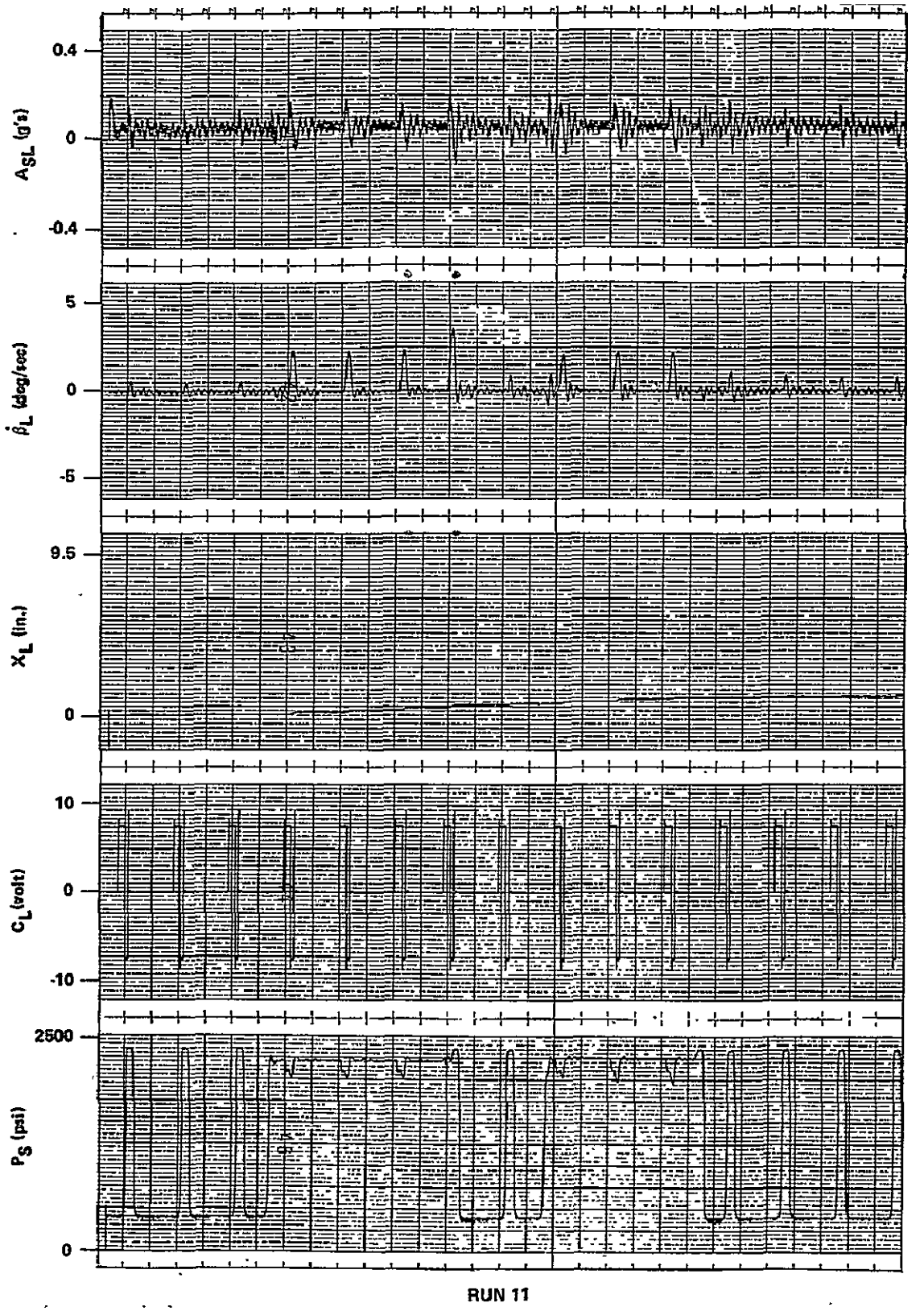

Figure 36. Dynamic response of the left boom for Run 1.

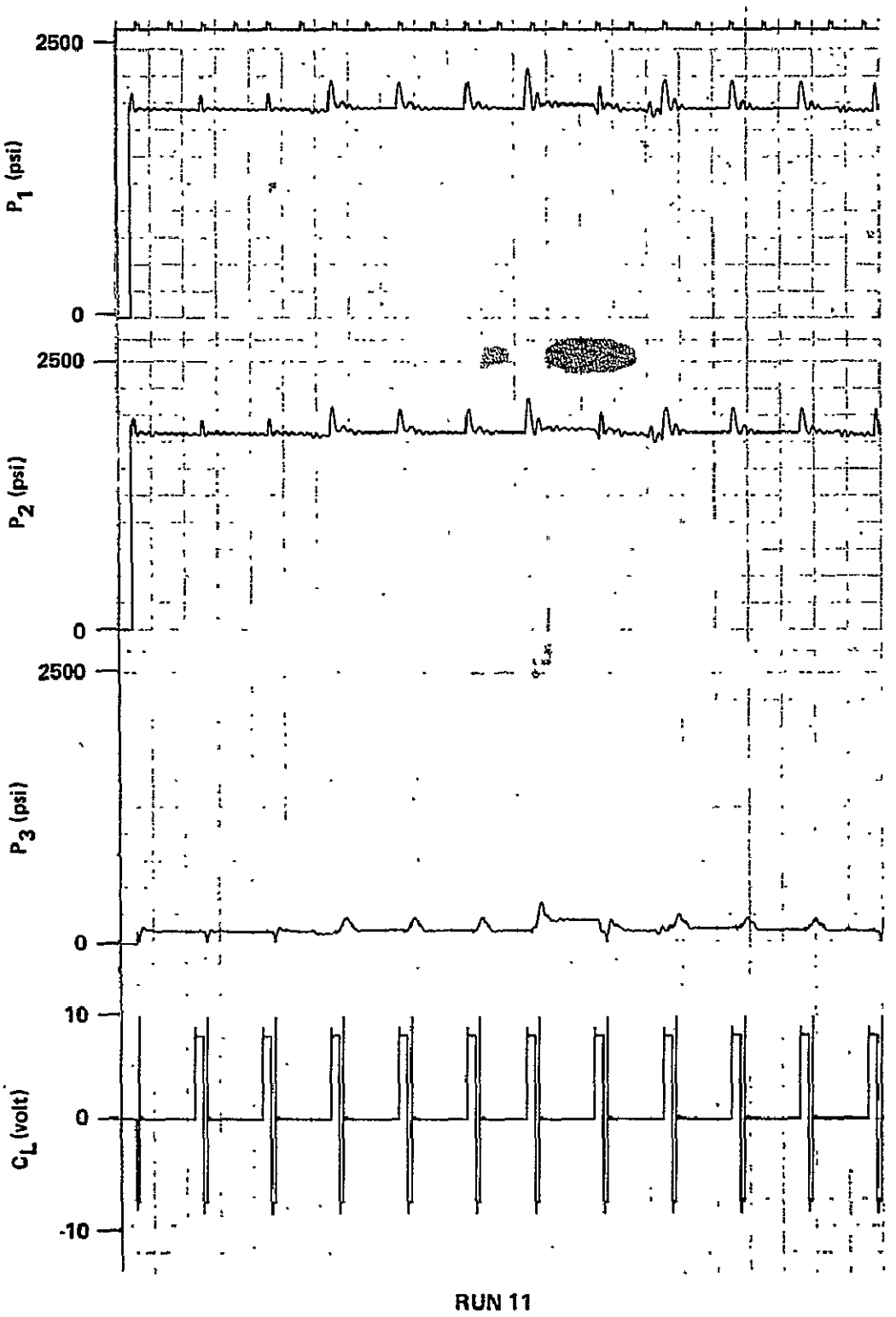

Figure 37. Pressure response of the left boom for Run 11.

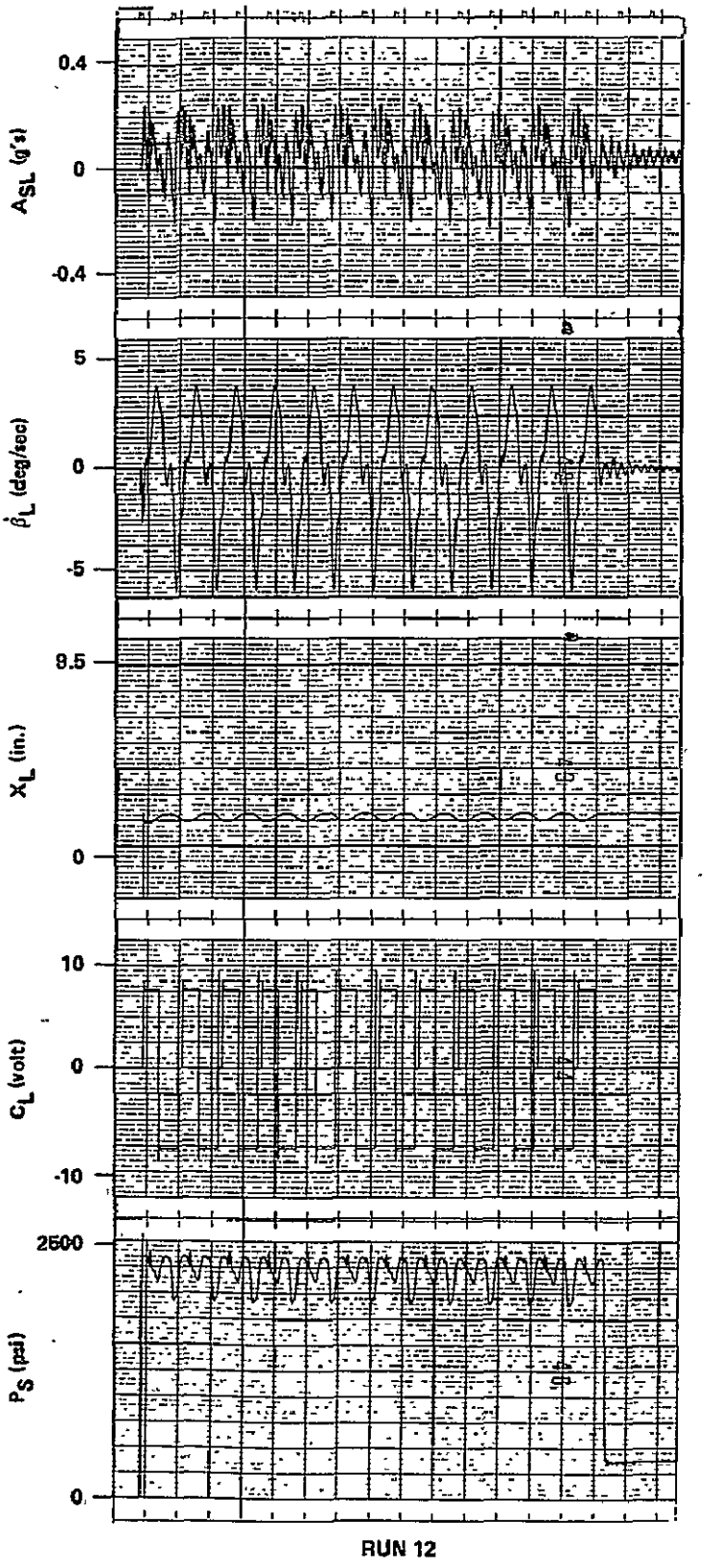

Figure 38. Dynamic response of the left boom for Run 12.

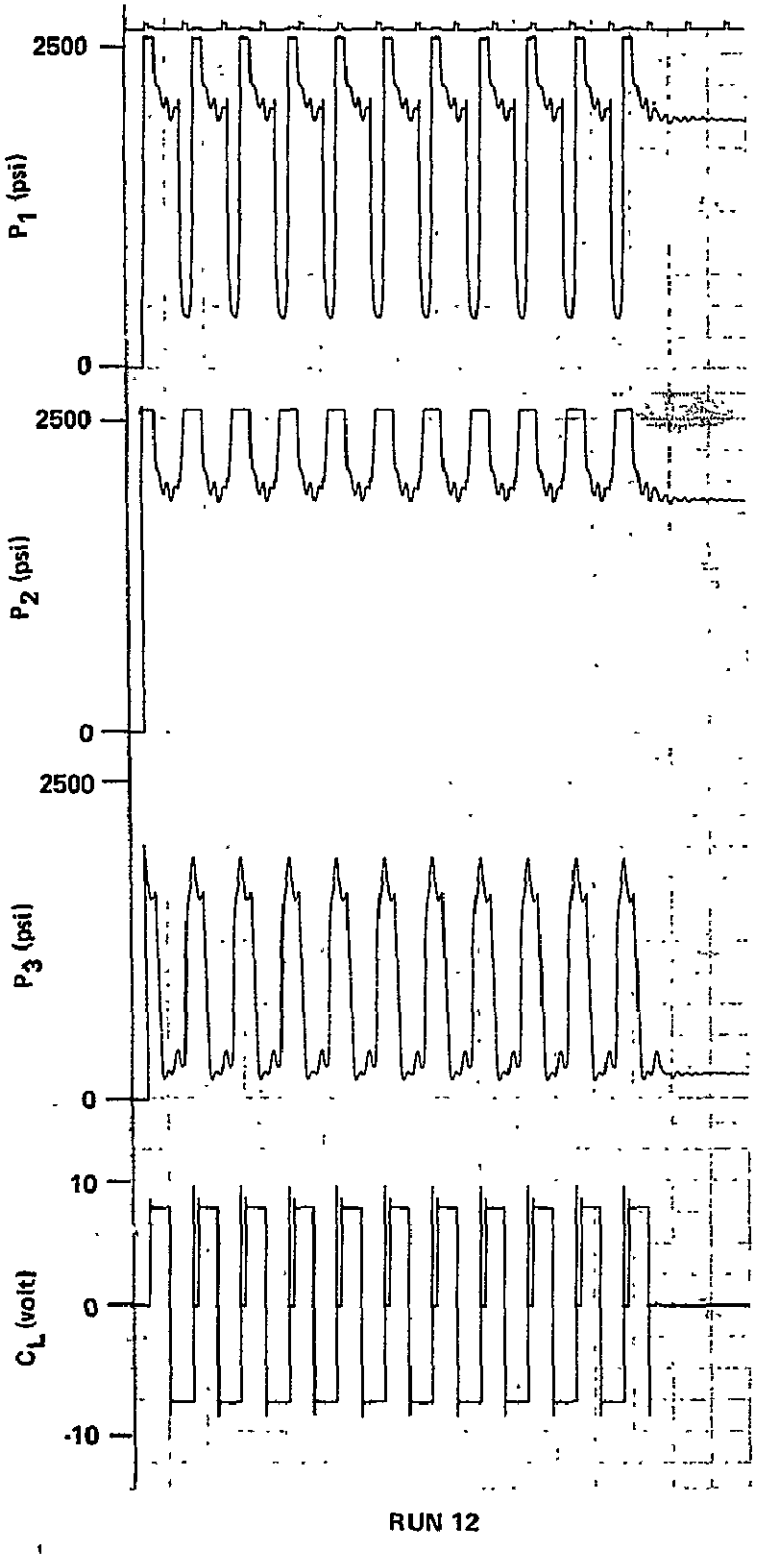

Figure 39. Pressure response of the left boom for Run 12.

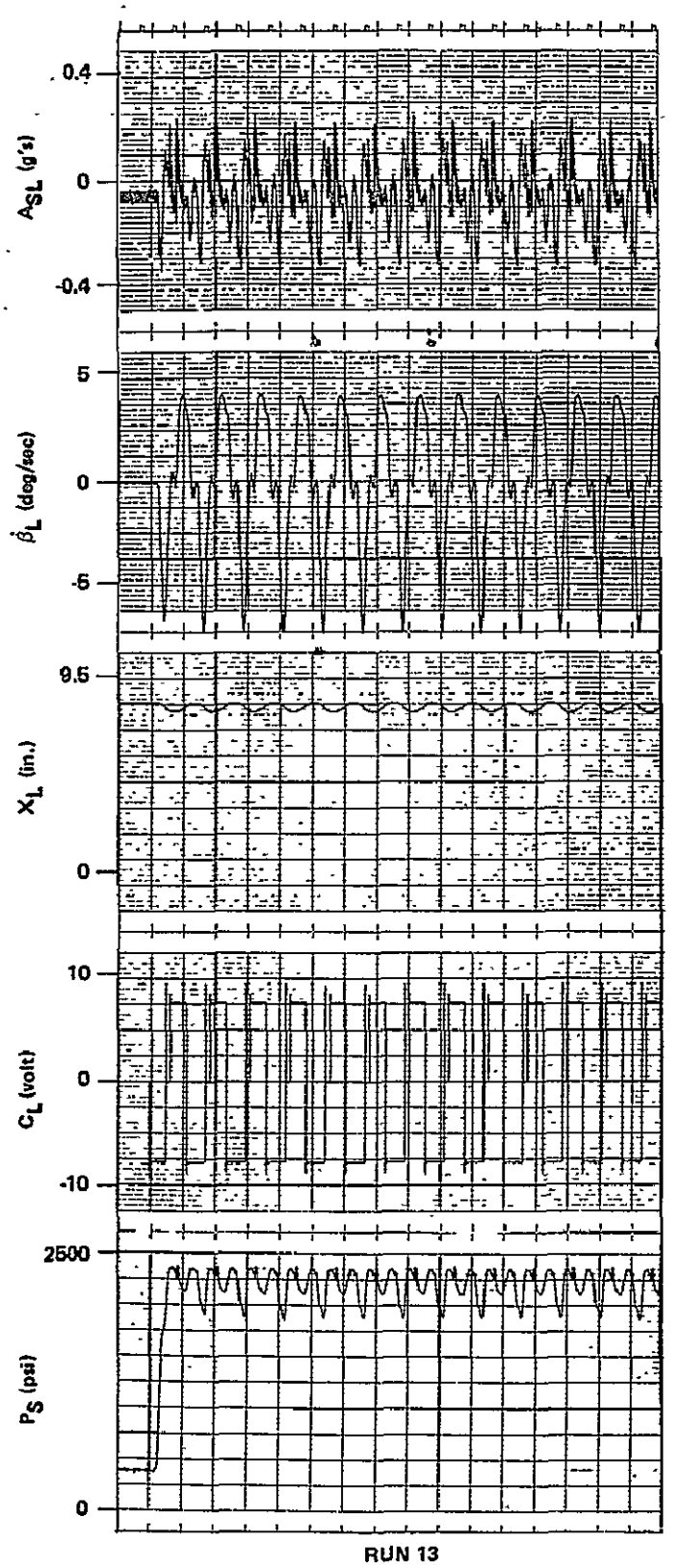

Figure 40. Dynamic response of the left boom for Run 13.

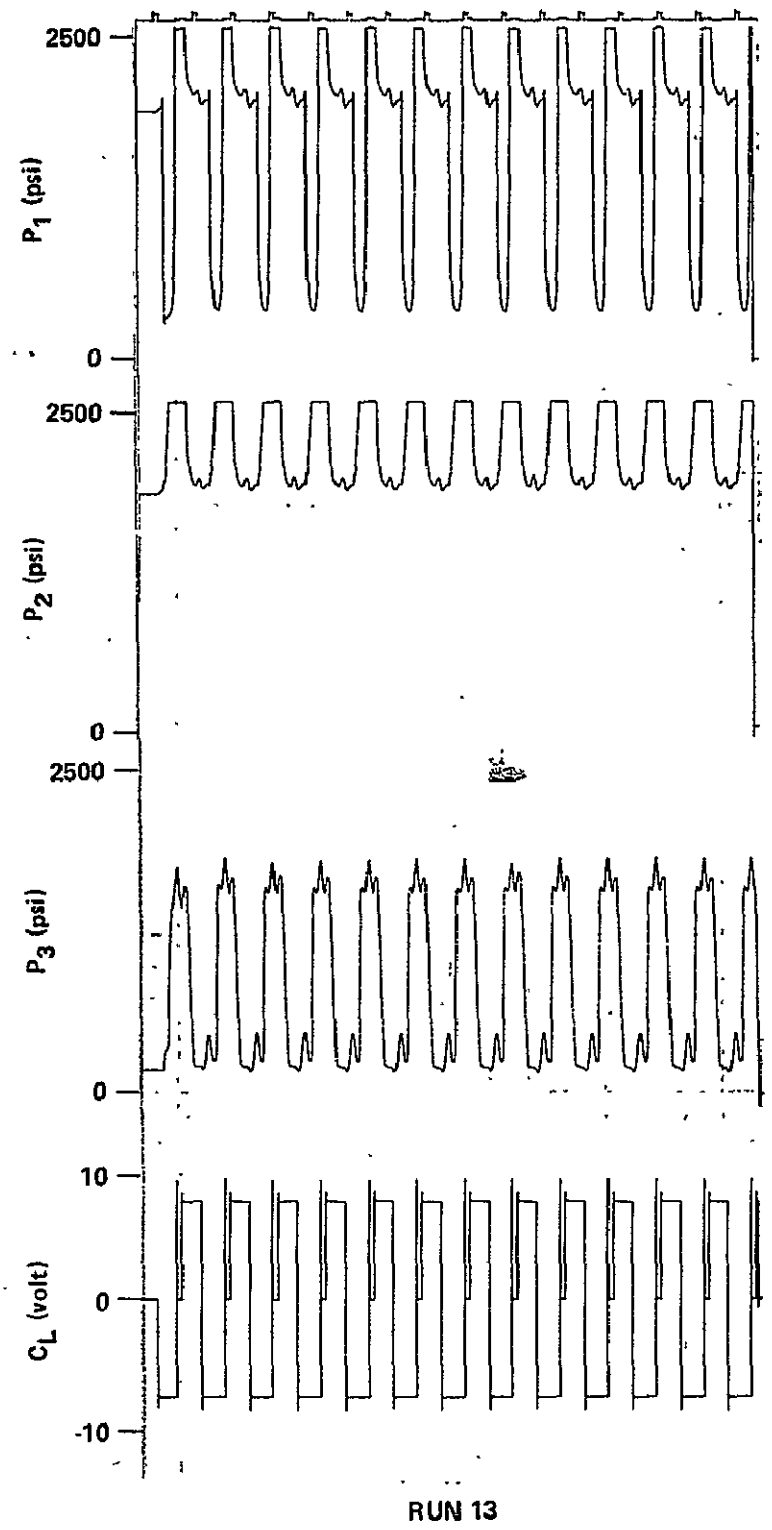

Figure 41. Pressure response of the left boom for Run 13.

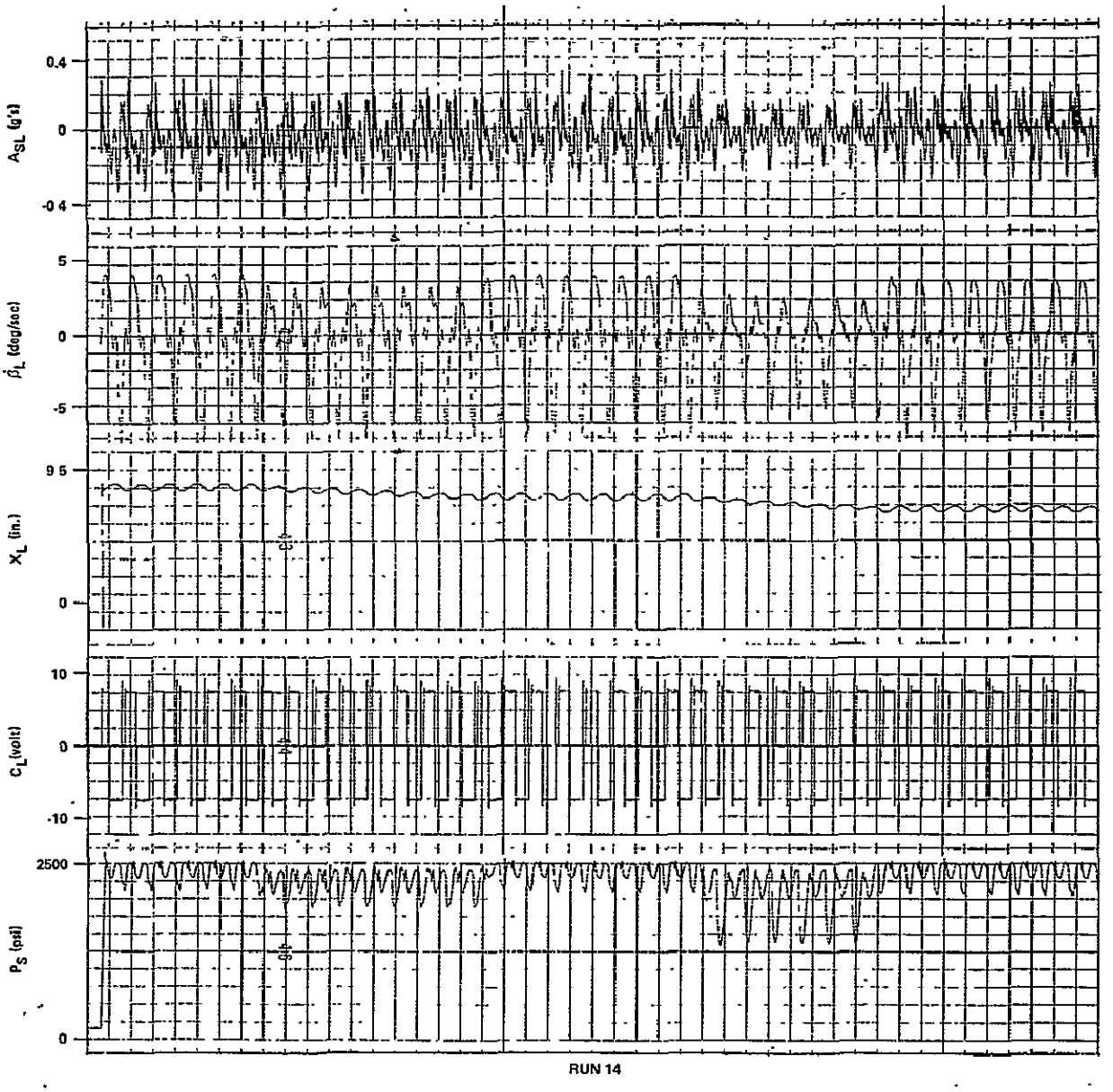

Figure 42. Dynamic response of the left boom for Run 14.

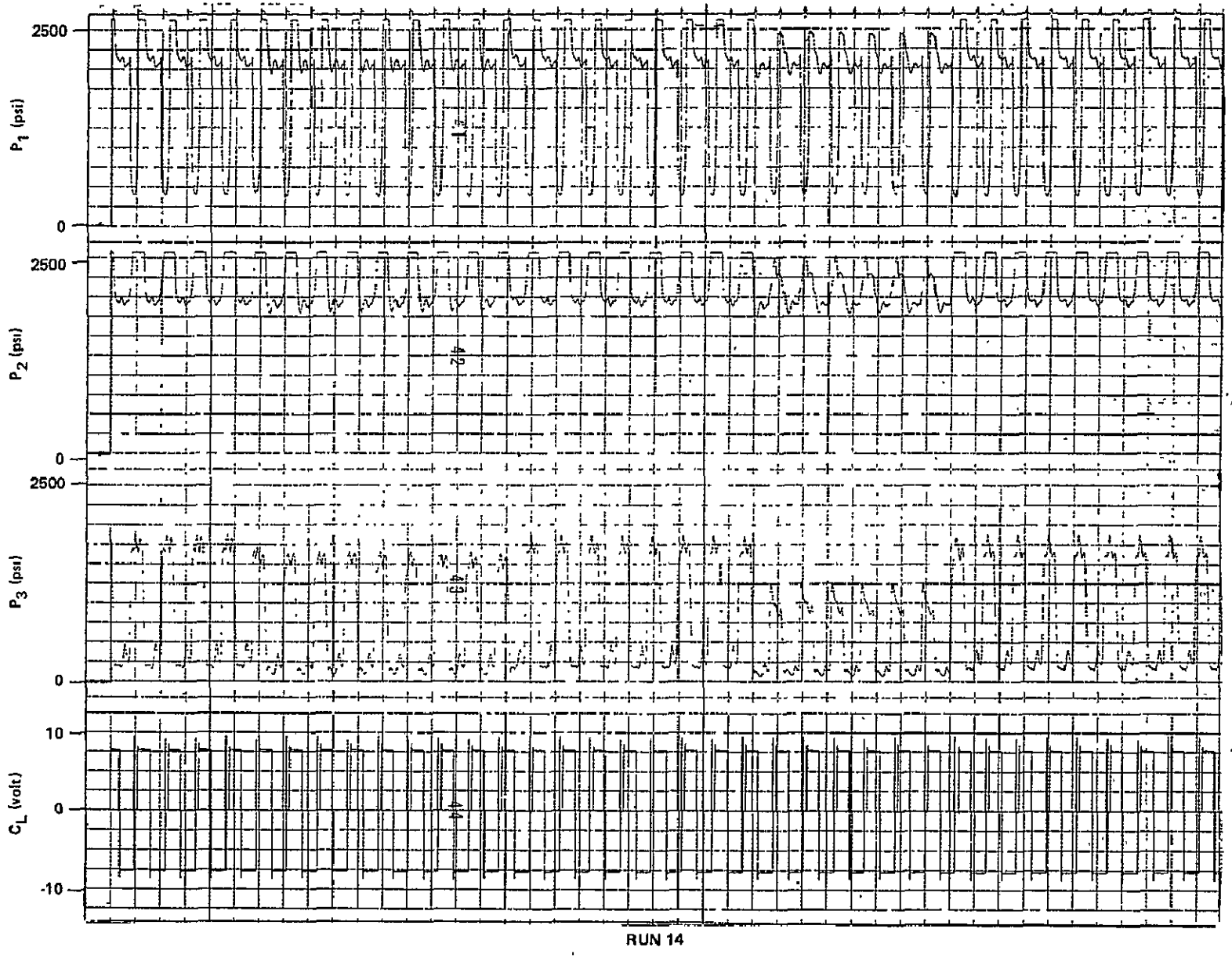

Figure 43. Pressure response of the left boom for Run 14.

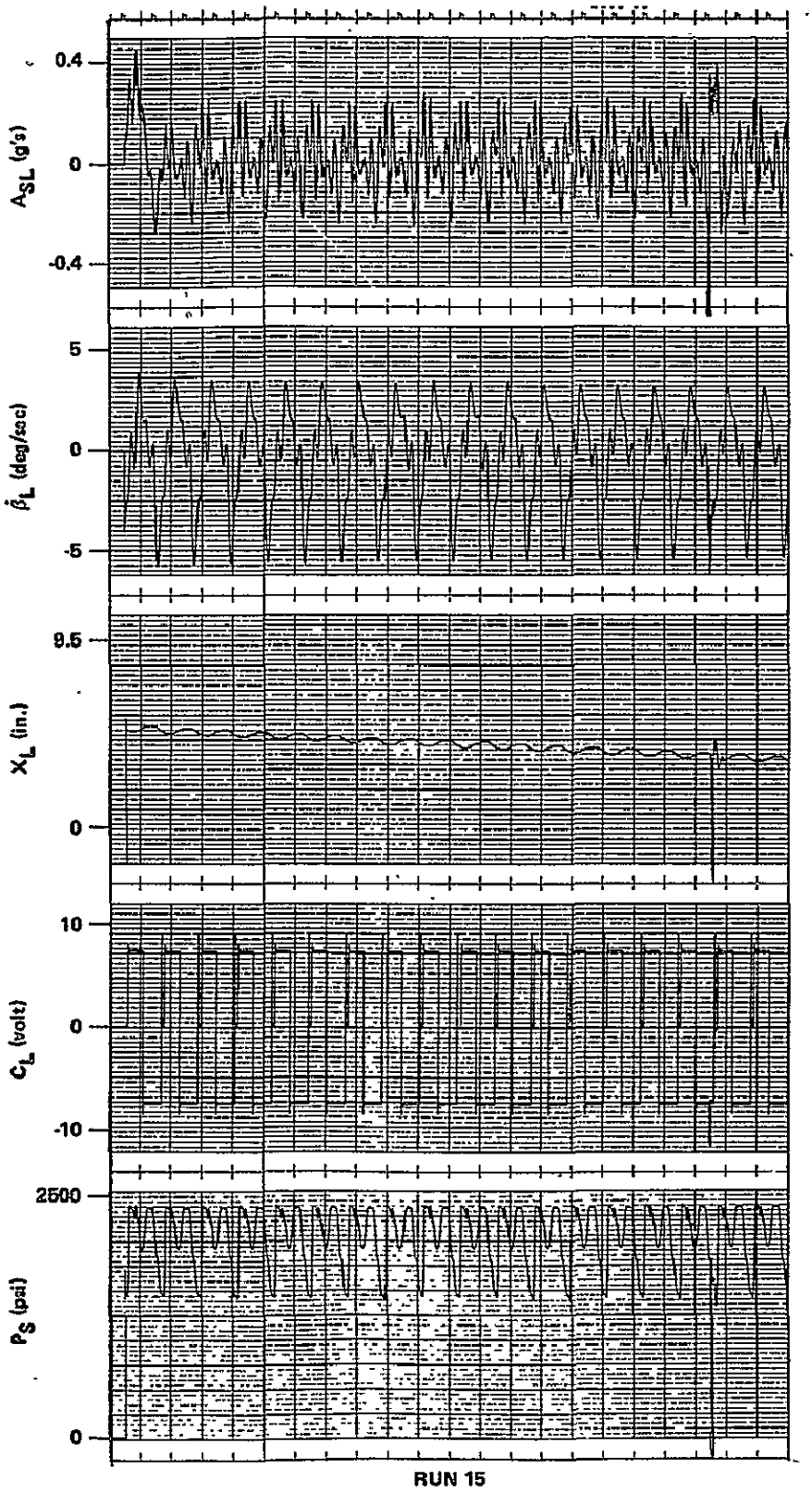

Figure 44. Dynamic response of the left boom for Run 15.

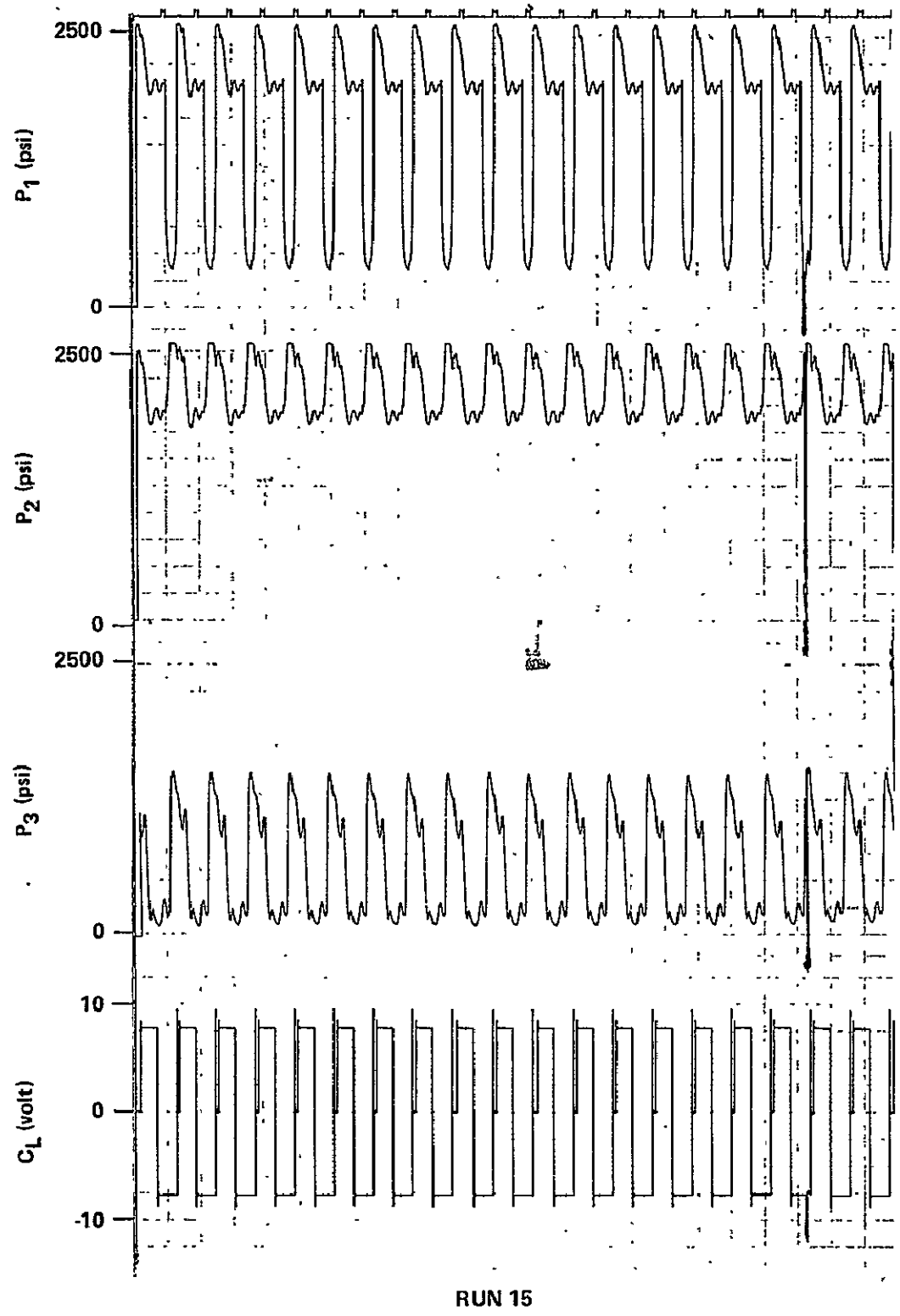

Figure 45. Pressure response of the left boom for Run 15.

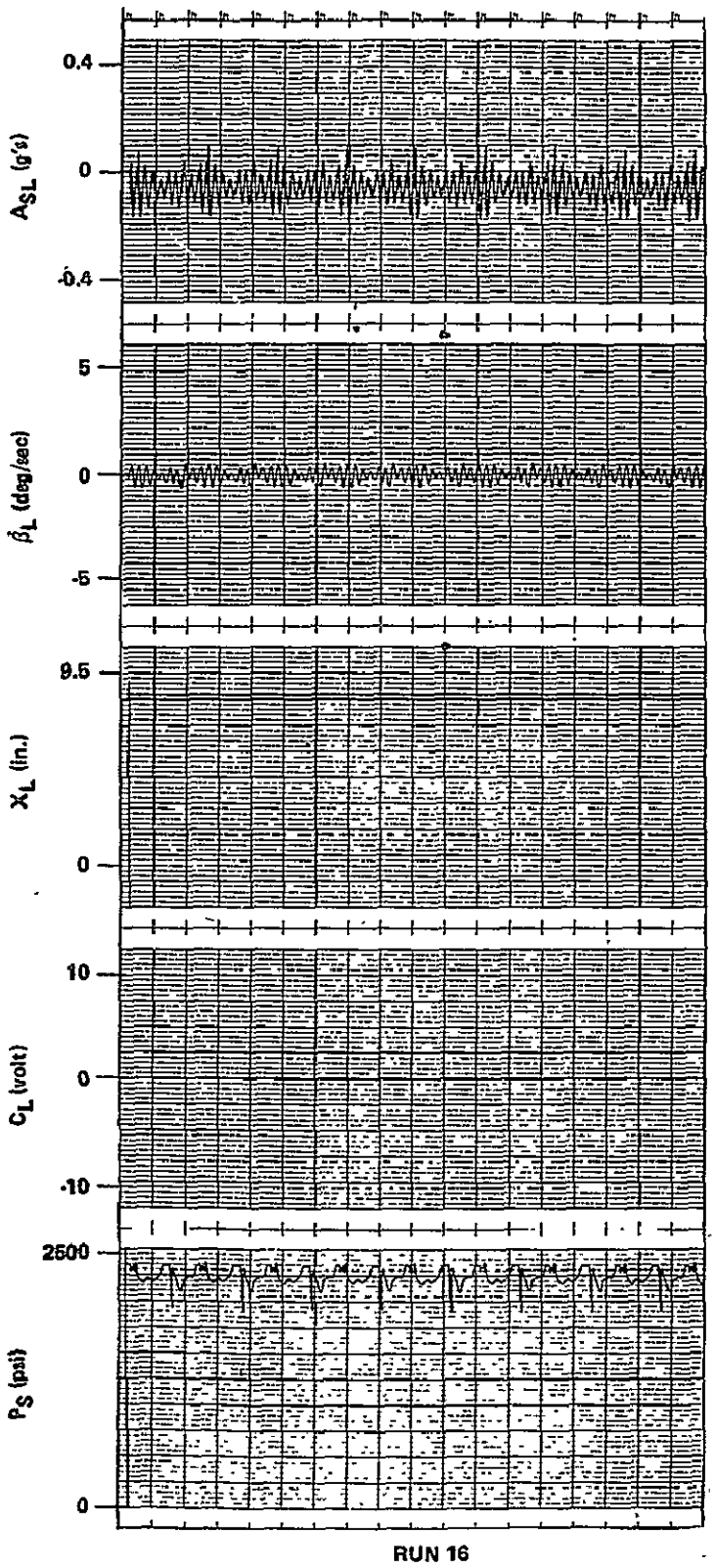

Figure 46. Dynamic response of the left boom for Run 16.

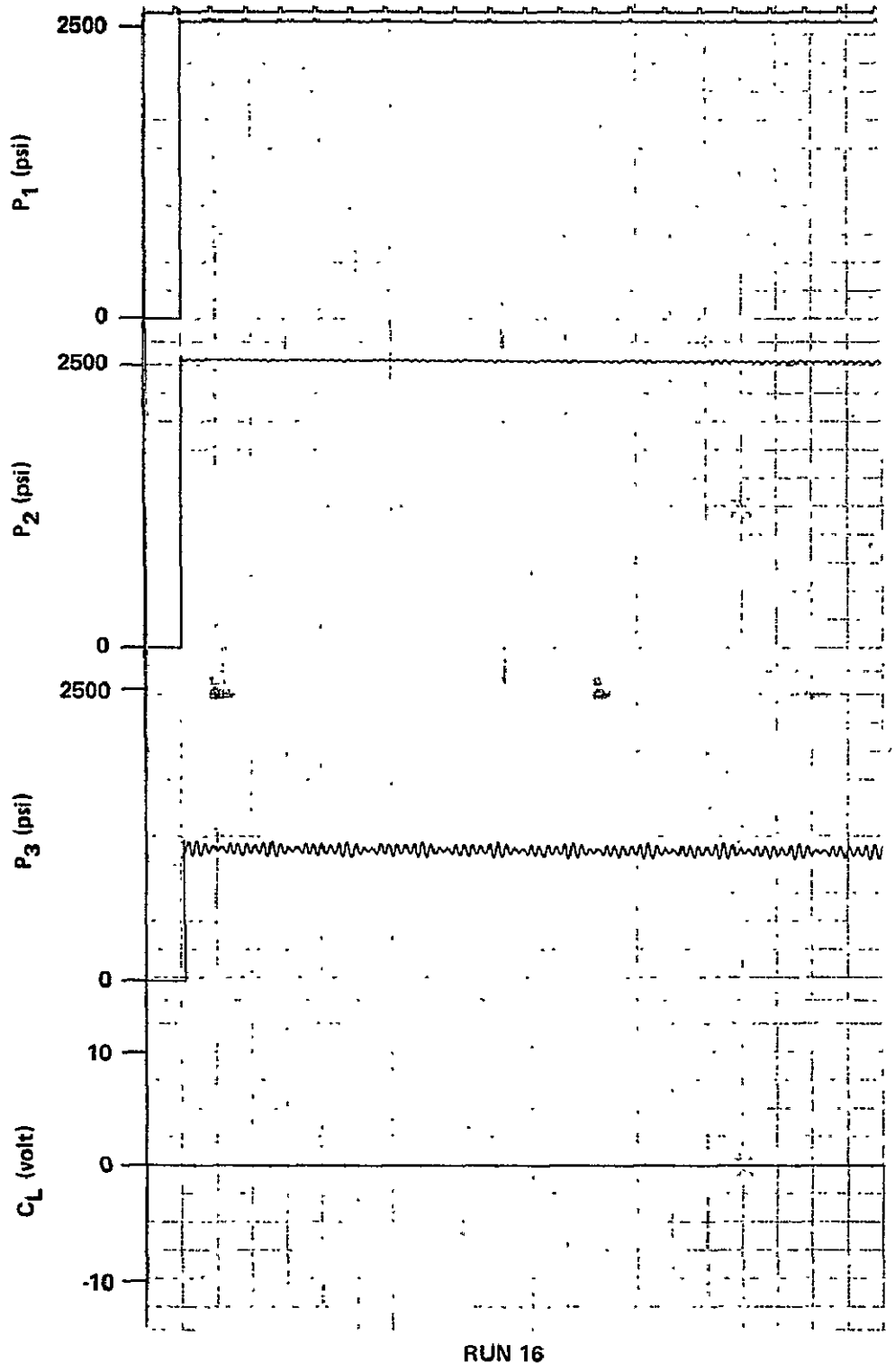

Figure 47. Pressure response of the left boom for Run 16.

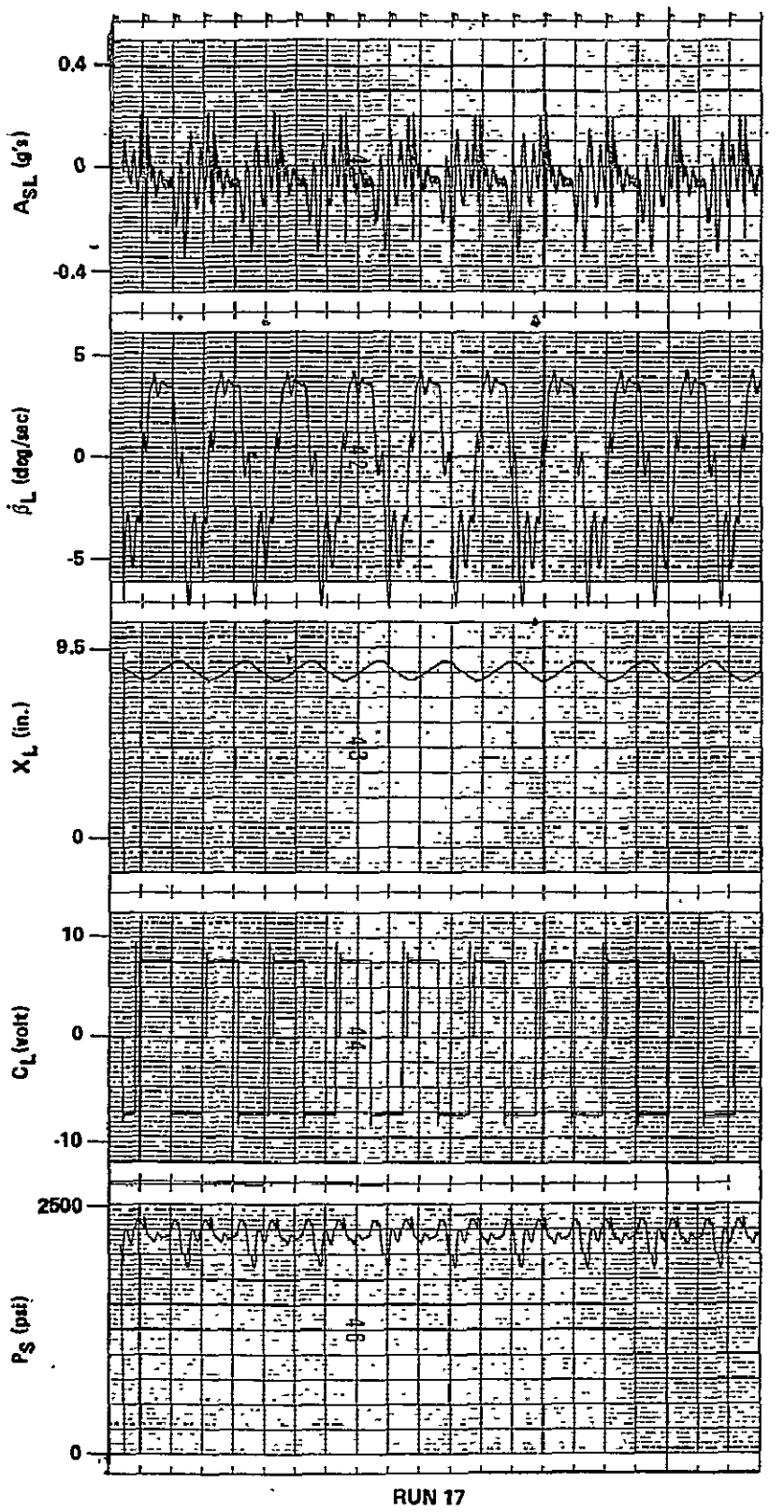

Figure 48. Dynamic response of the left boom for Run 17.

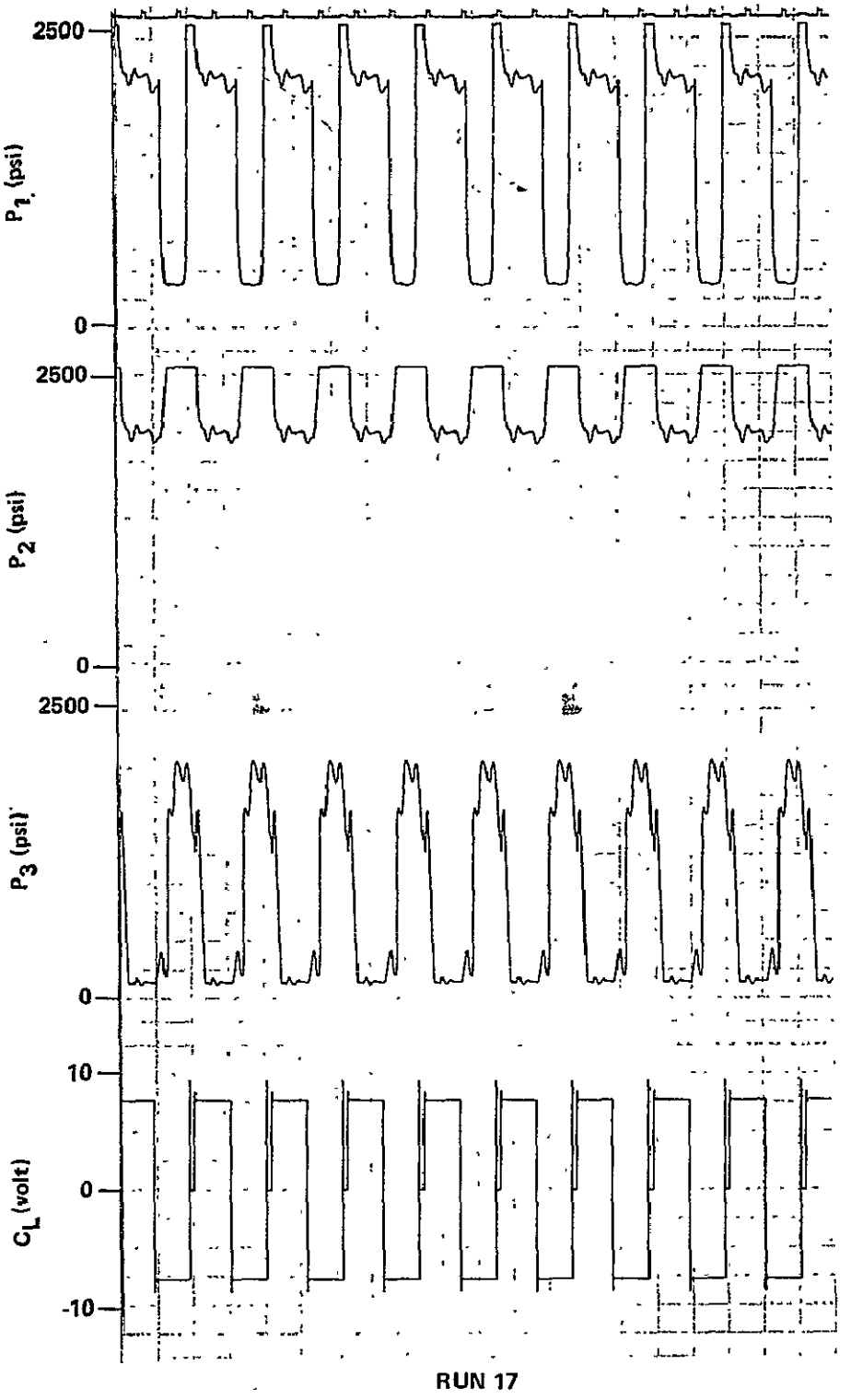

Figure 49. Pressure response of the left boom for Run 17.

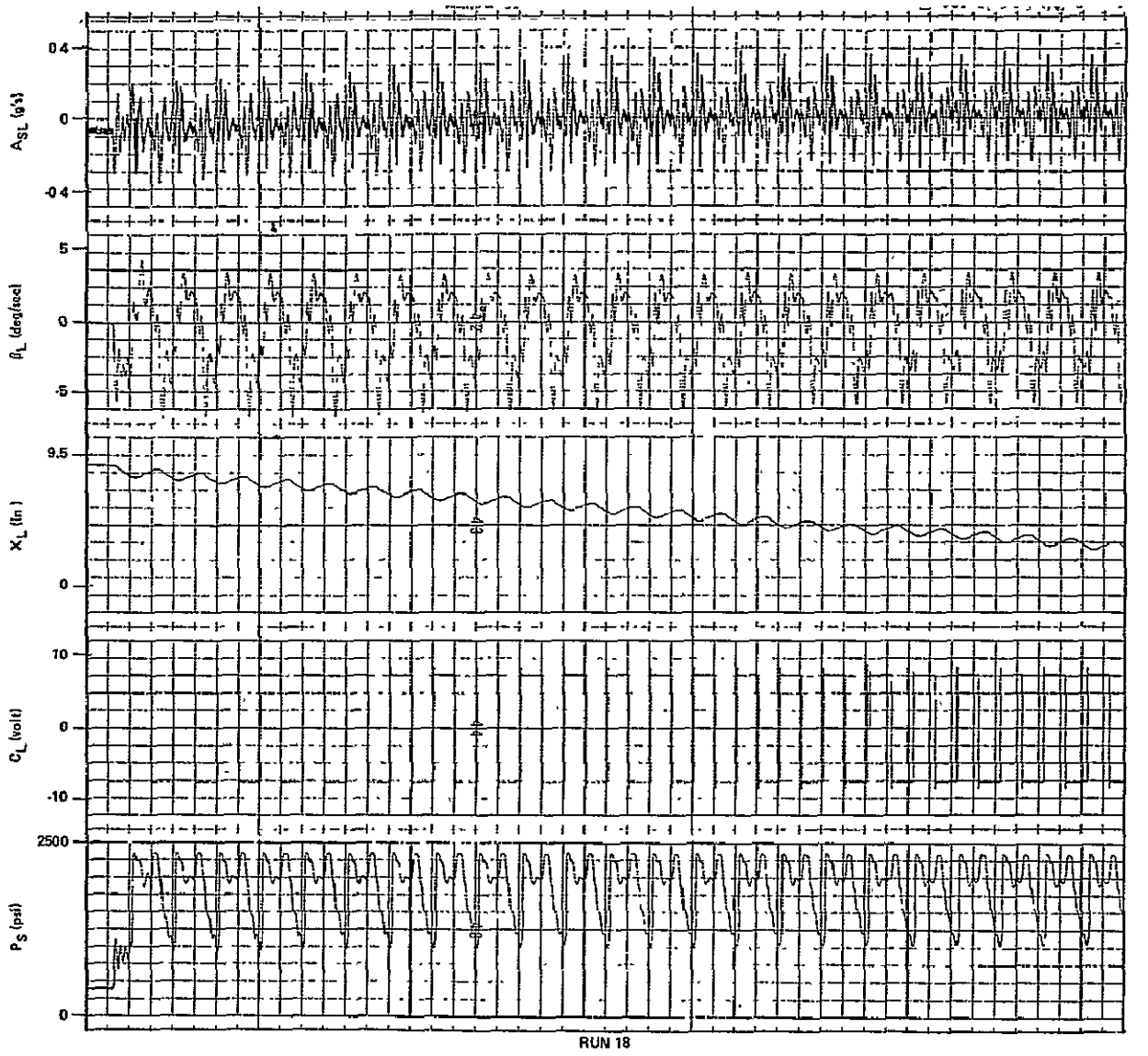

Figure 50. Dynamic response of the left boom for Run 18.

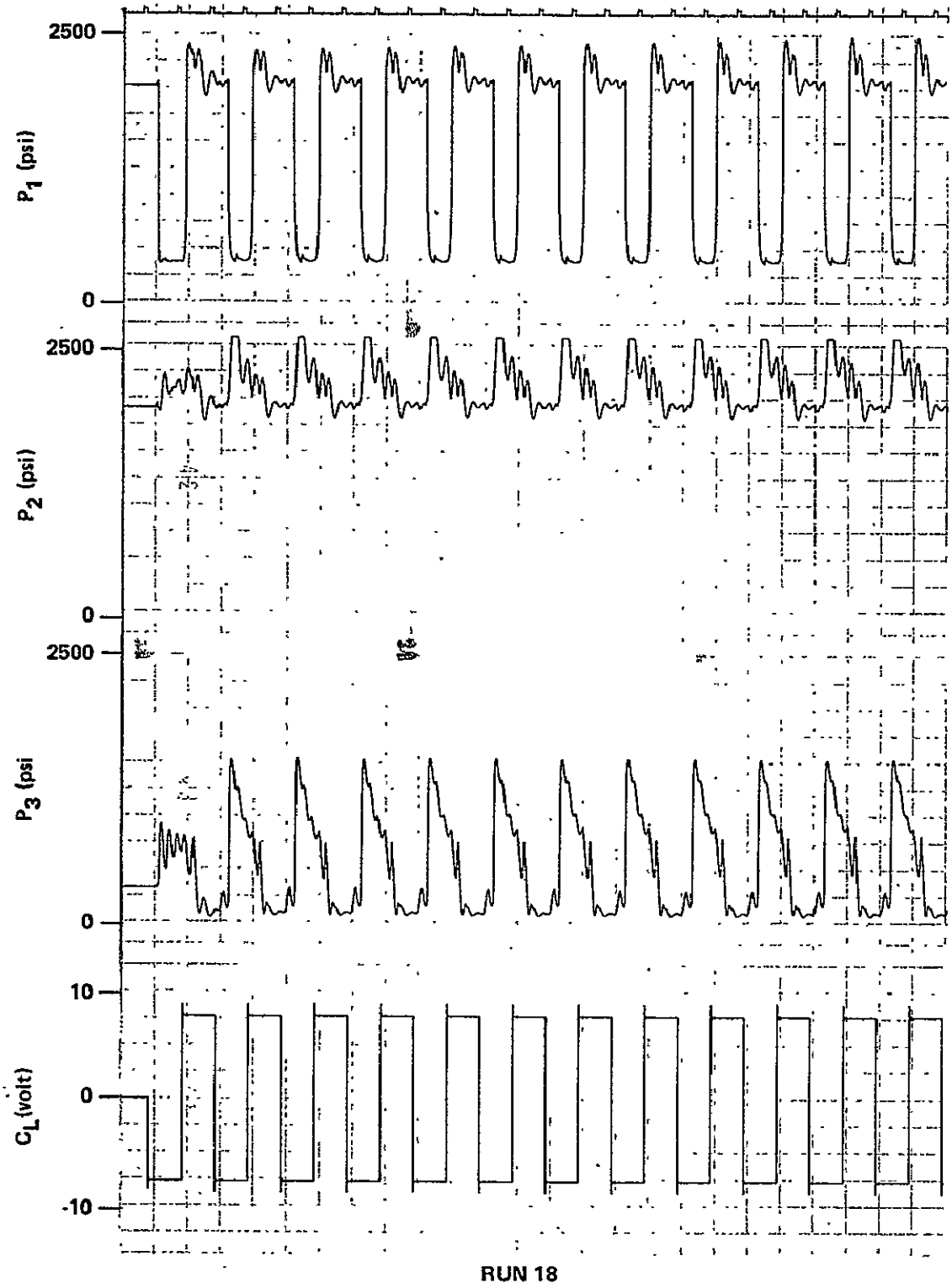

Figure 51. Pressure response of the left boom for Run 18.

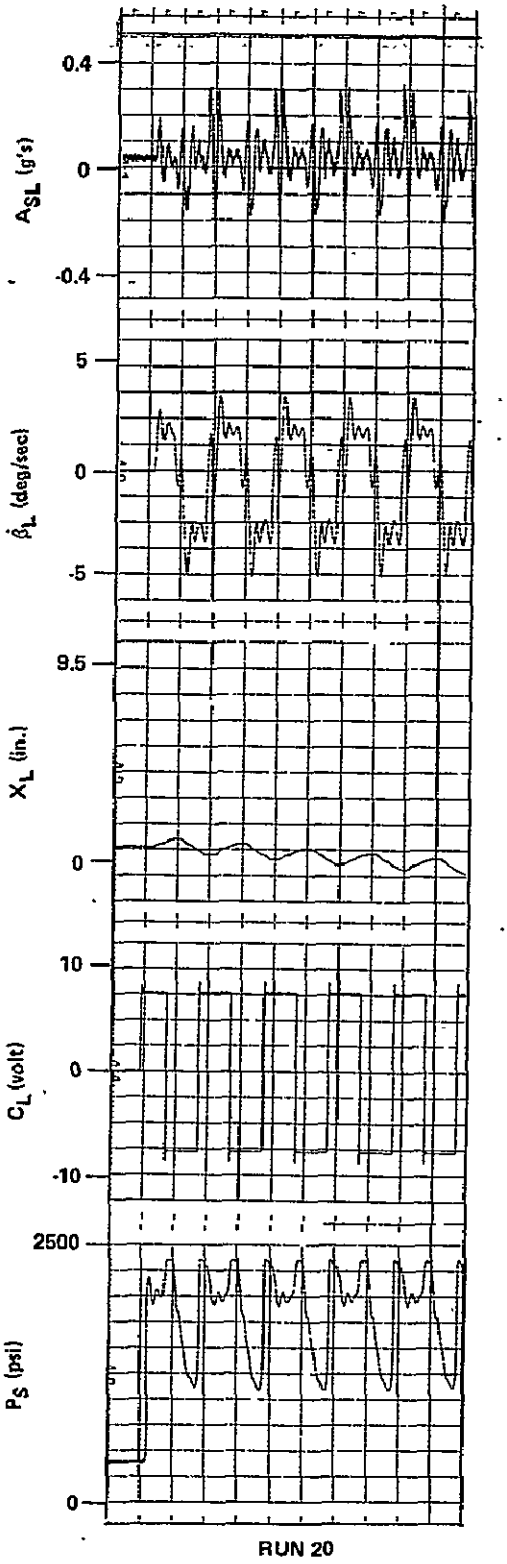

Figure 52. Dynamic response of the left boom for Run 20.

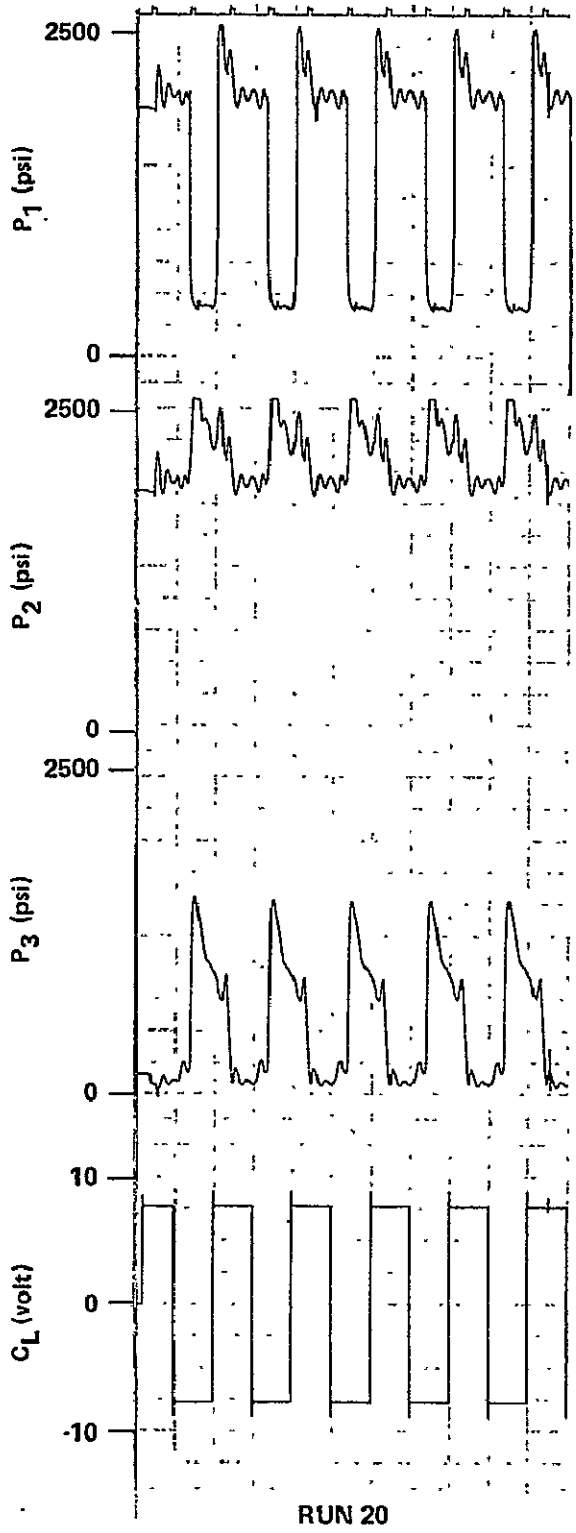

Figure 53. Pressure response of the left boom for Run 20.

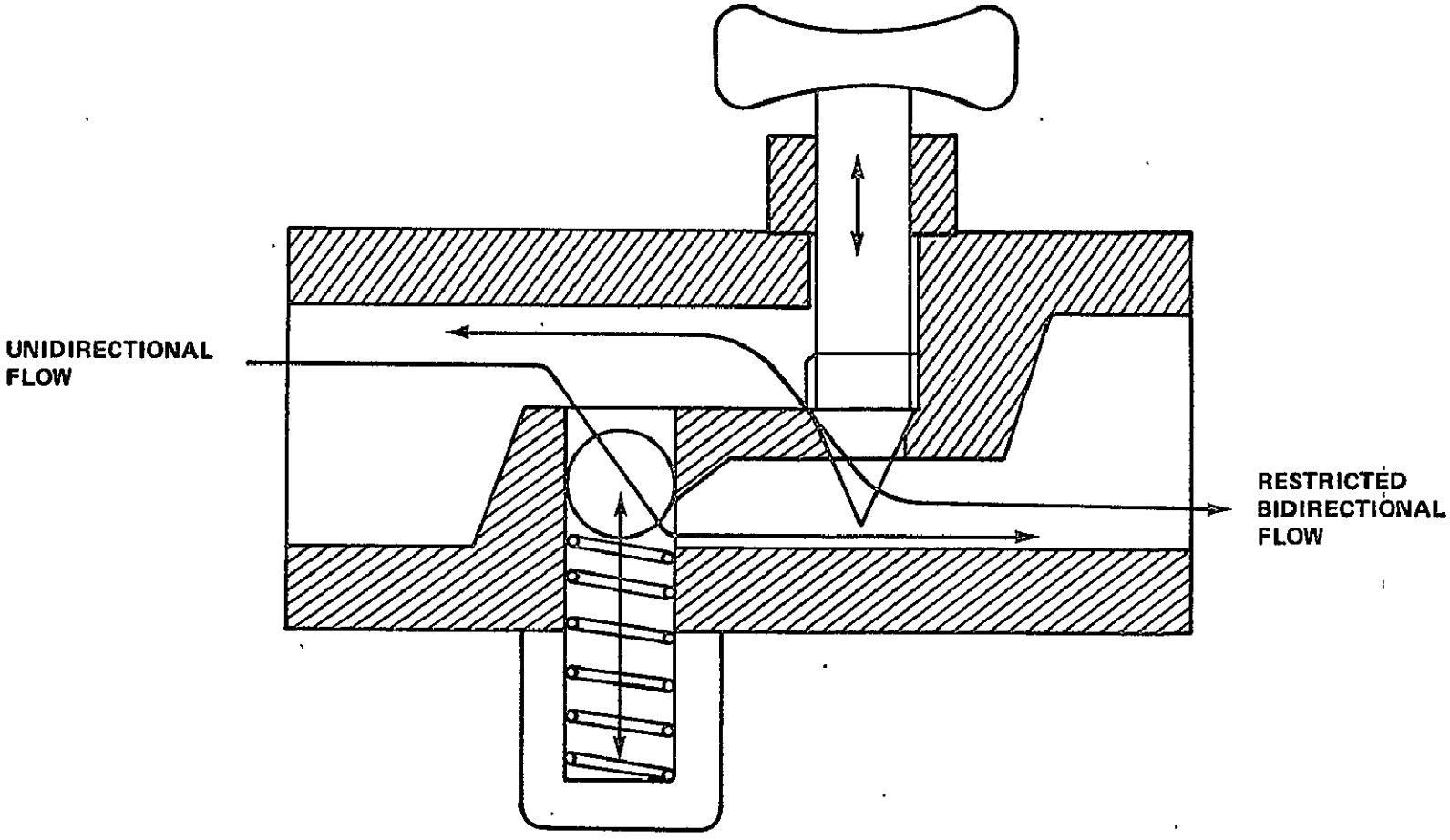

Figure 54. Needle and check valve.

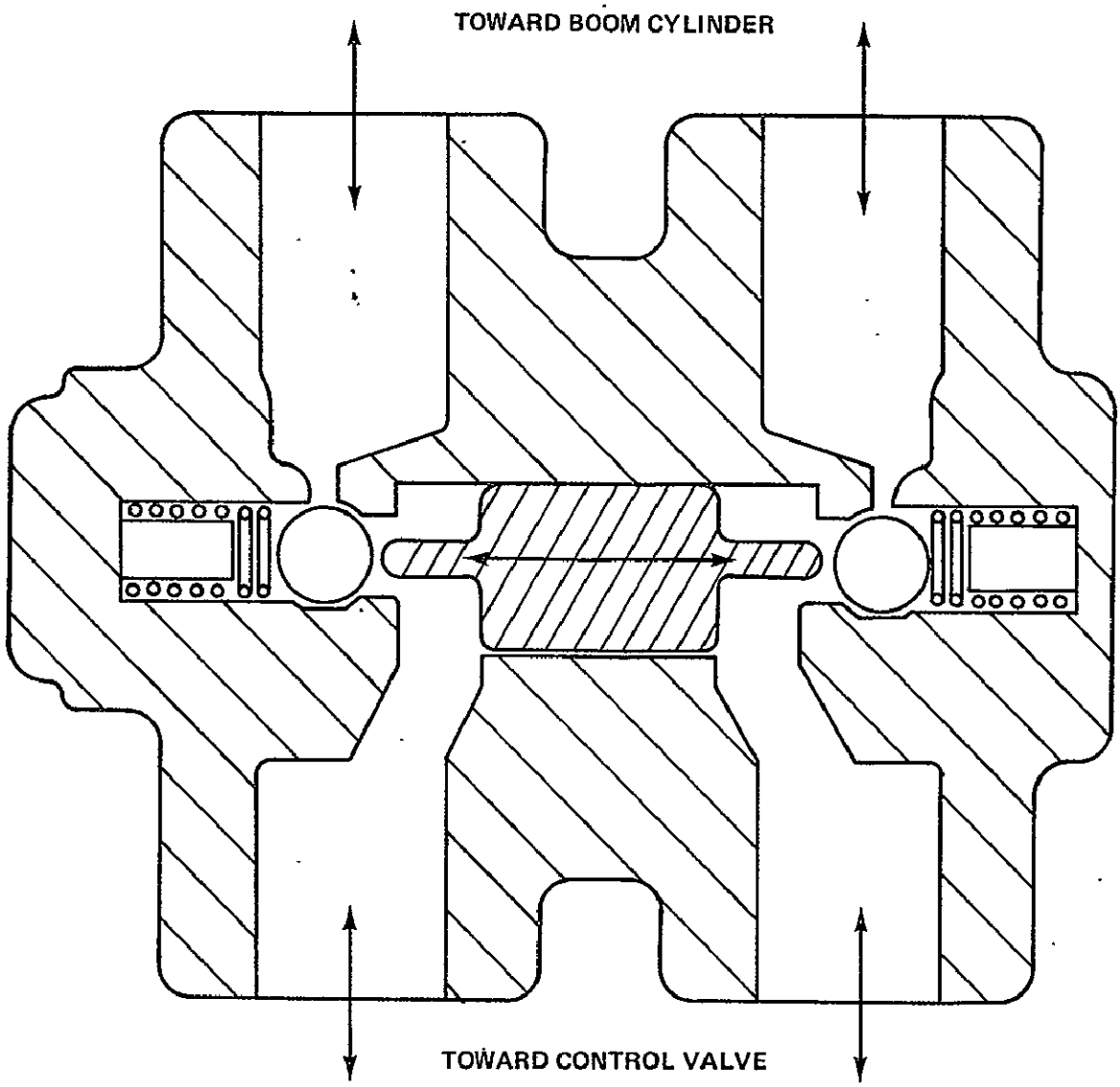

Figure 55. Pilot check valve.

APPENDIX A

TRANSFER FUNCTION MODEL OF THE LONGWALL SHEARER

A simulation model has been developed from the results obtained during the Bruceton tests of the longwall shearer. This model is an end-to-end type development since the individual component transfer functions were not determined at the time of the tests. Prior to testing the Joy machine it had been decided not to break into the system to obtain component characteristics. The block diagrams in Figures A-1 and A-2 are structured with the components such that each may be replaced with its individual transfer function and characteristics when they have been obtained.

The control valve, dual pilot check valve, and boom cylinder are shown in Figure A-1. The equivalent spring constant (K_{EQ}), boom inertia (J), and boom displacement (Y_L) are shown in Figure A-2. The control valve in Figure A-1 has a 30 percent threshold K'_D and a limited input level of 8 V K'_L. The input to K_s is E_1 such that $\pm E_1 = \pm(|C_L| - 2.4)\ K'_s$ for $2.4 < |C_L| < 8$ V. The control valve has a natural frequency of 6 Hz with a 0.9 damping factor. The flow to the valve from the pump is Q_S. Since the control valve is capable of 10 gal/min flow but the pump flow to the valve is 8 gal/min, the maximum flow to the dual pilot check valve occurs before the valve is fully opened. The flow to the boom cylinder determines the rate of the actuator displacement. The position of the boom cylinder piston is X_I and has a range from 0 to 9.5 in. at full stroke. When the boom is horizontal the stroke is 3.25 in. and X_B and β in Figure A-2 is zero. The boom displacement Y_L is an approximation for small angles.

If an 8 V command is introduced at t = 0 sec and a -8 V command is introduced at t = 4 sec, each for a 2 sec duration, then the command C_L is as shown in Figure A-3. The response of the boom cylinder to this command is shown in Figure A-4. The deviation from a constant rate is apparent during the

initial acceleration. It is greater when the boom is lowered as shown by the increased peak of boom rate ($\dot{\beta}_L$) in Figure A-5. This figure shows the response of the boom rate to the input command of Figure A-3. The oscillation that is present in the boom rate of this figure is also present in the height of the cutting drum centerline Y_L.

Simultaneous operation of the right and left boom decreases the boom rate to half its valve whenever either is raised. Whenever either is lowered simultaneously or individually the boom rate is not reduced. Figure A-6 shows the response of the boom to input command of Figure A-3 when the other boom was raised for 8 sec. The response was the same when the other boom was lowered for 8 sec. The simultaneous operation of both booms is modeled by duplicate definition of the block diagrams shown in Figures A-1 and A-2. The hydraulic flow for the booms Q_P are identified as Q_{PL} for the left boom and Q_{PR} for the right boom model. The boom cylinder constant K_G is identified as K_{CL} and K_{CR} for left and right boom models. The valves of gains for K_C are indicated for the left and right booms in Table A-1.

TABLE A-1. VALUES OF GAINS FOR K_C FOR THE LEFT AND RIGHT BOOMS

$+C_L$	$-C_L$	$+C_R$	$-C_R$	Q_{PL}	Q_{PR}	K_{CL}	K_{CR}
Individual Commands							
1	0	0	0	1	0	K_{CL}	0
0	1	0	0	1	0	K_{CL}	0
0	0	1	0	0	1	0	K_{CR}
0	0	0	1	0	1	0	K_{CR}
Simultaneous Commands							
0	1	0	1	1	1	K_{CL}	K_{CR}
1	0	1	0	1	1	$K_{CL/2}$	$K_{CR/2}$
1	0	0	1	1	1	$K_{CL/2}$	K_{CR}
0	1	1	0	1	1	K_{CL}	$K_{CR/2}$

The results given in Table A-1 for the simulation model are based on saturation commands of ±8 V to the control valves and are not valid for proportional operation. External loads to the boom may vary the constants in this model, but their effects are not known at this time.

A listing of the values and constants is provided in Table A-2.

TABLE A-2. LISTING OF VALUES AND CONSTANTS FOR THE SIMULATION MODEL

Symbol	Units	Definition
A_{SL}	g's	Linear acceleration normal to boom and at drum axis
C_L	volt	Step command to control servovalve, ±8
d	ft	Moment arm from pivot to boom cylinder tie point, 0.875
E_1	-	Input to K_s
J	lb-ft-sec^2	Moment of inertia of boom, drum, cowl, and components, 8886.6
K_A	lb/in.	Spring constant of the boom cylinder
K_B	in./rad	Actuator displacement per radian boom rotation, 10.5
K_C	$\frac{\text{in.-min}}{\text{sec-gal}}$	Actuator velocity gain factor, 0.933
K_D	$\frac{1}{\text{sec}}$	Inner loop damping gain factor of control valve, 67.9
K'_D	volt	Control valve dead band, 2.4

TABLE A-2. (Continued)

Symbol	Units	Definition
K_{DB}	$\frac{1}{sec}$	Inner loop damping gain factor, 5.8
K_{DF}	$\frac{1}{sec}$	Inner loop damping gain factor, 2.95
K_{DV}	$\frac{1}{sec}$	Inner loop damping gain factor of dual pilot check valve, 7.04
K_{EQ}	lb/in.	Equivalent system linear spring constant, 610 967
K_F	$\frac{1}{sec^2}$	Outer loop gain of a boom frequency component, 872
K_{FO}	$\frac{rad}{ft\text{-}lb\text{-}sec}$	Input gain factor, 3.488×10^{-7}
K'_L	volt	Input voltage limit, 8
K'_s	$\frac{1}{sec^2}$	Control valve input gain, 0.179
K_s	$\frac{1}{sec^2}$	Control valve outer loop gain, 1421
K_S	lb/in.	Spring constant of boom structure and pivot and actuator tie points
K_T	$\frac{gal/min}{ft\text{-}lb}$	Torque to flowrate conversion factor, 5×10^{-14} if C_L is positive and 7.5×10^{-4} if C_L is negative
K_V	$\frac{1}{sec^2}$	Outer loop gain factor of dual pilot check valve, 25.27

TABLE A-2. (Concluded)

Symbol	Units	Definition
L1	$\frac{1}{\text{sec}}$	Control valve rate limit, 4
L2	-	Position limit, 1
L3	in.	Stroke limit, 9.5
P_S	psi	System supply pressure
Q_S	gal/min	Hydraulic flow supplied to boom control valve, 8
T_L	ft-lb	Torque on boom cylinder due to weight of boom, 54×10^3
Δt	msec	Simulated response time of the dual pilot check valve, 140
W_t	lb	Weight of boom, drum, cowl, and motors 12 185
X_A	in.	$(X_A = X_L)$ actual position of the boom cylinder when T_L applied
X_I	in.	Ideal position of boom cylinder, X = 3.25 when $\beta = 0$
Y_L	in.	Linear change of boom height at drum centerline
β	rad	Position angle of boom from a horizontal position
$\dot{\beta}$	rad/sec	Angular rate of boom
$\ddot{\beta}$	rad/sec^2	Angular acceleration of boom

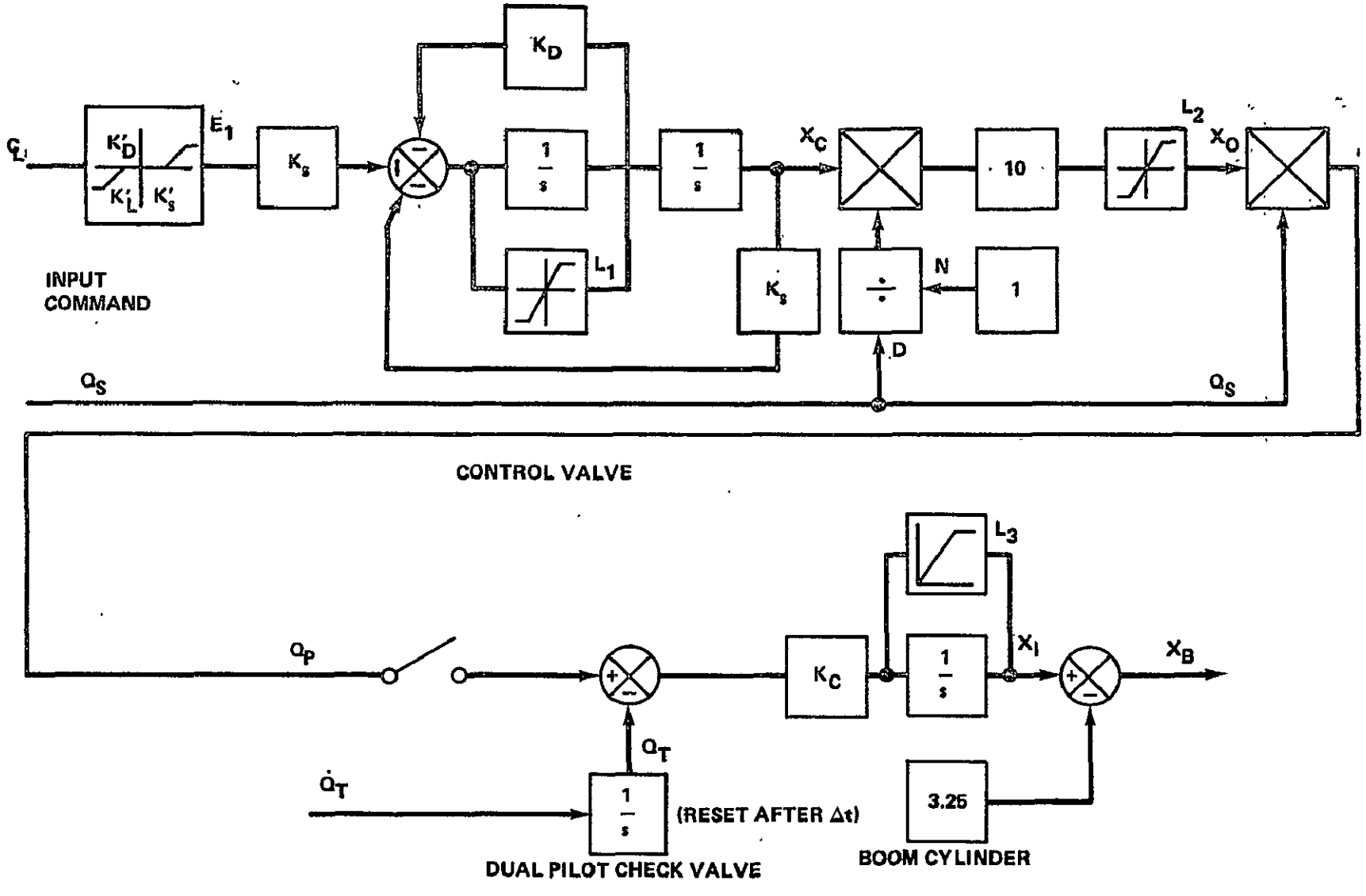

Figure A-1. Control valves and actuator.

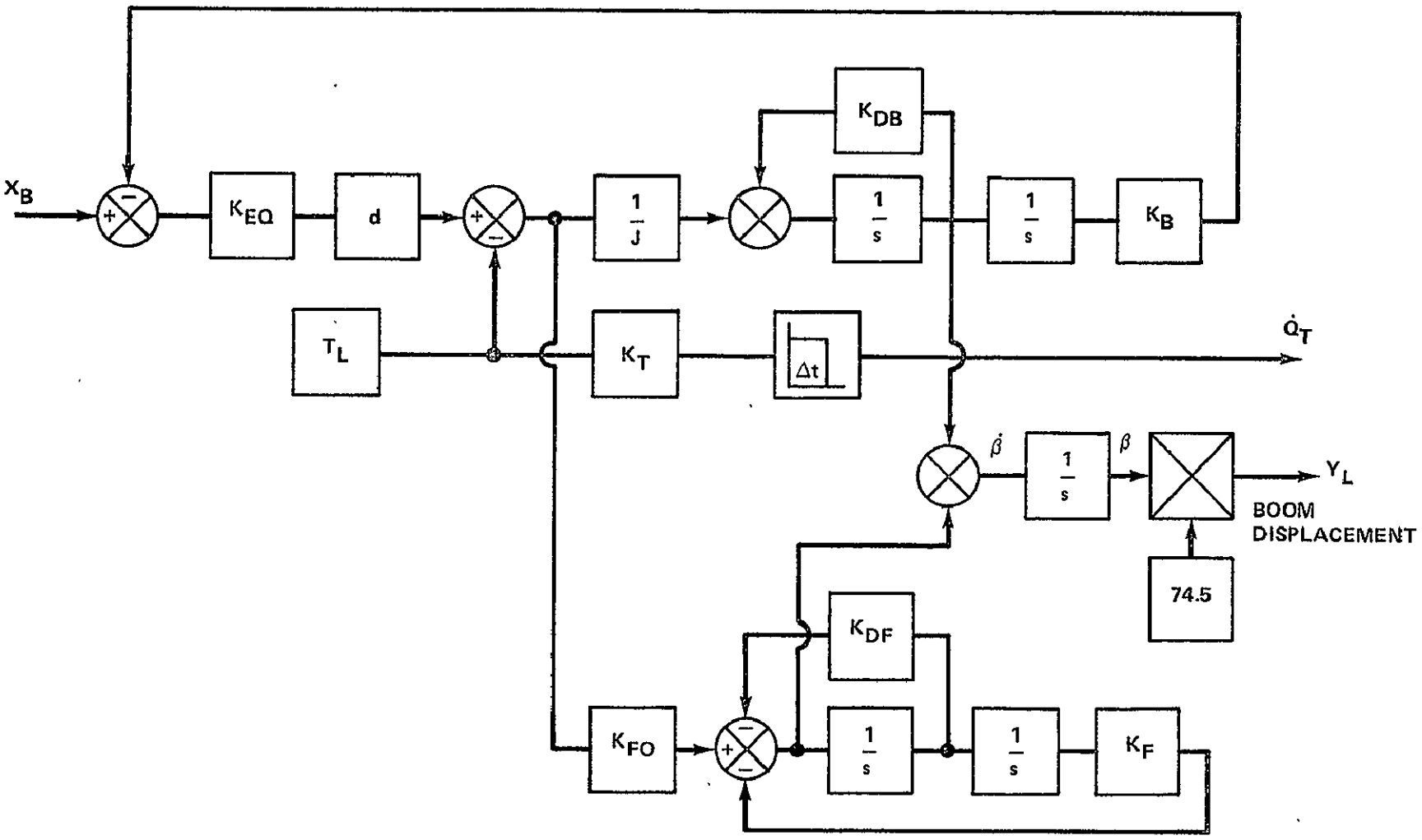

Figure A-2. Boom dynamics.

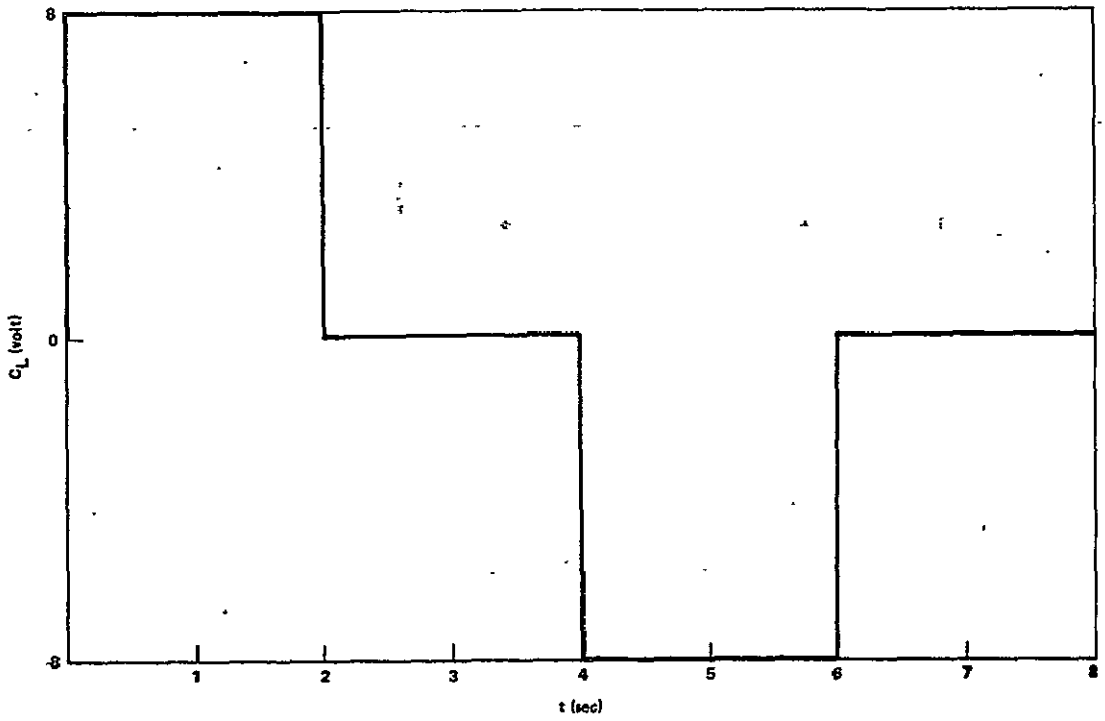

Figure A-3. Command to left boom.

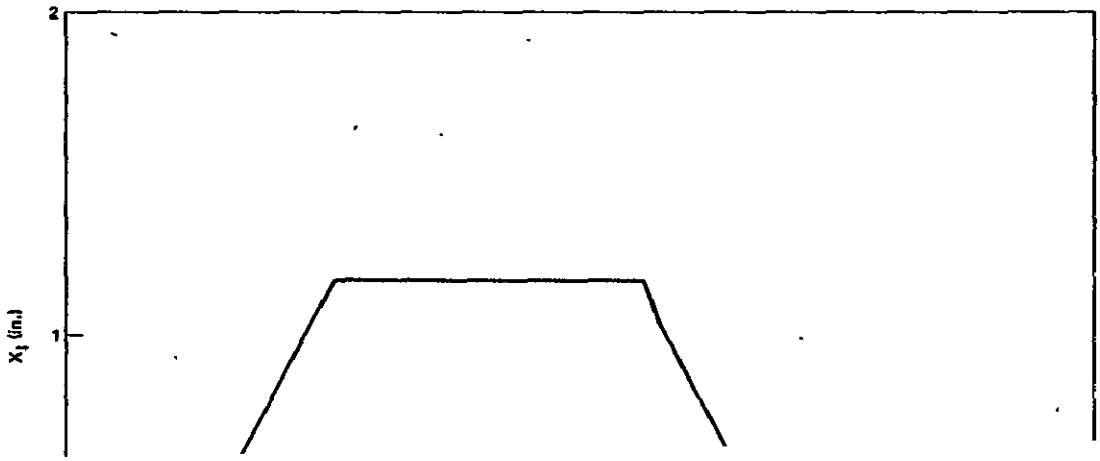

Figure A-4. Boom cylinder displacement.

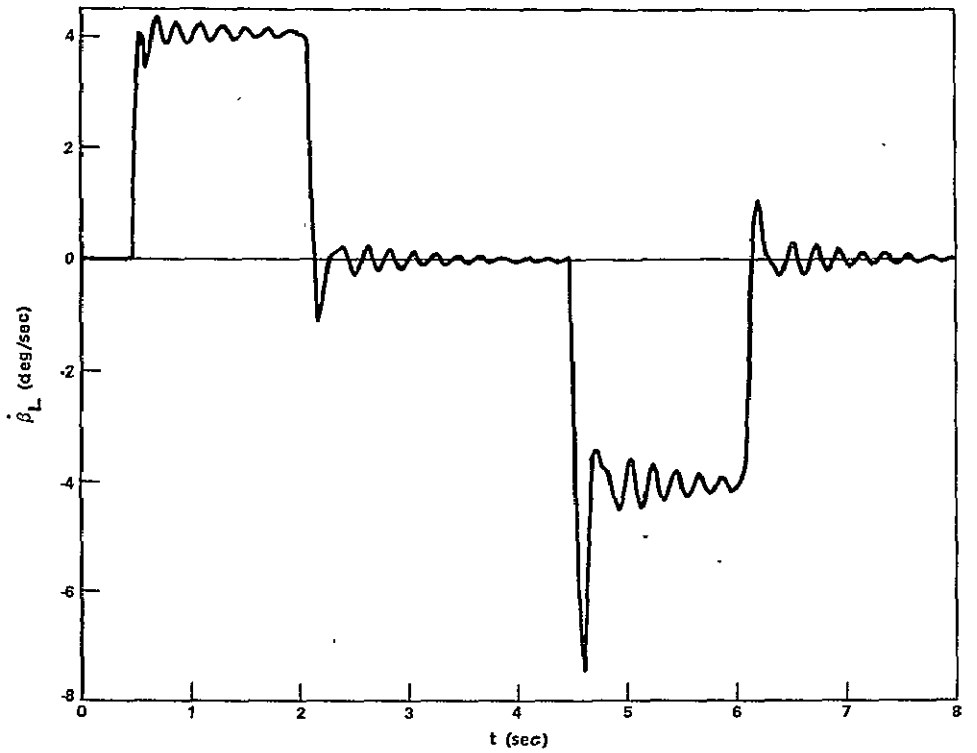

Figure A-5. Rate for left boom operation — individual operation.

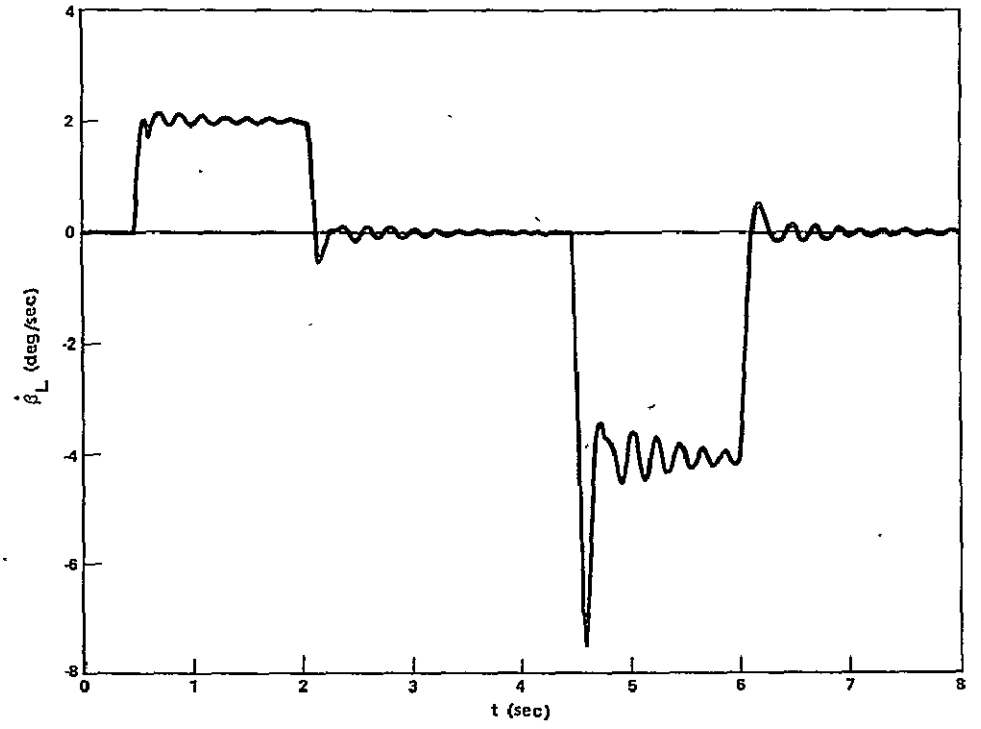

Figure A-6. Rate for left boom operation — simultaneous operation.

APPROVAL

TRANSFER FUNCTION TESTS OF THE JOY LONGWALL SHEARER

By Paul H. Fisher, Jr.

The information in this report has been reviewed for security classification. Review of any information concerning Department of Defense or nuclear energy activities or programs has been made by the MSFC Security Classification Officer. This report, in its entirety, has been determined to be unclassified.

CLYDE S. JONES, JR.
Chief, Electronics and Servo-Analysis Branch

J. L. MACK
Chief, Control and Instrumentation Division

F. BROOKS MOORE
Director, Electronics and Control Laboratory

☆U.S. GOVERNMENT PRINTING OFFICE 1978—640-081/357 REGION NO. 4